Doctoral Dissertation

博士論文

Neuroendocrinological studies on the neural circuit that activates female sexual behavior in a teleost medaka

（メダカを用いた真骨魚類のメス性行動を賦活する神経回路に関する神経内分泌学的研究）

A Dissertation Submitted for the Degree of Doctor of Philosophy

December 2021

令和 3 年 12 月 博士（理学）申請

Department of Biological Sciences, Graduate School of Science,

The University of Tokyo

東京大学 大学院理学系研究科

生物科学専攻

Soma Tomihara

富原 壮真

Abstract

Reproduction is one of the most important and vital biological phenomena for all animals. In most of vertebrate species, there are two sexes, female and male, and successful reproduction is accomplished by coordinated occurrence of gonadal maturation for attaining fertility and smooth execution of sexual behavior in conspecific individuals of other sex. For the regulation of such phenomenon, sex steroid hormones released from mature gonads are supposed to serve as the signals to convey the gonadal status to the brain in order to synchronize the activation of sexual behavior with gonadal maturation, which is widely observed among vertebrate species. The neuroendocrine regulatory mechanisms have been unraveled at neural/molecular levels in mammalian species, on the other hand, little is understood in non-mammalian vertebrates including teleosts.

In the present thesis, I aimed to elucidate the neuroendocrine mechanism that elicits the female sexual behavior, using medaka as a teleost model, which have many advantageous features for this study.

In chapter 1, I established open-source semi-automated behavioral recording/analysis suite for analysis of sexual behavior of medaka. This analysis suite drastically reduced the time for the analysis, and behavioral analyses can be performed more efficiently and sophisticatedly. It should be noted that it is possible to apply it for almost all behavioral analysis, which contributes to the progress of various fields of biology.

In chapter 2, I examined the possible involvement of a sex steroid hormone estrogen, which is released from mature ovary, in the control of female sexual behavior. From the observation of female sexual behavior after ovariectomy or pharmacological treatment, I found that estrogen has an important and essential role in the activation of female receptivity. I also found that one of the estrogen receptor subtypes *esr2b* deficiency caused severe defect in the female receptivity,

although *esr2b*-deficient female medaka shows normal gonadal function. Considering the previous studies demonstrated that *esr2b* is expressed in the brain, it is suggested that *esr2b*-expressing neurons play a crucial role in the activation of female receptivity in accordance with signals from the gonadal estrogen.

In chapter 3, I explored the neural circuitry that elicits the female sexual behavior. Activity mapping with an immediate early gene revealed that the neurons in ventral telencephalon specifically show high neural activity during the spawning behavior but not during the reception of courtship by male, and this neurons expressed a GABA marker gene, *gad1.1*, suggesting that GABAergic inhibitory neurotransmission is involved in the spawning behavior in female, but not in female receptivity. Furthermore, I found that *esr2b*-expressing neurons are closely located in the GABAergic neurons and supposed to release the neuropeptides, NPB, CCK, and CNP1. Interestingly, the genes of receptors for CCK and CNP1 were expressed in the ventral telencephalic region where the above-mentioned GABAergic neurons were located. These findings may suggest that the existence of local peptidergic neuromodulation between these two populations in the ventral telencephalon, which contribute to facilitate the spawning behavior in response to estrogenic signal.

Using medaka as teleost model animal, the present thesis revealed the neuroendocrine regulatory mechanism that elicits the female sexual behavior in teleosts, which independently controls the activation of female receptivity and facilitation of spawning behavior.

Table of Contents

Abbreviations

cck	cholecystokinin
cckbr	cholecystokinin b receptor
cGMP	cyclic GMP
cnp1	C-type natriuretic peptide 1
Cy3	cyanine 3
DAPI	4',6-diamidino-2-phenylindole
DHP	17α,20β-dihydroxy-4-pregnen-3-one
DIG	digoxigenin
DMSO	dimethyl sulfoxide
E2	17β-estradiol
EPS	Encapsulated Postscript
Esr1	estrogen receptor 1
Esr2a	estrogen receptor 2a
Esr2b	estrogen receptor 2b
Fad	fadrozole hydrochloride
FL	fluorescein

fps	frames per second
FSH	follicle stimulating hormone
fshb	follicle stimulating hormone beta subunit
GABA	ɤ-aminobutyric acid
GFP	green fluorescence protein
GnRH	gonadotropin-releasing hormone
GPCR	G-protein coupled receptor
GPIO	general-purpose input/output
HPG	hypothalamic(hypothalamo)-pituitary-gonadal
IEG	immediate early gene
IHC	immunohistochemistry
ir	immunoreactive
ISH	*in situ* hybridization
KO	(gene) knock out
LH	luteinizing hormone
lhb	luteinizing hormone beta subunit
LMD	laser-microdissection
MPG	motor pattern generator

MS-222	tricaine methanesulfonate
NAS	network-attached storage
npb	neuropeptode B
npbwr2	NPB/W receptor 2
NPPv	nucleus posterioris peroventricularis
NVT	nucleus ventralis tuberis
olgc7	*Oryzias latipes* gyanylyl cyclase
OVX	ovariectomy
PBS	phosphate-buffered saline
PGE2	prostaglandin E2
PGF2α	prostaglandin F2α
POm	nucleus preopticus pars magnocellularis
PWM	pulse width modulation
qRT-PCR	quantitative real-time PCR
RNA-seq	RNA-sequencing
rPOp	rostral part of nucleus preopticus pars parvocellularis
rps13	ribosomal protein s13
SEM	standard error of the mean

SSC	saline sodium citrate
TBS-T	Tris-buffered saline with Tween 20
Tg	transgenic
TPM	transcripts per kilobase million
UGP	urogenital papilla
VBA	Visual Basic for Applications
Vd	ventral telencephalon pars dorsalis
VMH	ventromedial hypothalamic nucleus
VMHvl	ventrolateral part of VMH
Vp	ventral telencephalon pars posterior
Vs	ventral telencephalon pars supracommissuralis
WLAN	wireless local area network
WT	wild type

General Introduction

Reproduction is one of the most vital and essential phenomena for all animals to leave the offspring. Most of vertebrate species have two sexes, female and male, and successful reproduction is accomplished by gonadal maturation for attaining fertility and smooth execution of the sexual behavior at the best timing for fertilization. Such coordinated occurrence of gonadal maturation and activation of sexual behavior is supposed to be precisely regulated by the central nervous and endocrine systems that integrate and process various information from external environments and physiological status of each individual. Actually, many vertebrate species show seasonal breeding, during which animals perform sexual behavior in accordance with their gonadal maturation [1, 2]. For such regulation, the sex steroid hormones released from mature gonads are supposed to serve as signals for tuning the regulatory mechanism of sexual behavior for successful reproduction in the brain. Thus, the sex steroid hormones play pivotal roles in such neuroendocrine regulatory mechanisms to synchronize behaviors with the physiological conditions, and this phenomenon is widely observed among vertebrates even though there is an enormous diversity in the ecological niche, life history, physiological feature, morphology, and behaviors.

For the regulation of the gonadal functions, hypothalamic(hypothalamo)-pituitary-gonadal (HPG) axis is regarded as an important neuroendocrine and endocrine regulatory system in vertebrates. Here, a well-known phenomenon called the sex steroid feedback is operative in which sex steroid, especially estrogen, released from gonads regulates the upstream regulator in hypothalamus as a feedback signal. In mammals, hypothalamic kisspeptin neurons are considered to directly regulate the neural activities of gonadotropin-releasing hormone (GnRH) neurons in an estrogen-dependent manner [3-8], which results in the periodical folliculogenesis and ovulation in female [9-11]. Although there are some differences in the precise mechanism, accumulating evidence strongly suggests the importance of estrogen in the HPG axis regulation

in non-mammalian species as well [12-17].

It has also been suggested that the sex steroid hormones, especially estrogen, contributes to the neural control of female sexual behavior, and not a few studies have been carried out to elucidate that mechanism mainly using mammalian species. In 1968, Davidson *et al.* demonstrated that estrogen administration reinstates lordosis behavior, a female-specific sexual behavior, in ovariectomized-adrenalectomized female rats, which are devoid of sex steroid hormones and does not perform lordosis behavior [18], suggesting that estrogen plays some crucial roles in the activation of lordosis behavior in rats. In addition, the ventromedial hypothalamic nucleus (VMH) has been suggested to be the target for the estrogenic signals, because VMH neurons express estrogen receptors, and the electrolytic lesion of VMH disrupts, while electrical stimulation facilitates, lordosis behavior in rats [19, 20]. It is revealed that estrogen receptor 1 (*esr1*)-expressing neurons is involved in the activation of lordosis behavior in mice [21], and recent studies using mice suggested that estrogen receptor 1 (*esr1*)-expressing neurons in the ventrolateral part of VMH (VMHvl) are involved in promoting the lordosis behavior, although optogenetic/chemogenetic acute stimulation of these neurons in ovariectomized female does not elicit the lordosis behavior, suggesting that activation of stimulated neurons does not directly elicit the lordosis behavior [22]. It has also been revealed that estrogen/*esr1* signaling is involved in the activation of lordosis behavior by modification of the gene expression patterns and synaptic connection of this neural population [22, 23]. As described above, in mammals, the neural mechanisms that elicit the female sexual behavior, especially lordosis behavior, and its essential modulation by estrogen, have been gradually unraveled at the neural circuit/cellular level.

On the other hand, in non-mammalian species, search for the neuroendocrine mechanisms involved in the control of sexual behaviors have been conducted mainly using teleost fishes. Many teleosts are seasonal breeder, which suggests the existence of a principal regulatory mechanisms

that synchronize the activation of sexual behavior with gonadal maturation in teleosts, probably mediated by sex steroid hormones, although there are the diverse habitats and patterns of sexual behavior in teleosts. Thus, it may be worth analyzing the neuroendocrine mechanism of a model teleost for understanding the evolution of neuroendocrine mechanisms that control the sexual behavior in teleosts. In addition to this, teleosts have been frequently used since the era of Tinbergen and Lorenz, and neural mechanisms of teleost behavior have been interested for a long time.

Unfortunately, however, available information is still limited compared to that in mammals. In 1980s, a couple of studies indicated that ventral telencephalon and preoptic area are involved in the activation of sexual behavior in male goldfish (*Carassius auratus*) and female himé/kokanee salmon (*Oncorhynchus nerka*), which are useful for such studies due to their steleotypical and obvious patterns of sexual behavior [24-26]. Because recent studies have demonstrated in some teleost species that these areas express genes for sex steroid hormone receptors [27-30], it may be speculated that these nuclei contain neurons that play important roles in the activation of sexual behaviors by receiving sex steroid signals in teleost. However, goldfish and himé/kokanee salmon, which has were used for studying the brain regions involved in the activation of sexual behavior, may have some technical limitations for further mechanistic analyses, mainly because of the difficulty of applying various molecular genetic tools to these fish. Although zebrafish has most frequently been used in the field of neuroscience because of its easy accessibility to various molecular genetic tools, gene-knockout (KO) of sex steroid hormone receptors causes sex-reversal [31], which makes it difficult to simply analyze the intrinsic effects of sex steroid hormones on the brain functions that are involved in the female sexual behavior. Thus, further analyses of the neural mechanisms that elicit sexual behaviors in female teleost have been difficult.

In order to overcome these technical limitations in the studies using teleost fishes, I used a model

teleost, medaka (*Oryzias latipes*), which has recently been intensively used for neuroendocrinological analyses. Medaka has many advantageous features for the neuroendocrinological studies; for instance, a wealth of information about their genome, accumulating information on the mechanisms of neuroendocrine regulation of reproduction by sex steroid hormones, and sophisticated experimental methods including various molecular genetic tools [32, 33]. Furthermore, medaka shows stereotypic patterns of sexual behavior [34, 35], which gives us an easy access to quantitative behavioral analyses. By taking advantage of these features of medaka, I performed multidisciplinary analyses to elucidate neural mechanisms regulating the female sexual behavior in medaka.

In chapter 1, I established a suite of experimental system for behavioral analyses that should enables us to perform efficient and sophisticated analyses by alleviating tasks and eliminating human errors, using a single-board computer, Raspberry Pi^{TM} in combination with Microsoft Excel Macro. The analysis suite drastically reduced the times and laboriousness of the behavioral analysis. By using this suite, I analyzed the sexual behavior of laboratory and wild strain medaka and found a difference in sexual motivation in male, perhaps resulting from the influence of domestication [36].

In chapter 2, I examined the possible involvement of estrogen and one of its receptors, estrogen receptor 2b (Esr2b) in the activation of female sexual behavior in medaka by behavioral analyses using the analysis suite established in chapter 2. I found that *esr2b* KO female medaka refused to be clasped by male, thus did not perform the subsequent spawning behavior, egg release, although they have normal gonadal function. The results suggest that *esr2b*-expressing neurons in the female brain are involved in the activation of female receptivity.

In chapter 3, I explored the neural circuit that elicits female sexual behavior of medaka. I histologically analyzed the gene expression patterns of the immediate early gene *egr1* during the

female sexual behavior in some experimental groups, and found an increase in *egr1* expression in the ventral telencephalic region specifically in the individual that showed oviposition. RNA-sequencing followed by histological analysis revealed that this neural population is GABAergic, which suggests that tail-bending/oviposition behavior are activated by GABAergic neurons in the ventral telencephalon. Interestingly, *esr2b*-expressing neurons, which are supposed to be involved in the control of female sexual behavior, are closely located to these GABAergic neurons. In addition, I obtained histological evidence to suggest the existence of functional anatomical relationship (perhaps neuromodulatory) between these two neural populations. These findings suggest that there is a local neural circuit in ventral telencephalon that is involved in the control of spawning behavior for oviposition following activation of estrogenic signaling.

Chapter 1

Establishment of open-source semi-automated behavioral analysis system and quantification of the difference of sexual motivation between laboratory and wild strains

Abstract

Behavioral analysis plays an important role in wide variety of biological studies, but behavioral recordings often tend to be laborious and are associated with inevitable human-errors. It also takes much time to perform manual behavioral analyses while replaying the videos. On the other hand, presently available automated recording/analysis systems are often specialized for certain types of behavior of specific animals. Here, I established an open-source behavioral recording system using Raspberry Pi, which automatically performs video-recording and systematic file-sorting, and the behavioral recording can be performed more efficiently, without unintentional human operational errors. I also developed an Excel macro for behavioral annotation, which enables us to easily perform behavioral analysis with simple manipulation. Thus, I succeeded in developing an analysis suite that mitigates human tasks and thus reduces human errors. By using this suite, I analyzed the sexual behavior of a laboratory and a wild medaka strain and found a difference in sexual motivation presumably resulting from domestication.

Introduction

Animal behavior is one of the most important factors that represent the animal's features, and the behavioral analysis often gives a lot of information complementally to the other analyses using methods in physiology, *in vitro* biochemistry, etc. In addition to the behavioral analyses of wildtype animals, the recent development of genetic tools such as genome editing technology [37-40] has increased the importance of analyzing behaviors of genetically modified animals as the most salient phenotypes. Thus, the demands of behavioral analyses are increasing, and the easier and more efficient method has been awaited.

So far, the majority of researchers have recorded the videos of animal behavior by using video camera and manually annotated the behavioral events while replaying the videos [41-47]. However, simultaneous video-recording inevitably tends to be associated with human-errors with increasing number of cameras. After video recording, it is also a confusing task to transfer the data from multiple video cameras to a storage, change their filenames systematically, and sometimes encode them. Furthermore, it is also painstaking to replay the entire video, pause and identify each behavioral event, and manually record the timing and/or duration of each behavioral event. Thus, the manual behavioral annotation takes much time. While there are some automated recording/analysis systems for the solution of these problems [48-57], these are exclusively designed for certain species and/or behavior, and such systems often may not be applicable to the studies of non-model animals or rare behaviors. In addition, although commercially available systems are convenient and sophisticated, they are often expensive. Thus, such conventional onerous methods have been the only choice to analyze behaviors for many researchers.

In the present study, I established an open-source automated behavioral recording/file-sorting system with a single-board computer, Raspberry Pi and performed behavioral analysis efficiently

without unintentional human errors caused by experimental operations. Raspberry Pi is an inexpensive credit card-sized computer, and we can remotely operate multiple Raspberry Pi at the same time via wireless local area network (WLAN) connections. By utilizing them, I have succeeded in automating a large part of experimental procedure of behavioral analysis: video-recording by multiple cameras, file-naming, encoding, and transferring video data from multiple cameras to a network-attached storage (NAS). In addition, Raspberry Pi can switch on and off external devices via general-purpose input/output (GPIO) pins and a simple relay circuit, which enables to automate simple experimental manipulations, such as feeding and illumination. This customization reduced the experimental procedures and made efficient/reproducible analyses of behaviors at low cost.

Furthermore, I established a Microsoft Excel macro for behavioral annotation. By using this tool, it became possible to annotate the behavioral events by only pressing the assigned PC keys when the behaviors of interest occur. As this tool makes manual notetaking unnecessary, the time taken for quantification of the behaviors was drastically shortened. This tool also enables the generation of raster plots that indicates the time course of the behaviors, thereby making it easier to get an overview of the behavioral transition.

Using the combination of these two, the behavioral analyses can be carried out more efficiently, and consequently it may mitigate human errors. In the present study, I analyzed and compared the sexual behaviors of a laboratory and a wild strain of teleost medaka, and the time spent for the analysis was drastically shortened compared to the conventional method. Here, I found a difference in the sexual motivation between the strains probably caused by the different selection pressure in the laboratory and the wild environments.

Materials and Methods

Hardware

Two versions of Raspberry Pi, Raspberry Pi Zero W (Raspberry Pi Foundation, Cambridge, UK) and Raspberry pi 3B (Raspberry Pi Foundation) installed with Raspbian (ver.3.1.1; latest version of which is called Raspberry Pi OS) were used in the present study. Each component of video-recording (hereafter "RP-units") consists of a Raspberry Pi Zero W and a Raspberry Pi Camera V2 (Raspberry Pi Foundation), which is a camera module designated for Raspberry Pi (Figure 1-1A). I put them in the designated case for Raspberry Pi Zero W, Raspberry Pi Zero Case (Raspberry Pi Foundation). To remotely operate RP-units, I built a WLAN including 16 RP-units and a wireless rooter, WARPSTAR Aterm WR8370N (NEC, Tokyo, Japan) (Figure 1-1B). A NAS (LS210DC; Buffalo INC., Nagoya, Japan) was also connected to this WLAN through an Ethernet cable. I accessed and operated the RP-units through Secure Shell (SSH) remote login by using a Windows PC that is connected to this WLAN.

For developing a system that operates external devices, Raspberry pi 3B, which is equipped with GPIO pins, was used (Figure 1-1C). In the present study, I used a green LED lamp, an auto-feeding device (Eheim auto feeder, Eheim, Deizisau, Germany), and an electric circuit including 9 V alkaline battery (6LR61Y(XJ), Panasonic, Kadoma, Japan) as external devices, and I connected some of GPIO-output pins to a custom-made relay unit, which switches on and off external devices by turning on and off the power to the circuit. The block diagram of the relay unit is described in Figure 1-D. Video-recording was carried out by Raspberry Pi Camera V2.

Software

All of the shell script for operating Raspberry Pi were Bash Unix shell, and the Python script was written in Python (ver.2.7.13). For video-recording and file-sorting, I created a shell script "*Record.sh*" (Figure 1-2). *Record.sh* runs a Python script "*Camera.py*", which executes video-recording during the recording period and with a camera resolution defined in it. *Camera.py* also defines the file-names and saves the temporary files in a storage of the Raspberry Pi. By default setting, each file-name of contains machine ID, date and time to run *Record.sh*. Machine ID is an assigned number of each RP-unit written in a text-file "*MachineID*". Furthermore, *Camera.py* includes scripts to operate external devices through GPIO. In this part, the trigger settings for GPIO pins (signal output, the timing and duration of the signal) can be configured. Hence, once *Camera.py* is run, video-recording, file-naming and GPIO interfacing are carried out according to the script. After running *Camera.py*, recorded files in each RP-unit are moved to the NAS storage. Note that conversion of the video file to another format was designed to be done automatically by the main PC in this study. In case of Raspberry Pi 3B, this conversion can be done in the Raspberry Pi itself before moving the video to the NAS. In my experience, Raspberry Pi Zero W takes too much time to achieve format conversion because of its smaller CPU power. I also created a shell script *Setup.sh* for cloning the RP-units easily. When *Setup.sh* is run, interactive command line for setting the machine ID and IP-address appear in the terminal window. After filling them in, *Record.sh* and *MachineID* will be automatically generated. Although a PC keyboard and a display are initially required during this step, they become unnecessary after that, since all operations can be done via SSH remote login (See RP-units instruction web site (https://github.com/Neuroendo-mdLab/RP-units)).

I made a tool for behavioral annotation by using an Excel macro written in Visual Basic for Applications (VBA), which is here called "*Ethogramer*". In the worksheet- "*Sheet1*" of the Excel

macro, I made four columns and a cell for filling in the following settings: names of behavioral repertoires indicating what we want to analyze ("Repertoires Name"), duration of behavioral repertoires ("Continuous/Intermittent"), Color for drawing raster plots ("Color"), key for recording behavioral repertoires ("Key"), and total time duration of the analysis ("Time (s)") (Figure 1-3A). For the behavioral annotation, I made a user-form (GUI window) "*Analyze*" that was programmed to generate a worksheet (by default, sheet2,3,4…) for recording the data, based on the settings defined in the worksheet "*Sheet1*". After pressing "." to reset the time, the behavioral annotation was carried out by pressing the assigned PC keys based on the worksheet "*Sheet1*". After completing the behavioral annotation, the raster plot is generated by running another user-form "*Draw_Rasterplot*". The output for the raster plot was made in Encapsulated Postscript (EPS) format. Since EPS is a text-based format for drawing a graphic, I converted the timing information of each behavioral events to the line widths of the raster plots (Figure 1-3B).

Animals

Two strains of medaka (*Oryzias latipes*), d-rR and Kiyosu were used in the present study. Since d-rR strain has been inbred over 50 years by the researchers, I treated them as a laboratory strain that is influenced by the selection under the breeding environments. In contrast, Kiyosu was the 5th generation of inbreeding of wild fish that had been caught in Toyohashi City, Aichi Prefecture, Japan, and I treated them as a wild strain. In the both strains, female and male were paired and maintained in fish tanks with water circulation (Labreed, IWAKI Co., Ltd., Tokyo, Japan) under 14-hour light/10-hour dark photoperiod (light on at 08:00 and off at 22:00) condition at a water temperature of 27 ± 2 °C. These were fed three or four times per day with live brine shrimp and/or commercial flake food (Tetra Medaka-bijin; Spectrum Brands, Yokohama, Japan). All of the fish maintenance and the experiments were conducted in accordance with the protocols approved by

the Animal Care and Use Committee of the University of Tokyo (permission number 17-1).

Analysis of sexual behavior

The pairs of medaka that showed spawning for three consecutive days before the experimental day were used. On the day before behavioral testing, the pairs were placed and habituated to experimental tanks which had transparent bottom (15 × 15 cm) and white walls (Figures 1-4A-C). The water depth was maintained at ~5 cm. Each pair of female and male were kept separated until the analysis by putting a transparent perforated partition diagonally set across the tank. These tanks were placed on a transparent acrylic plate, and their upper side was covered with a thin white paper to spread the light evenly from above. The RP-units were put 20 cm under the acrylic plate for each tank to record the behavior from ventral side of medaka. At 9:00 (1.0 hour after the onset of the light period) of the following day, I ran *Record.sh* for each RP-unit by SSH remote login. The camera resolution and framerate were set to 640 × 480 pixels and 15 frames per second (fps), respectively in *Camera.py*. The partitions were slowly removed, then the interactions of female and male were recorded for one hour.

By using *Ethogramer*, I identified the behavioral repertoires and annotated four behavioral repertoires during the sexual behavior: following, courtship, clasping, and spawning (Figure 1-4D), while replaying the first 30 minutes of the videos from the time the partition was removed, with a playing speed of ×2 (actual time required for playing is 15 minutes per videos). Each behavioral repetoire was identified by referring to the previous studies [34, 35] (also see a brief description of each behavioral repertoire in the Results section). I regarded and set following and clasping as continuous behavior, while courtship and spawning as intermittent behavior when using *Ethogramer*. After behavioral annotation for all four behavioral repertoires, I calculated the following behavioral parameters: the latency to first following, the percentage of the time spent

for following before spawning, the frequency of courtship before spawning, the percentage of following with successful courtship before spawning, the number of clasping ceased by female before spawning, and the latency to spawning. The parameters were calculated according to the following formulae.

$$\text{Percentage of time spent for following before spawning (\%)} = \frac{\text{Cumulative time for following before spawning (min.)}}{\text{Latency to spawning (min.)}} \times 100$$

$$\text{Frequency of courtship before spawning (min.}^{-1}) = \frac{\text{Number of courtship}}{\text{Latency to spawning (min.)}}$$

$$\text{Percentage of following with successful courtship before spawning (\%)} = \frac{\text{Number of following with courtship in rapid succession}}{\text{Total number of following}} \times 100$$

All of the analysis was performed by blind test.

Statistical analysis

All the values are presented as mean ± standard error of the mean (SEM). Statistical analyses and graph drawing were performed by using R (R Core Team 2020). All of the parameters except for the latency to the first following/spawning were analyzed by Mann-Whitney *U* test and are shown by the whisker and scatter plot. I used the *beeswarm* package (https://cran.r-project.org/web/packages/beeswarm/index.html) to perform the scatter plot. The latency to the first following/spawning was analyzed using Kaplan-Meier plot, and the differences between each Kaplan-Meier curve were tested for statistical significance using Log-Rank test. The *survival*

package (https://cran.r-project.org/web/packages/survival/index.html) was used to conduct Kaplan-Meier plots. A *P*-value less than 0.05 was considered statistically significant.

Results

Automated behavior recording system with Raspberry Pi enables efficient and reproducible video-recordings

I established an automated behavioral recording system by using Raspberry Pi. Behavioral recording was performed by running *Record.sh* through SSH remote login. In the present study, I simultaneously accessed 16 RP-units and ran *Record.sh* for recording the sexual behavior of medaka (described below in detail). After 1-hour video-recording, it only took approximately 30 minutes to perform required operatations automatically for all 16 videos, such as file-naming, encoding and transferring data to the NAS storage (Figure 1-5). The 16 video files encoded in the mp4 format were correctly named with the machine ID number and the current timestamp, and stored in the NAS storage. The remote video-recording reduces unintentional human disturbances against the animal behavior, and the automated systematic file-sorting function removes the risk of the erroneous video data storage. In addition, since RP-units are small and easy to install, it requires less space to perform behavioral experiments. In the present study, I made wooden frames that can accommodate twelve tanks and RP-units and carried out simultaneous video-recording of the sexual behavior of twelve medaka pairs in only 100 × 45 cm space (Figures 1-4A and B).

Behavioral annotation tool, *Ethogramer* enables easier and more informative behavioral analysis

I developed *Ethogramer*, which enables behavioral annotation for all behavioral events of interest by only pressing the assigned PC keys while replaying the video. I performed the behavioral annotation of sexual behaviors of 16 pairs of medaka while replaying the first 30 minutes of the videos played at double speed (Figure 1-5). Also, I successfully analyzed the

behavioral repertoires that last for certain time, following and clasping, by continuously pressing the assigned key during these two behavioral repertoires. Since I gave the macro the function to record the pressed time and duration of 40 keys (26 alphabet keys (a-to-z), ten numeric keys (0-to-9) and four cross-keys (left/right/up/down)), the observers can assign up to 40 behavioral repertoires and then theoretically annotate up to 40 behavioral repertories during the video replay. Moreover, the raster plots that visualize the behavioral transition along the accurate time scale are generated by only pressing the button. Also, I roughly estimated the time spent for the analysis with or without these systems. In the conventional manual method, video-recording was performed by home-video cameras, and I manually annotated the behavioral events. It was painstaking to annotate the continuous behavior, following and clasping, because I must record both the start and end timing of each behavioral event and calcurate the duration. It took approximately 40 minutes per 30-minite videos, and then it is estimated that it should take more than ten hours for the annotation of all 16 videos. In addition, since it is difficult to genereate the raster plots by manual behavioral annotation, it will result in the lack of information to get an overview of the behavioral transition. On the other hand, by using the system established in this study, it is not necessary to switch on each video camera, transfer the video data and rename the filenames. Behavioral annotation took approximately four hours, which is the same as the time for replaying the 16 videos at double speed. Also, the present system allowed me to generate 16 raster plots indicating the behavioral transition of each pair, which makes the behavioral data more informative. Thus, *Ethogramer* enables efficient and informative analysis of behaviors.

The combination of the Raspberry Pi system and Excel macro enabled an efficient and informative comparative analysis of the sexual behavior of medaka between laboratory and wild strains

Here, I show the result of the comparative analysis of the sexual behavior of a teleost medaka as a successful application of the combination of the Raspberry Pi system and Excel macro. Adult medaka is a useful animal model for the studies of reproductive biology, behavioral neuroscience, etc [6, 7]. Since the d-rR (domesticated rR) strain of medaka, which is one of the most frequently used laboratory strains, have been empirically recognized to spawn readily compared with the wild strain, and there is an anecdotal report that laboratory strain spawns more readily than the wild ones, I compared the sexual behavior between the two strains, d-rR and Kiyosu as a wild strain.

Male and female medaka pairs show stereotypical sequence of sexual behavior repertoires [34, 35]. This sequence begins with the male approaching the female closely from behind and following at the same speed (termed 'following'), and the male performs courtship display (swimming in front of the female by making a quick circular turn) only when the female slows down swimming (termed 'courtship'). If the female accepts the male's courtship, the male wraps the female body by using dorsal and anal fins and quivers their body to promote spawning (termed 'clasping'). After the successful clasping, the male and female spawn sperms or eggs respectively, resulting in fertilization (termed 'spawning'). If the female is not receptive, however, she does not slow down nor accept the male's courtship but changes direction and rapidly swims away from the male. The female also shows unreceptive behavior in which she ceases clasping before successful spawning. I recorded such behavior repertoires by using RP-units, quantified and analyzed by using *Ethogramer* (Figure 1-6). Figure 1-6A shows the raster plots that indicate the transition of the sexual behavior in the present observation. I found that the latencies to first

following and spawning of d-rR were shorter than those of Kiyosu (Figures 1-6B and C). It was found that the latency to first following approached significance, suggesting a difference (Figure 1-6B). Also, significant difference was detected in the latency to spawning (Figure 1-6C). I further analyzed some indices that reflect male motivation of sexual behavior (Figures 1-6D and E), and found that the frequency of courtship before spawning of d-rR is significantly higher than that of Kiyosu (Figure 1-6E), while there was no significant difference in the percentage of the time spent for following before spawning (Figure 1-6D). This result suggests that the d-rR males perform courtship display more frequently than the Kiyosu males. On the other hand, I did not find differences in the indices that reflect female receptivity (Figures 1-6F and G). There was no significant difference in the percentage of following with successful courtship before spawning (Figure 1-6F) and the number of clasping ceased by female before spawning (Figure 1-6G). These results suggest that the d-rR male is more motivated and tends to get more chances of mating compared to the Kiyosu male, and therefore d-rR pairs spawn more readily than Kiyosu, as shown in Figure 1-6C.

Discussion

In the present study, I established an open-source automated behavioral recording system by using Raspberry Pi. I also used Raspberry Pi for automation of simple experimental treatments such as feeding and illumination by operating external devices through GPIO interfacing. This system drastically reduced experimental operation and enabled us to carry out the efficient and reproducible behavioral recording, which may result in improved quality of behavioral analysis. In addition, I developed the behavioral annotation tool, *Ethogramer*, by using Microsoft Excel macro. It became possible to easily annotate the behavioral events and automatically generate the raster plots, and thus the behavioral analysis became more efficient and informative than the conventional one. I could successfully apply this system to the comparative analysis of the sexual behavior of medaka between laboratory and wild strains and found that the laboratory strain spawn more readily than the wild strain, which is probably caused by the increase in the sexual motivation in males of the laboratory strain.

Establishment of efficient and sophisticated tools for behavioral analysis

Since the animals respond to many cues from external environments and change their behavior accordingly, it is essential to minimize human errors caused by experimental operations. Behavioral recording system established in the present study succeeded in automating the greater parts of behavioral experiments including video-recording and in minimizing human errors. Also, the shell script *Record.sh* were programmed to perform not only video-recording but also file-naming, encoding and transferring to the storage, which freed us from such laborious procedures, and the behavioral recordings could be performed more efficiently. In fact, the time spent for video-recording and file-sorting of 16 pairs of medaka was drastically shortened compared to the

conventional method. In addition, RP-units is very small and its smallness also enables us to perform behavioral experiment with less space.

Furthermore, external devices could be controlled by GPIO interfacing with Raspberry Pi, which make it possible to automate various experimental protocols. For the future application, I examined practical ability of the GPIO interfacing. First, I examined the control of external devices via a custom-made relay unit connected to GPIO pins on Raspberry Pi (Figure 1-7). My system enabled switching on/off the auto-feeding device and green LED lamp as described in Materials and Methods section (Data not shown). Next, to check the time resolution of the relay-switching, I generated the rectangular voltages by changing the timing of switching on the power to the circuit connected to 9 V alkaline battery to switch on/off the relay for various durations (5/10/25/50 milliseconds) and examined the waveform of the rectangular voltages. The rectangular waves with amplitudes of 9 V at 10/20/50/100 Hz were faithfully observed (Figure 1-8). In the present study, I used the relay with 5.0 milliseconds recovery time, so that the result indicated that this relay unit worked as I programmed, without impairing functionality of the relay. Thus, the external devices could be regulated with high time resolution via GPIO interfacing. The system that switches on/off the auto-feeding device and LED lamp can be applied to the learning experiment in which the LED light serves as the signal for feeding synchronized to the timing of switching on the auto-feeding device. While these learning experiments require repetitive conditioning trials, it is possible to automatically execute such trials anytime we want by using "cron", which is one of the daemons of Raspberry Pi and can be scheduled to run the shell scripts. This option drastically reduce human-tasks in repetitive experiments such as daily observation and repetitive learning. Furthermore, it is also possible to output pseudo-analog signals by using pulse width modulation (PWM) method, which enables us to perform the operations in a manner other than all-or-none. On the other hand, GPIO pins can not only perform signal output but also

signal input. Since the most of biological signaling are analog, it is necessary to convert analog to digital signals, which can be accomplished by connecting an analog-to-digital (A/D) converter to GPIO pins on Raspberry Pi. Thus, by customizing Raspberry Pi, it will be possible to develop various experimental systems. In addition, Raspberry Pi can be remotely operated via WLAN, so that it is possible to perform efficient and reproducible analyses by applying the system proposed in the present study. I also create a shell script "*Setup.sh*" for easy setup and cloning RP-units, so that it became easier to start behavioral recording by using RP-units. All the source codes for operating Raspberry Pi are publicly available on GitHub at https://github.com/Neuroendo-mdLab/RP-units.

One of the most important parts of the behavioral analyses is the quantification of the behavior. For this step, there are some full-automated behavioral analysis systems applied for the model animals in which their behavior has been frequently studied, such as rodents [48-52] or fruit flies [53-57]. Although these systems are useful, these can be applied exclusively for certain behavioral repertoires of specific species and are thus less flexible. On the other hand, we are often faced with experimental needs for analyzing unique/rare behaviors or for using non-model animals. In such cases, we are forced to perform painstaking behavioral annotation that require pausing the video and record the timing and duration manually every time the behaviors occur. However, by using the macro developed in the present study, *Ethogramer*, it is possible to perform behavioral annotation by only pressing the PC keys. It frees us from laborious analyses described above, and the behavioral quantification will be performed much easier. In addition, *Ethogramer* enables us to simultaneously analyze multiple and/or continuous behavioral repertoires, so that such multi-directional perspective makes behavioral analysis more informative. Thus, *Ethogramer* will be especially useful in such situations where the above-mentioned full-automated systems cannot be applied. Moreover, since *Ethogramer* automatically generates raster plots showing the behavioral

time course, we can also visually understand the temporal transition of the behavior. Therefore, by using *Ethogramer*, it will be possible to quantify and analyze the behaviors that are difficult to analyze by using conventional analysis methods.

Recently, automated behavioral annotation systems have been established by using machine learning method. For example, *JAABA* is a behavioral annotation tool using a supervised learning method, which can annotate any behaviors that the observer want to analyze [58]. Also, *DeepLabCut* is a sophisticated animal tracking system, which enables us to track the trajectory of animal movement regardless of the animal species [59]. These are very useful tools when the supervised learning is successfully performed. However, these systems require a certain level of knowledge or skills of computing to utilize. In addition, these kinds of machine learning tools often require consistent background and high contrast images for precise tracking. For this reason, it is difficult to apply them to the videos taken in the natural environment, in which many movements other than the objective animal are contaminated. Furthermore, supervised learning systems often require highly repetitive training to perform the appropriate annotation of the behavior that can distinguish subtle differences of animal movement, and the researchers must verify whether the behavioral annotation has been correctly performed by manually checking the video and annotated data. On the other hand, the macro in the present study supports behavioral annotation by human, and it can be applied in any condition as long as human can judge the behaviors. An instruction for *Ethogramer* is described in Supplementary Note 1-1.

Difference of sexual motivation between wild and laboratory strains of medaka perhaps resulting from domestication

By using the combination of Raspberry Pi and Excel macro in the present study, I analyzed sexual behavior of two strains of medaka. While there is an anecdotal report that laboratory strain

spawns more readily than the wild strain, the latency to spawning was significantly shorter in d-rR compared to Kiyosu (Figure 1-6C). The latency to first following was shorter almost significantly (Figure 1-6B) and the frequency of courtship before spawning were significantly higher in d-rR (Figure 1-6E). I analyzed two indices that reflect male motivation of sexual behavior; the percentage of the time spent for following before spawning and the frequency of courtship before spawning, and it was found a significant increase in the frequency of courtship before spawning for d-rR as compared with Kiyosu (Figure 1-6D). These data suggest that the d-rR male is more motivated for mating and court more frequently to female compared to Kiyosu male. Medaka is a commonly used teleost fish in various fields of biology, and d-rR is one of the most frequently used laboratory strains of medaka. d-rR has been maintained for decades, and it is well-known among the researchers of medaka that egg collection from d-rR is much easier than that from wild medaka. However, it has been unclear whether d-rR actually spawn more readily than the wild medaka and what underlies this phenomenon. In the present study, the analysis by using the present systems revealed that d-rR male is more motivated for mating compared to the male of wild strain Kiyosu, which are suggested to have afforded more scientifically verifiable hypothesis to the anecdotal reports of the difference in the sexual behavior between laboratory strain and wild individuals. It may be caused by the evolutionary pressure, which is an unconscious selection by researchers for easiness of egg collection. While I did not detect significant difference in the indices that reflect female receptivity in contrast with the indices that reflect male motivation of sexual behavior (Figures 1-6F and G), it cannot be sure that there is no difference in female receptivity by only analyzing these two indices in the present study, which were susceptible to male behavior that is different between two strains. To verify this, it is required to analyze these two indices by using F1 hybrid male as mating partner for mitigating the influence of genomic background of mating partner. Since I have been maintaining d-rR and

Kiyosu in the completely same breeding method (described in the “Materials and Methods” section), the phenomenon found in the present study is unlikely to be caused by epigenetic factors, but rather by genetic factors, and it can be called “domestication.” It is well known that domestication can affect various animal behaviors [60-64] including fishes [65, 66]. However, to our knowledge, the effect of laboratory domestication on the sexual behavior in fishes have not been clarified yet. Thus, the present study is the first report to suggest a possible effect of domestication on the sexual motivation in a teleost, medaka and there is no doubt that the behavioral recording/analysis system established here has made a substantial contribution to this finding. It can be an important future topic to quantify sexual motivation of multiple laboratory and wild strains to determine whether differences observed in this study is due to domestication effects or not.

In summary, I established automated behavioral recording systems and behavioral annotation tool by using Raspberry Pi and Microsoft Excel macro, respectively. Using the combination of these two, behavioral analysis will be performed more efficiently, which will bring us more informative results and contribute to the progress of various fields of biology.

Figure legends

Figure 1-1

Hardware setup. (A) Photograph of RP-unit with their cases open. Raspberry Pi Camera V2 is connected to Raspberry Pi Zero W through the flat flexible cable. Scale bar indicates 1 cm. (B) Connection diagram of automated behavioral recording system. 16 RP-units are wirelessly connected to WLAN, while NAS is connected to WLAN router through Ethernet cable. I accessed and operated RP-units through SSH remote login by using a Windows PC, which is represented as "Main PC for analysis" on this figure. (C) Schematic diagram of another RP-unit for automated switching of LED lamp, auto-feeding device, and the electric circuit including 9 V alkaline battery. These external devices are connected a custom-made relay unit that is connected to GPIO pins on Raspberry Pi 3B. Raspberry Pi Camera V2 is also connected to Raspberry Pi 3B for video-recording. This unit can be replaced to each RP-unit drawn in B. (D) Block diagram of the system for operating external devices. The electric current is passed through the relay, accompanied with driving the transistor by the current from GPIO pins (GPIO.Voltage / GPIO.Feeding). At this time, the relay makes a connection with a fixed contact, and the current flows to the entire the circuit. Since current supplied from GPIO is not enough to run the relay, this circuit containing transistor applies current from PW in response to GPIO current flow. GPIO.Voltage, GPIO.LED, GPIO.Feeding indicate the pins that connected to the GPIO pins on Raspberry Pi 3B for operating the electric circuit including the battery, LED lamps and auto-feeding device, respectively. To absorb coil surge to the transistor, diodes are connected between the relay and the transistor.

Figure 1-2

Flowchart of *Record.sh*. Running *Record.sh*, Python script *Camera.py* is run. It executes video-

recording, file-naming and GPIO interfacing with the setting in itself. After running *Camera.py*, recorded file in each RP-unit is encoded to mp4 format and transferred to the NAS storage. In this step, the letters "converted.mp4" is added to the end of the file-name for distinguishing files that are completed to be encoded.

Figure 1-3

Conceptual diagram of *Ethogramer*. (A) Diagram that represents some indices for setting that filled in worksheet- "*Sheet1*" are reflected to each function for behavioral annotation. Data in columns- "Repertoire name" and "Continuous/Intermittent" in worksheet- "*Sheet1*" configure the setting of columns for annotations of the timing of the behavior in worksheet- "*Sheet2*…". Key assigning is performed by filling in the letters in column- "Key". Available keys are shown in Supplementary Note 1-1. Color information of the cells in column- "Color" are reflected in drawing raster plots. Filled in Data in cell- "Time (s)" is defined the length of raster plots. After setting these indices, it enabled to perform behavioral annotation by pressing assigned keys. (B) Image representing the example of the text-based data exported in EPS format (left, "Text data") and the graphical image actually outputted when opened by vector graphics editor (right, "Graphical output"). Time information of each behavioral event obtained by pressing keys (for example: a behavioral event is observed from t to t + Δt) are substituted like in the left box, and these text-based data define the coordinates for drawing a square in a raster plot like in the right box.

Figure 1-4

Experimental design for sexual behavior analysis. (A) Photograph of the whole experimental equipment for recording the sexual behavior of medaka. Wooden frame that was attached

transparent acrylic plate was placed onto the 100 × 45 cm stainless rack. Twelve tanks, which were covered their upper side by thin white paper, were put on the acrylic plate, and RP-units were placed inside the wooden frame. (B) Photograph of a part of experimental equipment taken from diagonally above. When performing experiments, thin white papers were put onto each tank, like the left tank of this figure. RP-units were placed directly below each tank. (C) Schematic illustrating of the experimental equipment. Since both the bottom of the tank and acrylic plate were transparent, it is possible for RP-units to record the videos from ventral side of the medaka. (D) Schematic diagram of the sexual behavior sequence of medaka. Images of each four behavioral repertoires were captured from the video data of one pair of d-rR. Colored frames and words in parentheses are corresponding with the setting of the *Ethogramer*.

Figure 1-5

Conceptual diagram of the experimental procedures and their estimated time required for the behavioral analysis with or without the systems. By using the combination of the two systems established in this study, video-recording and their organization were completely automated, and behavioral annotation was drastically shortened and became easier compared to conventional manual behavioral annotation. Without the systems, the observer is forced to manually switch on 16 video cameras. Also, it is necessary to manually perform file-naming/encoding/transferring to strage, which takes approximately 30 minutes. Furthermore, the behavioral annotation without the *Ethogramer* took 40 minutes per video. Accordingly, it is expected that behavioral annotation for 16 pairs takes approximately more than ten hours. On the other hand, with the systems, video-recording of 16 pairs of medaka was automatically/simultaneously performed by running *Record.sh* via SSH remote login. Immediately after recording, file-naming, encoding, and transferring to storage were automatically performed, and it took approximately 30 minutes. Since

the behavioral annotation was performed while replaying the first 30 minutes of each video at double speed by using *Ethogramer*, the time spent for the behavioral annotation of 16 pairs of medaka was only 4 hours.

Figure 1-6

d-rR pairs spawn earlier than Kiyosu pairs, probably because d-rR male is more motivative to mating than Kiyosu male. (A) Time-course data of 30-minute analyses of sexual behavior are shown as raster plots. Yellow, black, cyan and red bands represent the timing and duration of following, courtship, clasping and spawning, respectively. Red triangles are put on the right of each red bands for easy detection of them. (B, C) The latency data were further analyzed using Kaplan-Meier plots. Yellow and blue curves represent Kiyosu and d-rR, respectively. d-rR pairs showed first following and spawning earlier than Kiyosu pairs (Latency to first following: Kiyosu; 2.763 ± 0.602, d-rR; 0.963 ± 0.540, $P = 0.070$ (B), Latency to first following: Kiyosu; 8.779 ± 1.492, d-rR; 3.979 ± 0.556, $^{**}P = 0.009$ (C)). (D-G) Various parameters were measured and compared between Kiyosu and d-rR. Yellow and blue dots represent Kiyosu and d-rR, respectively. The frequency of courtship before spawning was significantly higher in d-rR than Kiyosu (Kiyosu; 0.435 ± 0.085, d-rR; 0.874 ± 0.128, $^{*}P = 0.0148$ (E)), while no significant difference was detected in the percentage of the time spent for following before spawning (Kiyosu; 18.674 ± 3.80, d-rR; 31.581 ± 7.18, $P = 0.235$ (D)), the percentage of following with successful courtship before spawning (Kiyosu; 39.221 ± 8.647, d-rR; 24.474 ± 4.376, $P = 0.195$ (F)), or the number of clasping ceased by female before spawning (Kiyosu; 0.875 ± 0.398, d-rR; 0.750 ± 0.313, $P = 0.957$ (G)).

Figure 1-7

Experimental design for operating external devices by GPIO interfacing. (A) Photograph of the experimental systems for operating external devices. External devices, LED lamp and auto-feeding device were connected to the relay unit via red-and-black leads and switched on/off via GPIO pins and the relay unit. (B) Schematic illustrating of the system of (A). This figure is represented in two dimensions, the width information is omitted. Also, red-and-black leads that connect external devices and the relay unit are omitted for not being complicated. (C) Schematic diagram of the system for testing the performance of relay unit. The rectangular voltages that have various wavelengths were generated by changing the duration of turning on the electricity, and the performance of relay unit was validated. Voltmeter and resistor were connected in parallel in order to decline the current flowed to the voltmeter.

Figure 1-8

Representative waveforms of voltage generated from the circuit that include the battery and was operated via GPIO pins and custom-made relay unit. Left numbers (10/20/50/100 Hz) represent the wavelengths that were set in the Python script, *Camera.py*. Each waveform was reflected the settings for generating the rectangular waves that have specific wavelength.

Figure 1-1

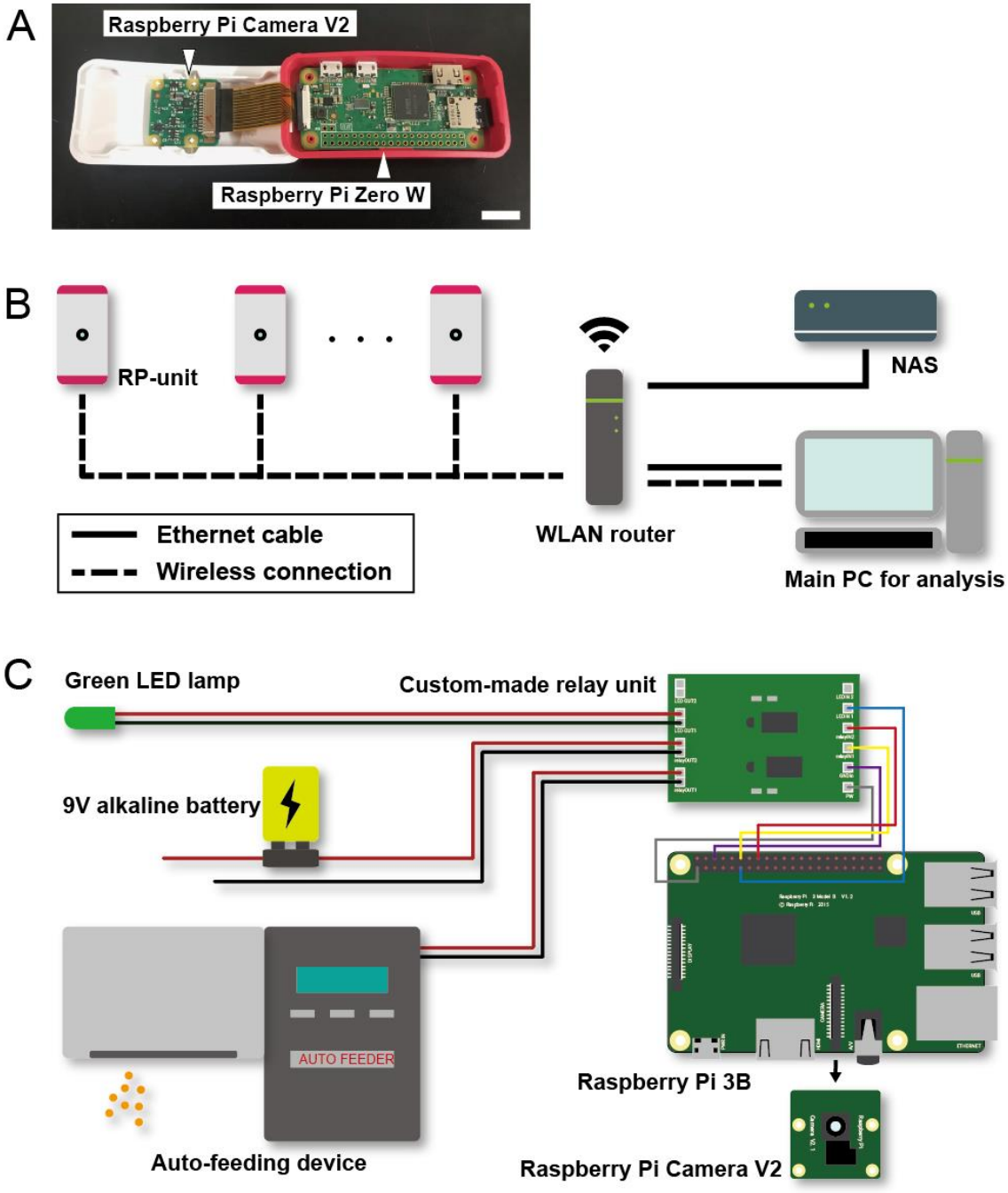
A
Raspberry Pi Camera V2
Raspberry Pi Zero W
B
RP-unit
NAS
WLAN router
Main PC for analysis
Ethernet cable
Wireless connection
C
Green LED lamp
Custom-made relay unit
9V alkaline battery
AUTO FEEDER
Raspberry Pi 3B
Auto-feeding device
Raspberry Pi Camera V2

Figure 1-1

D

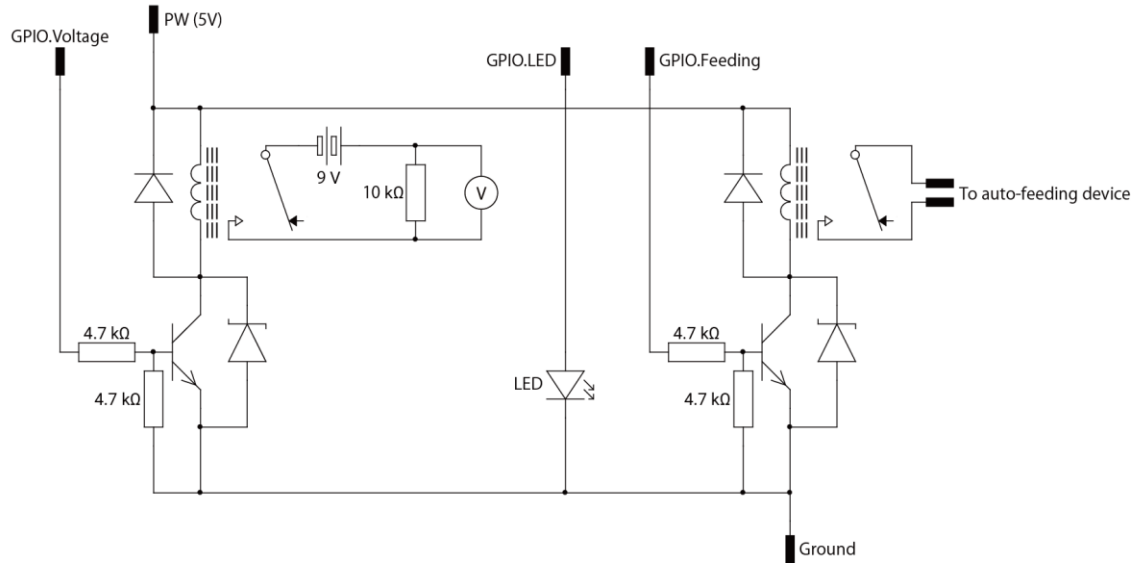
GPIO.Voltage
PW (5V)
GPIO.LED
GPIO.Feeding
9 V
10 kΩ
V
To auto-feeding device
4.7 kΩ
4.7 kΩ
LED
4.7 kΩ
4.7 kΩ
Ground

Figure 1-2

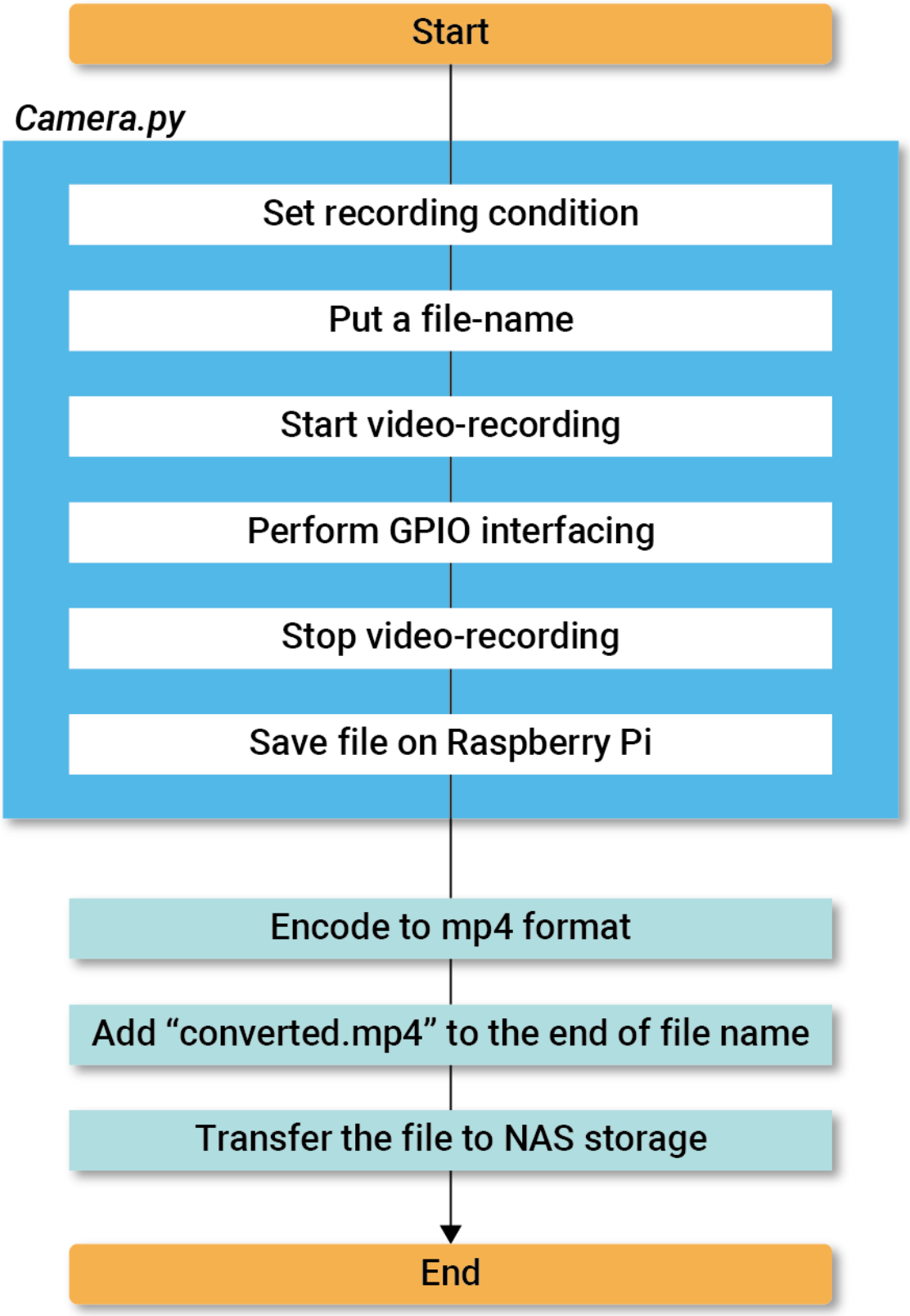
Start
Camera.py
Set recording condition
Put a file-name
Start video-recording
Perform GPIO interfacing
Stop video-recording
Save file on Raspberry Pi
Encode to mp4 format
Add “converted.mp4” to the end of file name
Transfer the file to NAS storage
End

Figure 1-3

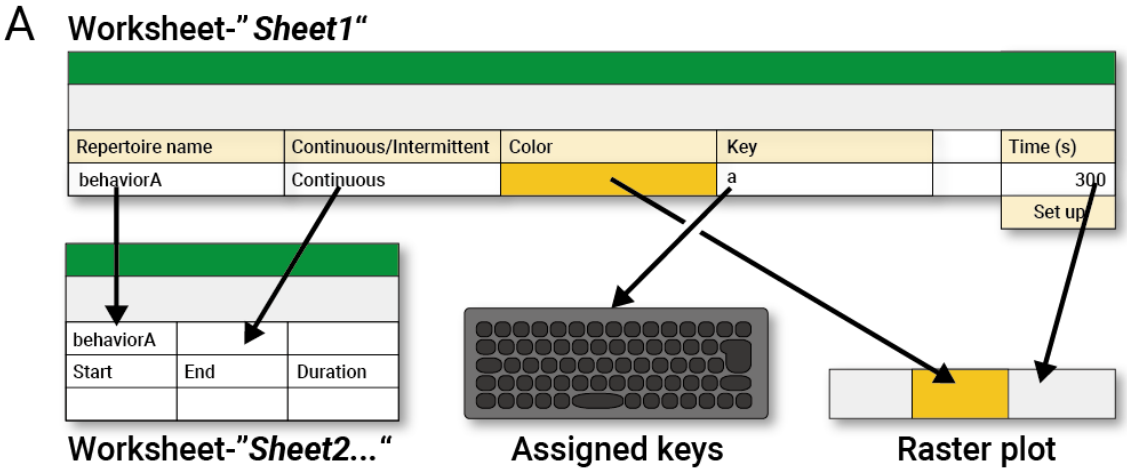
A
Worksheet-"Sheet1"
Repertoire name
Continuous/Intermittent
Color
Key
Time (s)
behaviorA
Continuous
a
300
Set up
behaviorA
Start
End
Duration
Worksheet-"Sheet2..."
Assigned keys
Raster plot

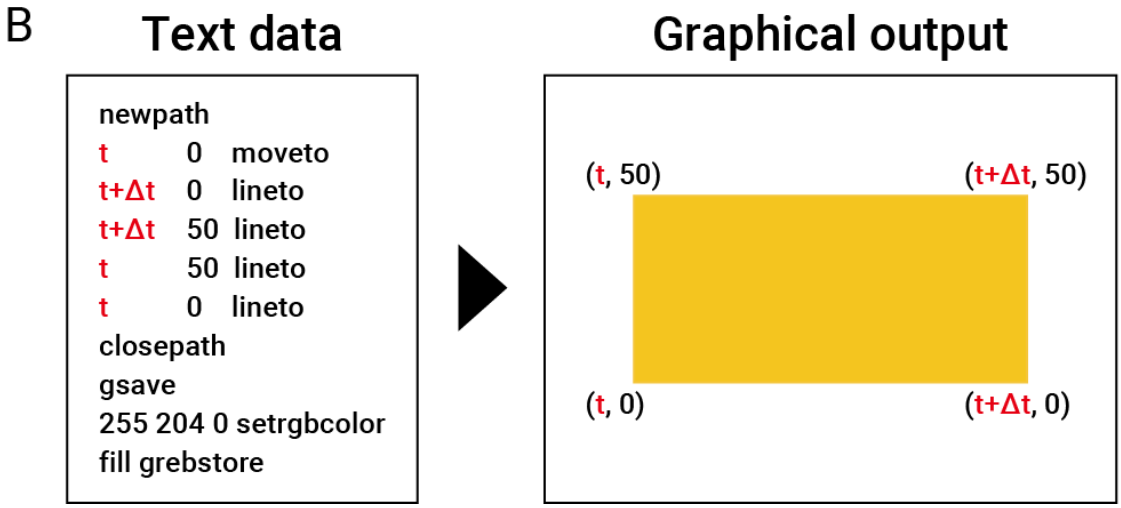
B
Text data
Graphical output
newpath
t 0 moveto
t+Δt 0 lineto
t+Δt 50 lineto
t 50 lineto
t 0 lineto
closepath
gsave
255 204 0 setrgbcolor
fill grebstore
(t, 50)
(t+Δt, 50)
(t, 0)
(t+Δt, 0)

Figure 1-4

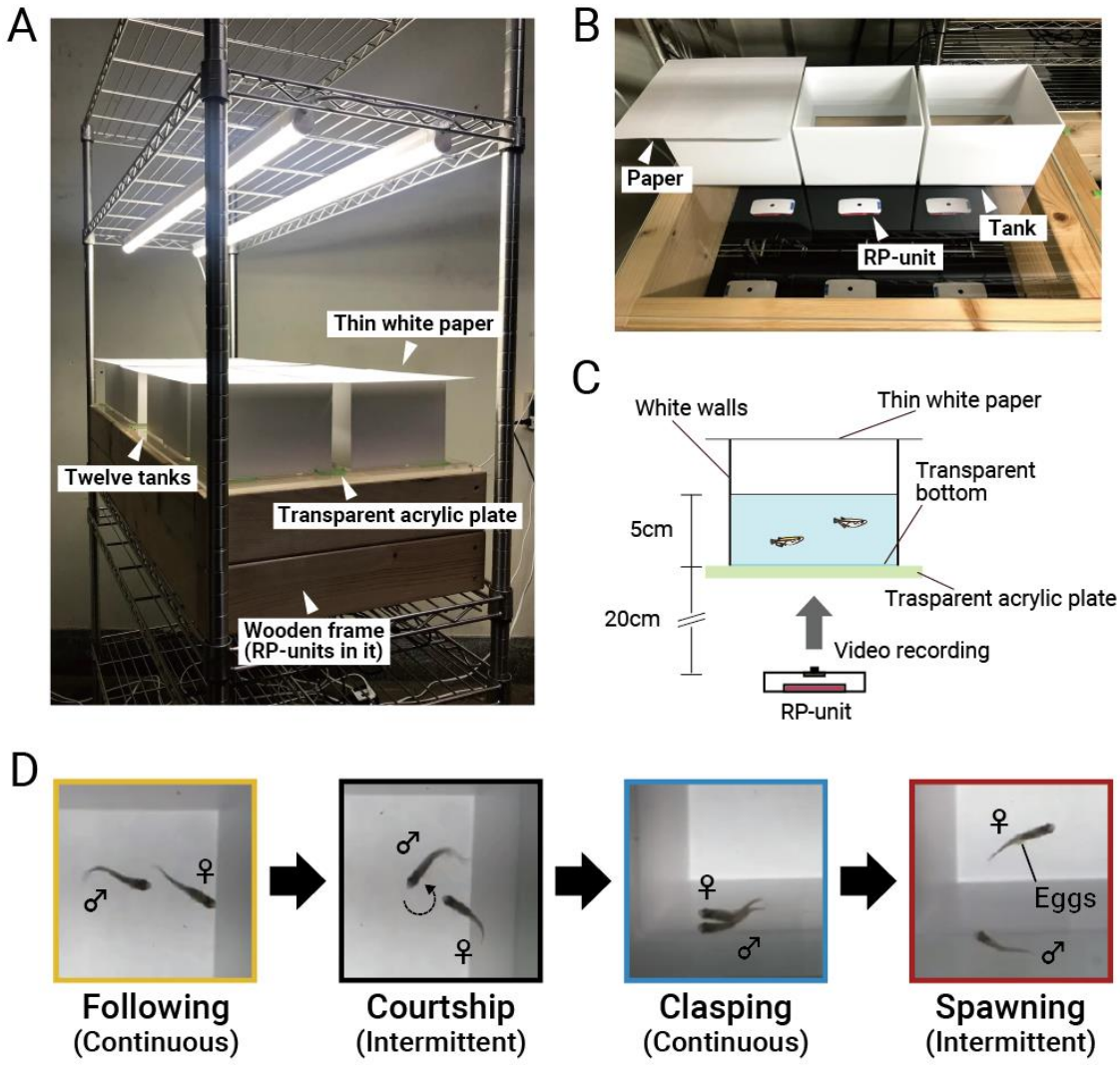
A
Thin white paper
Twelve tanks
Transparent acrylic plate
Wooden frame
(RP-units in it)
B
Paper
Tank
RP-unit
C
White walls
Thin white paper
Transparent
bottom
5cm
20cm
Trasparent acrylic plate
Video recording
RP-unit
D
Following
(Continuous)
Courtship
(Intermittent)
Clasping
(Continuous)
Spawning
(Intermittent)
Eggs

Figure 1-5

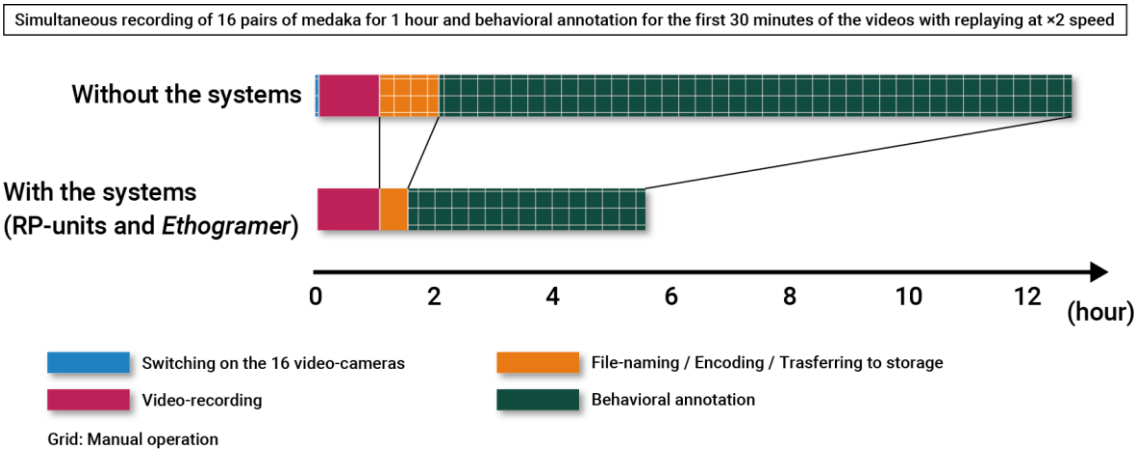
Simultaneous recording of 16 pairs of medaka for 1 hour and behavioral annotation for the first 30 minutes of the videos with replaying at ×2 speed
Without the systems
With the systems
(RP-units and *Ethogramer*)
0
2
4
6
8
10
12
(hour)
Switching on the 16 video-cameras
File-naming / Encoding / Trasferring to storage
Video-recording
Behavioral annotation
Grid: Manual operation

Figure 1-6

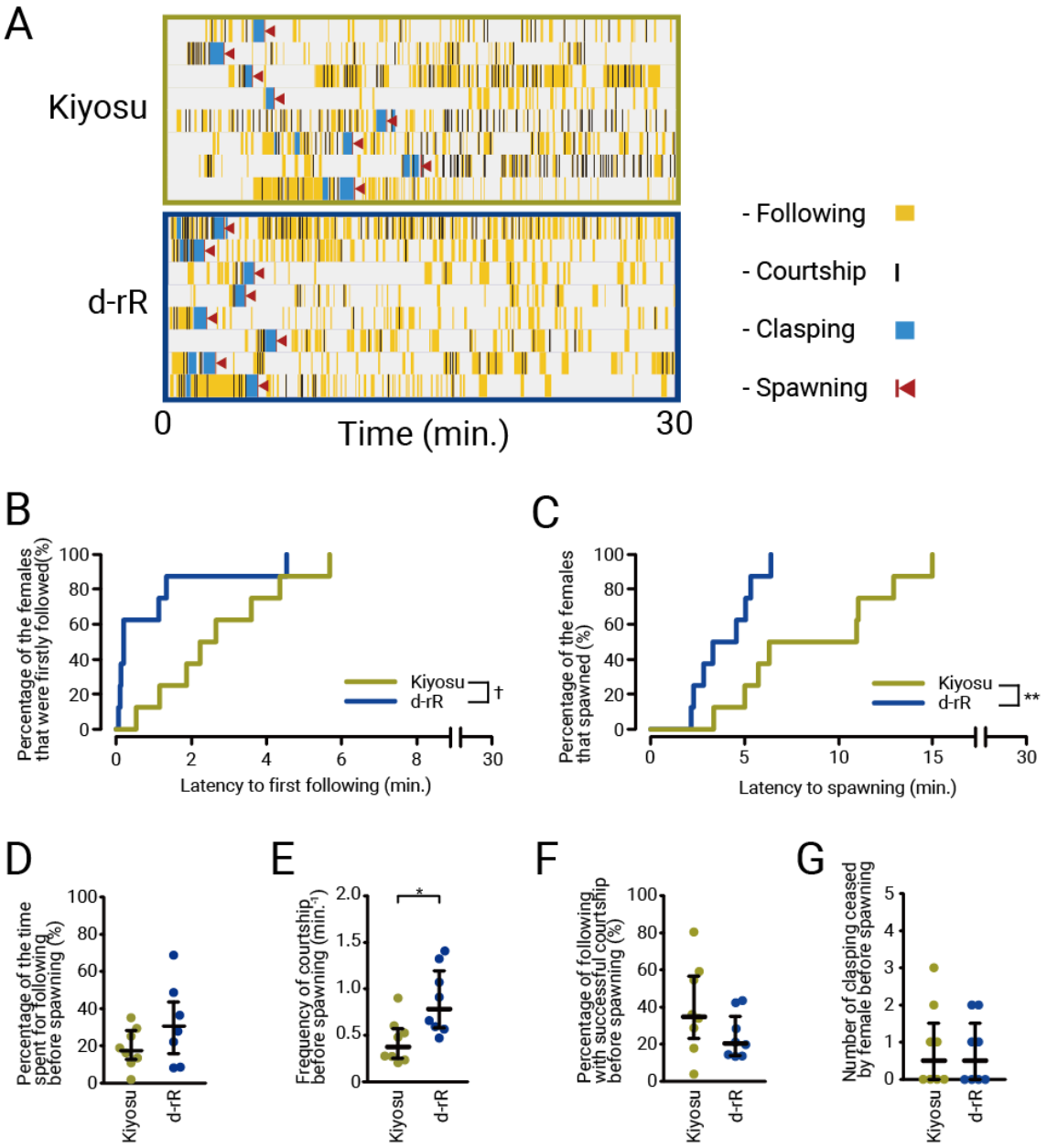
A
Kiyosu
d-rR
0
Time (min.)
30
- Following
- Courtship
- Clasping
- Spawning
B
Percentage of the females that were firstly followed(%)
Latency to first following (min.)
Kiyosu
d-rR
†
C
Percentage of the females that spawned (%)
Latency to spawning (min.)
Kiyosu
d-rR
**
D
Percentage of the time spent for following before spawning (%)
Kiyosu
d-rR
E
Frequency of courtship before spawning (min-1)
*
Kiyosu
d-rR
F
Percentage of following with successful courtship before spawning (%)
Kiyosu
d-rR
G
Number of clasping ceased by female before spawning
Kiyosu
d-rR

Figure 1-7

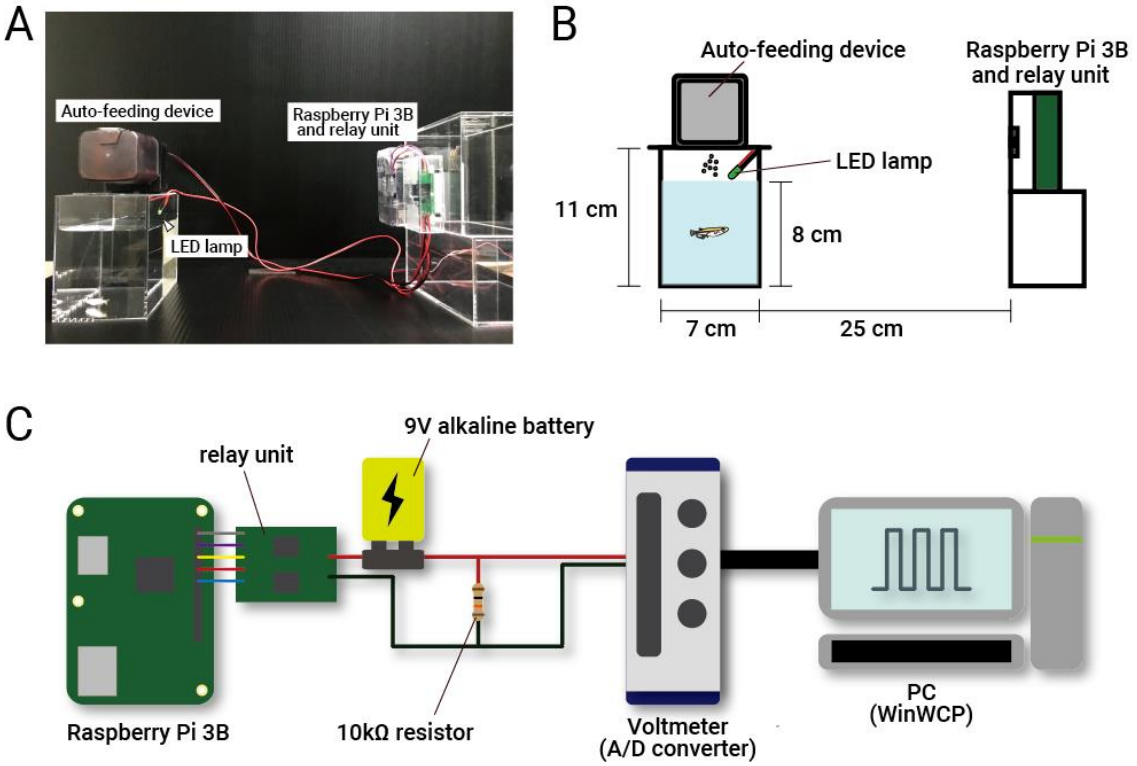
A
Auto-feeding device
Raspberry Pi 3B
and relay unit
LED lamp
B
Auto-feeding device
Raspberry Pi 3B
and relay unit
LED lamp
11 cm
8 cm
7 cm
25 cm
C
9V alkaline battery
relay unit
Raspberry Pi 3B
10kΩ resistor
Voltmeter
(A/D converter)
PC
(WinWCP)

Figure 1-8

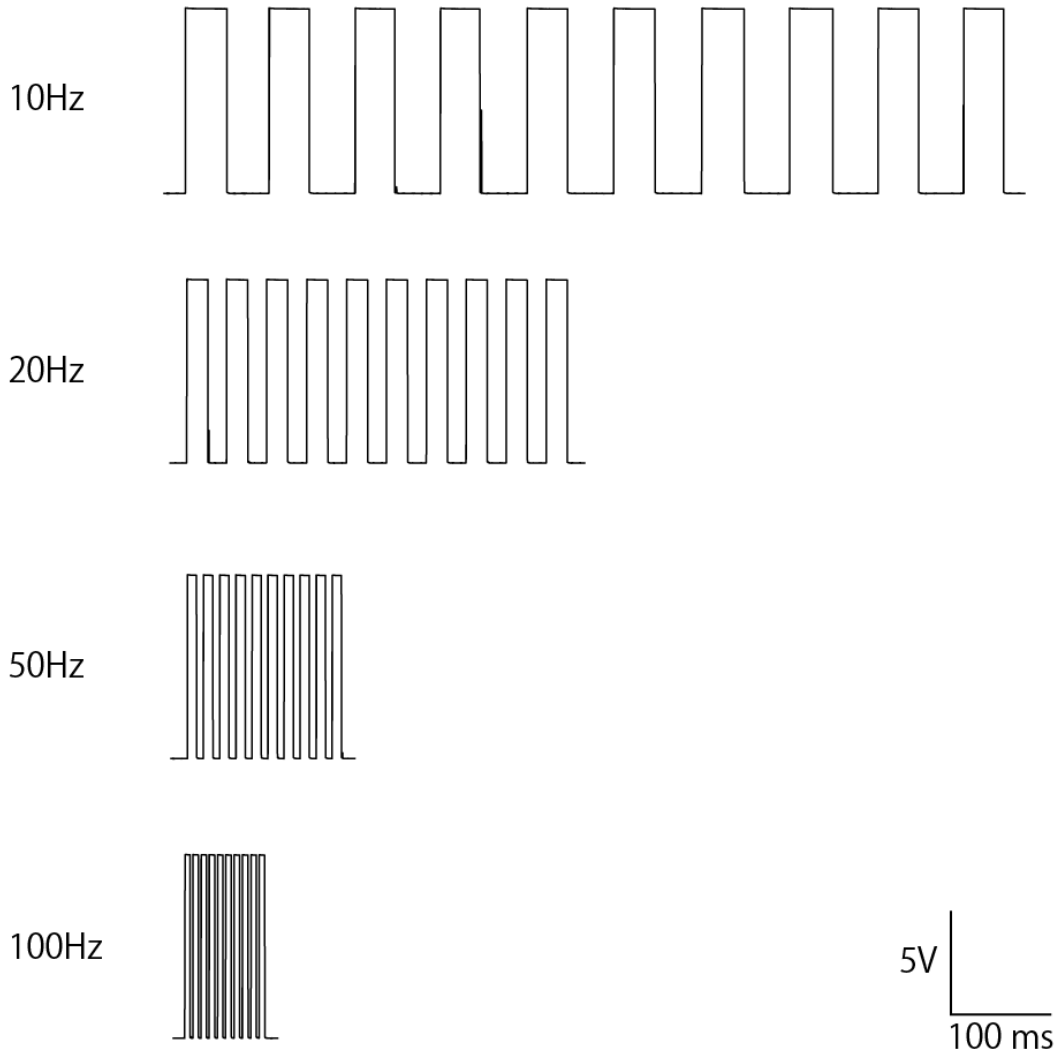

Supplementary Note 1-1

How to use *Ethogramer*

Before using

- This macro runs on Microsoft Excel.

- Install the Microsoft (MS) Excel. We had confirmed that this macro runs on version.2010 or later.

- Enable macros in Excel.

- The raster plots are output in the Encapsulated PostScript (EPS) format. Prepare the software that support to open EPS files (e.g. Adobe Illustrator, Affinity Designer).

How to use

1. Fill in the name of behavioral repertoires that indicate what you want to analyze in the Column A (Repertoires name).

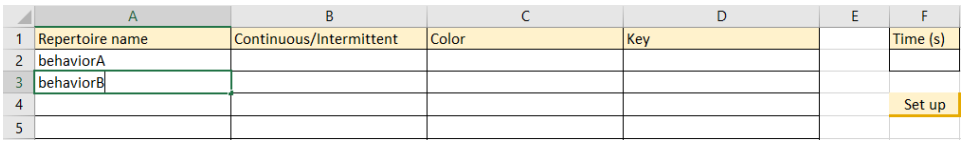

2. Select either “Continuous” or “Intermittent” according to the repertoires in the pull-down menu in the Column B (Continuous/Intermittent). If the behavior lasts for a certain time, select “Continuous.” In contrast, select “Intermittent” in case the behavioral repertoire is recorded as instantaneous event. If you choose “Continuous,” macro records the time during you are pressing a key.

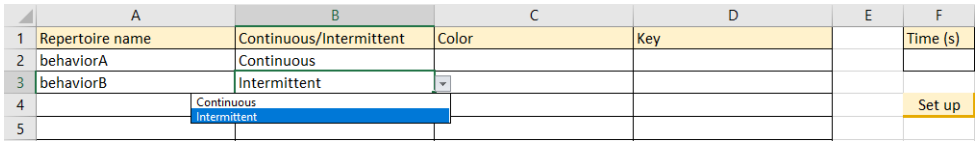

3. Assign color for drawing raster plots by changing the color of cell in the Column C (Color). The theme color of raster plots is set to gray (#E6E6E6) by default and we do not recommend to select colors close to gray.

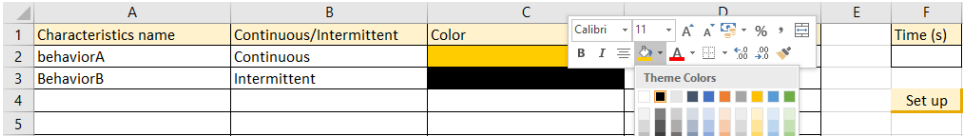

4. Register the keyboard's key to each behavioral repertoire in the Column D (Key). You can use 26 alphabet keys (A-Z), 10 numeric keys (0~9) and 4 cross-key (left/right/up/down). See the Table 1-1 (at the end of Supplementary Note 1-1) for how to assign keys.

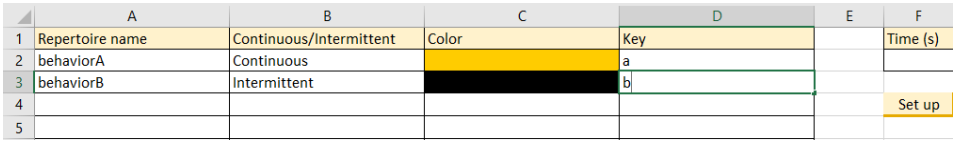

	A	B	C	D	E	F
1	Repertoire name	Continuous/Intermittent	Color	Key		Time (s)
2	behaviorA	Continuous		a		
3	behaviorB	Intermittent		b		
4						Set up
5						

5. Fill in the time for analysis. This information is used for setting of the length of raster plots.

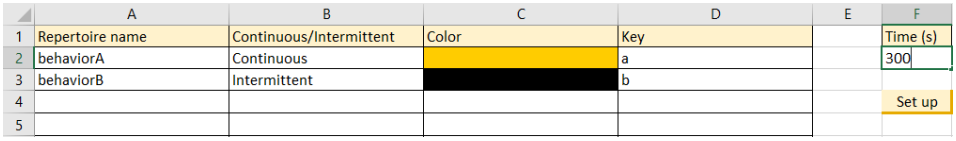

	A	B	C	D	E	F
1	Repertoire name	Continuous/Intermittent	Color	Key		Time (s)
2	behaviorA	Continuous		a		300
3	behaviorB	Intermittent		b		
4						Set up
5						

6. Double-click the "Set up" cell. Another worksheet and a pop-up ("*Analyze*") window for analysis will appear.

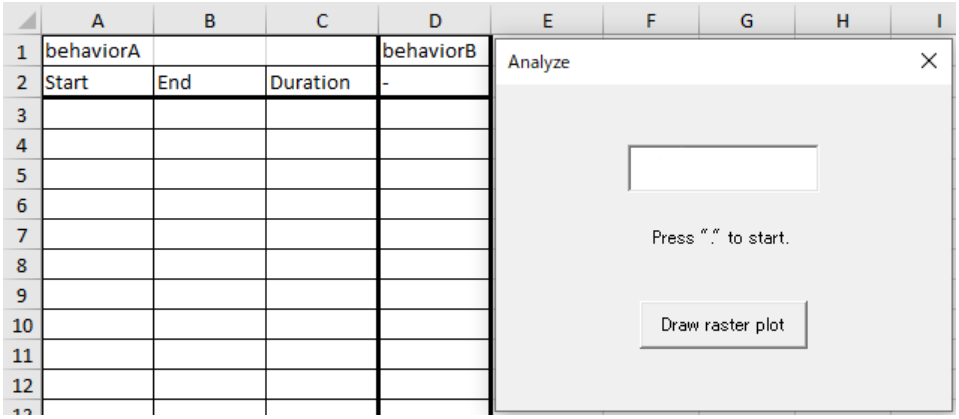

7. Start analysis by pressing period (“.”)-key. Watch the movies and press the registered keys when each behavioral repertoire is shown. When the continuous behavior is observed, keep pressing the key while observing.

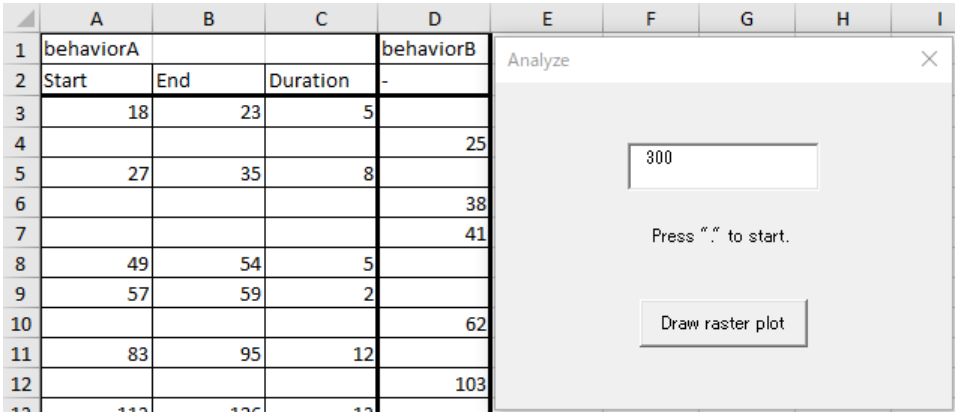

	A	B	C	D
1	behaviorA			behaviorB
2	Start	End	Duration	-
3	18	23	5	
4				25
5	27	35	8	
6				38
7				41
8	49	54	5	
9	57	59	2	
10				62
11	83	95	12	
12				103

8. Click the “Draw raster plot” button in the *Analyze* window. Another pop-up window (”*Draw_rasterplots*”) for generating raster plots appears. Then, click the “Save” button to generate raster plot data in the large box below and dialog box for file-saving appears. Note that these generated texts are the content of raster plot EPS file.

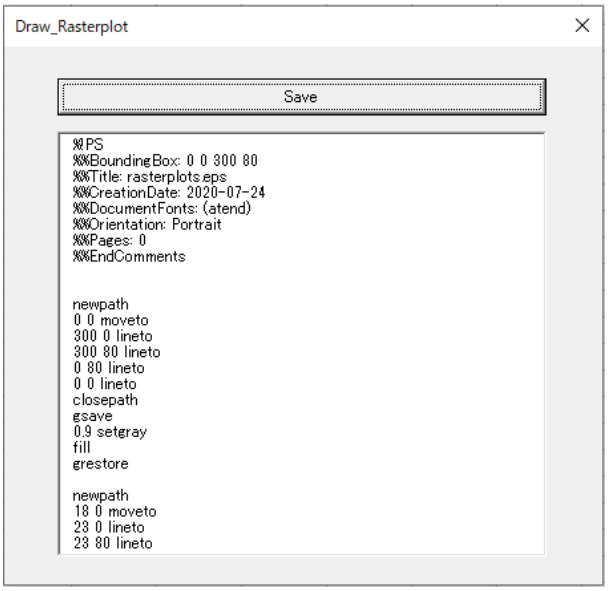

9. Open the EPS file with a vector graphics software and edit.

Alphabet keys		Numeric keys		Cross keys	
Assigned key	Filled in letter	Assigned key	Filled in letter	Assigned key	Filled in letter
A key	a	0 key	N0	← key	LEFT
B key	b	1 key	N1	↑ key	UP
C key	c	2 key	N2	→ key	RIGHT
D key	d	3 key	N3	↓ key	DOWN
E key	e	4 key	N4		
F key	f	5 key	N5		
G key	g	6 key	N6		
H key	h	7 key	N7		
I key	i	8 key	N8		
J key	j	9 key	N9		
K key	k				
L key	l				
M key	m				
N key	n				
O key	o				
P key	p				
Q key	q				
R key	r				
S key	s				
T key	t				
U key	u				
V key	v				
W key	w				
X key	x				
Y key	y				
Z key	z				

Table 1-1 Key assignment

Chapter 2

Detailed behavioral analysis revealed that estrogen/*esr2b* signaling plays a crucial role in the activation of female receptivity

Abstract

Sexual behavior is evoked in accordance with the gonadal maturation, although little is known about the neuroendocrine mechanisms that mediate such regulation in teleosts. In the present study, I used medaka to examine possible involvement of a sex steroid hormone, estrogen, which is secreted from mature ovaries, in the regulation of female sexual behavior. Pharmacological inhibition of estrogen synthesis suppressed the receptive behavior of the male by female (defined as female's acceptance of male courtship and clasping), which culminated in the failure of spawning behavior. Next, ovariectomized females, which are deprived of all the gonadal substances, failed to show receptive behavior, Furthermore, estrogen administration to the ovariectomized females partially reinstated the receptive behavior. These results suggest that estrogen has an important and essential role in the activation of acceptance behavior, which is supposed to reflect the female receptivity. Next, I examined the contribution of estrogen receptors for the behavioral activation by analyzing the phenotypes of female medaka in which estrogen receptor 2b (*esr2b*) gene was knocked out (KO) and found that *esr2b* KO females failed to show receptive behavior, although males also tried to court *esr2b* KO female. Interestingly. *esr2b* KO females showed normal gonadal functions and secondary sex characteristics, suggesting that *esr2b* KO females synthesize estrogen normally. Because it has been previously shown that *esr2b* is expressed by certain populations of neurons in the brain, it is reasonable that *esr2b*-expressing neurons play a crucial role in the activation of female receptivity in accordance with signals from the gonadal estrogen.

Introduction

Sexual behavior is specifically observed in the animals with mature gonad. For example, the breeding season is considered to represent the phenomena that reflects such synchrony. During the breeding season, females and males perform gametogenesis together with expression of the external morphology such as secondary sex characteristics or nuptial coloration, and not a few animals are known to release pheromones to attract the conspecific heterosexual mates. In addition to these physiological changes, species-specific sexual behaviors are displayed during this season.

For the appropriate synchronization of physiological conditions of the animals with sexual behaviors, it has been suggested that the sex steroid hormones, especially estrogen are involved in signaling gonadal status to the brain, which tunes the regulation of gonadal function and the activation of sexual behavior [67-69]. The central mechanisms of reproductive control have been called as the hypothalamic-pituitary-gonadal (HPG) axis in vertebrates, and estrogen is considered to play crucial roles in the neuroendocrine regulatory systems for gonadal maturation, by directly and indirectly modifying gonadotropin release from the pituitary [9-11, 13-17, 70]. In mammals, accumulating experimental results have shown that the hypothalamic kisspeptin neurons play the most essential roles in the HPG axis, by regulating the neural activities of gonadotropin-releasing hormone (GnRH) neurons via the kisspeptin receptors, Gpr54, in an estrogen dependent manner [3-8]. Also in non-mammalian vertebrates including teleosts, it has been suggested that estrogen is involved in the regulation of gonadotropin release from the pituitary, although the neural mechanisms appeared to be quite different from that of mammals [16, 17, 71]. As described above, it has been strongly suggested that estrogen play pivotal roles in the regulation of gonadal functions at the cellular/neural circuit levels. Also, numerous studies

have reported the effects of estrogen in the activation of sexual behavior in mammalian studies. For example, estrogen plays important roles in the activation of proceptive/solicitatory behavior and lordosis behavior via estrogen-receptive neurons in the brain in rodents [18, 21, 72-76]. On the other hand, relatively little is known about such mechanisms in non-mammalian vertebrates.

In the present thesis, I aimed to elucidate the neuroendocrine mechanisms for the synchronized and coordinated regulation of sexual behaviors in relation with the gonadal maturation, by focusing on estrogen and estrogen-receptive neurons by using a teleost, medaka (*Oryzias latipes*). Medaka has frequently been used as a teleost model organism in reproductive biology [33], which is one of the most widely used seasonal breeder, and many sophisticated experimental methods for validation of the effect of sex steroid hormones have been successfully applied [77, 78]. In addition, previous studies have shown that there are estrogen-receptive neurons in the medaka brain [29, 30], which can be considered as candidate neurons for the activation of sexual behavior. Also, medaka performs stereotypical patterns of sexual behaviors [34, 35], and it is therefore easy to perform quantitative analysis of sexual behaviors [36]. Here, I performed the behavioral analyses using female medaka and found that estrogen has an important role in the activation of specific repertoires of the female sexual behaviors to accept the male courtship behavior and clasping before spawning, which is supposed to reflect the female's sexual receptivity. I also demonstrated that female medaka whose *esr2b* gene, one of the estrogen receptor subtypes expressed in the brain, was knocked out failed to accept the courtship display and clasping behavior by male, which suggests that *esr2b*-expressing neuron in the brain plays a crucial role in the activation of female receptivity. This may be one of the most important mechanisms that elicit the sexual behavior in synchrony with the gonadal maturation.

Materials and methods

Animals

Female and male wild type (WT) d-rR medaka (*Oryzias latipes*) and the gene-knockout (KO) lines of *esr2b* (*esr2b*$^{+/-}$ and *esr2b*$^{-/-}$), which were generated in Kayo *et al.*, 2019 [17]) were used in this study. I collected the eggs of *esr2b*$^{-/-}$ from the pairs or harems that consisted of *esr2b*$^{+/-}$ females and *esr2b*$^{+/-}$ / *esr2b*$^{-/-}$ males. All fish were maintained in shoals until it was possible to distinguish their sex by their sexually dimorphic appearance. After breeding in shoals, I made the pair (one female and one male) or the harem (two to three females and one male) in fish tanks with water circulation (Labreed, IWAKI Co., Ltd., Tokyo, Japan) under 14-h light/10-h dark photoperiod (light on at 08:00 and off at 22:00) condition at a water temperature of 27 ± 2 °C. I fed live brine shrimp and/or commercial flake food (Tetra Medaka-bijin; Spectrum Brands, Yokohama, Japan) for three or four times per day. All experiments were performed using sexually matured 3-6 months aged females and males. All of the fish maintenance and the experiments were conducted in accordance with the protocols approved by the Animal Care and Use Committee of the University of Tokyo (permission number 17-1).

Genotyping and screening of *esr2b* KO medaka

To confirm the genotype of *esr2b* KO line medaka, I fin-clipped their caudal fin and put the fragments in 20 µL 20 µg/mL Protein-kinase K (KANTO CHEMICAL Co., INC., Tokyo, Japan) in TE buffer (10 mM Tris-HCl and 1 mM EDTA, pH8.0). After incubate it for 20 minutes at 75 °C, I added 80 µL water to dilute 5 times and use it as a template genome for PCR. For real-time PCR, the cDNA was amplified using KAPA SYBR FAST qPCR Kit (KAPA Biosystems, Nippon Genetics) with the LightCycler 96 system (Roche, Applied Science, Penzberg, Germany). The

temperature profile of the reaction was 95 °C for 3 minutes, 40 cycles of denaturation at 95 °C for 10 seconds, annealing at 60 °C for 10 seconds, and extension at 72 °C for 15 seconds. The qPCR product was verified using melting curve analysis (95 °C for 10 seconds, 65 °C for 60 seconds, and 97 °C for 1 second). The primer pairs used in the qPCR are listed in Table 2-1.

Fadrozole hydrochloride administration

An aromatese inhibitor, fadrozole hydrochloride (Fad) administration was performed by water exposure. I prepared 50 μg/L Fad water by dispensing 2 μL of Fad aliquot (25 g/L Fad in dimethyl sulfoxide (DMSO)) and placed the pair of WT medaka that showed spawning for three consecutive days before the administration. Behavioral recording was conducted three times for each pair. At first, behavioral recording was conducted one day after moving the pairs to the experimental tank ("Before"), which females were not administered Fad. Next, I administered Fad for three days and confirmed that all of the pairs (9 pairs) did not spawn. Behavioral recording was performed on the third day of Fad-administration ("During"). Finally, I suspended Fad-administration and record their behavior three days after suspension ("After"). All of the females were paired with a WT male (mating partner) and administrated in the experimental tank for the analysis of sexual behavior that was described in chapter 1.

For analyzing ovarian morphology, I administered Fad to different individuals for behavioral analysis, although by the administration method was same with behavioral analysis.

Ovariectomy and estradiol administration

Ovariectomy (OVX) was carried out by following the previous studies [77, 78]. Before the surgery, I deeply anesthetized the female fish with 0.02 % MS222 (Sigma-Aldrich, St. Louis, MO) and excise their ovary via intraperitoneal operation. After the removal of ovary, I sutured

the incision with a nylon thread. Post-surgery females were recovered in 0.8 % NaCl water for three days. Sham surgery was performed by insertion the forceps once, instead of the excision of ovary.

For estradiol (E2) administration, I prepared 10 nM (2.72 ng/ml) E2 water by dispensing 2.72 μL of E2 aliquot (1 mg/mL E2 in dimethyl sulfoxide (DMSO)) to 1 L water and place three OVX females in it. E2 administration was performed for 5 days by changing the water at the evening per day. The water for control group was made by dispensing DMSO at the same volume of E2 aliquot. All of the females were paired with a WT male and administrated by water exposure in the experimental tank for the analysis of sexual behavior that was described in chapter 1.

Analysis of sexual behavior

Analyses of sexual behavior were performed as described in chapter 1. On the day before the behavioral testing, I changed the water for the pairs that were exposed E2/Fad to intact water. The water depth was maintained at ~5 cm. Each pair of female and male were kept partitioned until the analysis by putting a transparent perforated partition diagonally across the tank. For the behavioral recording, I applied the RP-units [36] and set them and the tanks as described in chapter 1. At 9:00 of the testing day, the partition was removed and *Record.sh* was run with same recording setting with chapter 1.

After obtaining behavioral videos, I identified the behavioral repertoires and annotated four behavioral repertoires during sexual behavior; following, courtship, clasping, and spawning by using *Ethogramer*, while replaying the first 30 minutes of the videos from the time the partition was removed, and female and male started to interact. Each repertoire was referred to as approaching to courting orientation, head-up I to courting round dance, head up II to copulation, and spawning, respectively in the previous manuscript [34, 35]. After behavioral annotation, I

calculated the following behavioral parameters as described below:

For Fad-administration analysis (Figure 2-1)

- latency to first following (min.)
- latency to first clasping (min)
- percentage of the time spent for following (%)
- frequency of courtship (/min.)
- percentage of following with successful courtship (%)
- percentage of the females that spawned (%)

For OVX analysis (Figure 2-2) and *esr2b* KO female analysis (Figure 2-4)

- latency to first following (min.)
- latency to first clasping (min)
- percentage of the time spent for following (%)
- Number of following trials
- frequency of courtship (/min.)
- percentage of following with successful courtship (%)

Quantitative real-time PCR

Female medaka of *esr2b*$^{+/-}$ and *esr2b*$^{-/-}$ were deeply anesthetized with 0.02 % MS222, and their pituitaries were collected for quantitative real-time PCR (qRT-PCR) analysis. Total RNA was extracted by using the FastGene™ RNA Basic Kit (Nippon Genetics Co, Ltd, Tokyo, Japan) according to the manufacture's instruction. Total RNA was reverse-transcribed with PrimeScript™ RT Master Mix (TaKaRa, Kusatsu, Japan) or FastGene ScriptaseII 5x Ready Mix

OdT (Nippon Genetics) according to the manufacture's instruction. For real-time PCR, the cDNA was amplified using KAPA SYBR FAST qPCR Kit with the LightCycler 96 system. The temperature profile of the reaction was 95 °C for 90 seconds, 40 cycles of denaturation at 95 °C for 10 seconds, annealing at 60 °C for 10 seconds, and extension at 72 °C for 10 seconds. The qPCR product was verified using melting curve analysis (95 °C for 10 seconds, 65 °C for 60 seconds, and 97 °C for 1 second). The data were normalized to a housekeeping gene, ribosomal protein s13 (*rps13*). The primer pairs used in the qPCR are listed in Table 2-1.

Observation of secondary sex characteristics

To observe the female secondary sex characteristics, female medaka of *esr2b*$^{+/-}$ and *esr2b*$^{-/-}$ were anesthetized and lain down on the black board with their left side up. Dorsal/anal fin and urogenital papilla (UGP) were photographed under a Leica S9D (Leica Microsystems, Wetzlar, Germany) equipped with a digital camera Leica MC120HD (Leica).

Gonadal analysis

Female medaka of *esr2b*$^{+/-}$ and *esr2b*$^{-/-}$ were deeply anesthetized with 0.02 % MS222 and their body weight was recorded. After that, their ovaries were removed, weighed, and photographed under a Leica equipped with Leica MC120HD. Immediately after photographed, the ovaries were fixed overnight with Bouin's solution (picric acid saturated solution : formaldehyde : acetic acid = 15 : 5 : 1) at 4 °C. After fixation, specimens were dehydrated with ethanol, permeated with xylene, and embedded in paraffin (Histprep568, Wako Chemical CO., Tokyo, Japan). Embedded specimens were sectioned serially at a thickness of 5 μm and stained with hematoxylin and eosin. Photo images were acquired using OLYMPUS BX53 (OLYMPUS, Tokyo, Japan) equipped with OLYMPUS DP70 (OLYMPUS).

The gonadosomatic index (GSI) was calculated as the ovary weight / body weight ×100 (%).

Statistical analysis

All the values are presented as mean ± standard error of the mean (SEM). Statistical analyses and graph drawing were performed by using R (R Core Team 2020). For comparing between two groups, all of the parameters except for the latency to the first following/spawning were analyzed by Mann–Whitney *U* test. On the other hand, data were analyzed by the non-parametric Kruskal-Wallis test followed by Steel-Dwass test for more than two groups. Data were shown by the whisker and scatter plot using the *beeswarm* package. The latency to the first following/spawning was analyzed using Kaplan–Meier plot, and the differences between each Kaplan–Meier curve were tested for statistical significance using Log-Rank test. The *survival* package was used to conduct Kaplan–Meier plots. A *P*-value less than 0.05 was considered statistically significant.

Results

Estrogen-deficient female normally received male courtship but did not show the clasping behavior with male

To examine whether estrogen is involved in the activation of female sexual behavior, I first analyzed the sexual behavior of female medaka whose estrogen synthesis was inhibited by Fad-administration (Fig.2-1). WT males that were paired with Fad-administered ("During") female showed following/courtship behavior equivalent to the males with non-administered ("Before" and "After") female (Figures 2-1B, D-F). These results indicate that male approach to female occurs regardless of the presence/absence of estrogen in female, and estrogen-deficient female normally accept the male approach. However, significant difference was found in the latency to first clasping (Figure 2-1C), and the percentage of the spawned pair was decreased in Fad-administered female (Figure 2-1G). This result suggests that estrogen is involved in the activation of female receptivity, which is essential for the acceptance of male courtship display and clasping to culminate in female spawning (receptive behavior). It should be noted that Fad-administered females had abnormal ovary that did not contain oocytes with accumulated yolk (Figure 2-1H), which indicates that estrogen-deficiency not only affected the activation of sexual behavior, but also the regulation of gonadal functions. In fact, it is known that estrogen promotes vitellogenesis in the liver [79]. Therefore, it is reasonable that yolk accumulation was not observed in the ovaries of Fad-administered female. Then, the behavioral phenotype of Fad-administered females may be the secondary effect of the dysregulation of gonadal functions, and further analysis for revealing estrogenic actions on the sexual behavior is required.

Ovariectomized female refused male following and courtship, while estrogen administration partially reinstated the receptive behavior

Next, I performed the estrogen administration to ovariectomized (OVX) females and analyzed their sexual behavior (Figure 2-2). I did not find any significant differences in the latency to the first following and the percentage of the time spent for following among all groups (Sham/OVX/OVX+E) (Figures 2-2B and D). On the other hand, the number of following trials of Sham was significantly lower than that of OVX/OVX+E (Figure 2-2E), while the frequency of courtship and percentage of following with successful courtship of Sham was significantly higher than these of OVX/OVX+E (Figures 2-2F and G). These results indicate that males also tried to approach and court OVX/OVX+E females, which is equivalent to Sham females, but OVX/OVX+E females refused males' approaching; in other words it suggests that they showed avoidance behavior. However, some of OVX+E females performed the clasping behavior (Figure 2-2C), which occurred later and lasted for shorter period than that of Sham, whereas they refused male following/courtship to a similar extent as OVX female. It suggests that estrogen is necessary for the female receptivity, although it may not be sufficient to accomplish the sexual behavior.

***esr2b* KO female has normal gonadal function and shows normal secondary sex characteristics**

Since it is suggested that estrogen is involved in the activation of female receptivity, I focused on the estrogen receptor (Esr). Medaka have three subtypes of Esrs, Esr1, Esr2a, and Esr2b [80]. Recently, gene KO analysis revealed that Esr1 is dispensable for sexual development and reproductive function [81]. Also, *esr2a* KO females have dysfunction in follicle stimulating hormone (FSH) negative-feedback regulation and also show oviduct atresia, while they show apparently normal sexual behavior but without oviposition because of their oviductal atresia [17].

However, since the function of *esr2b* remained unclear, I performed detailed analysis of the *esr2b*$^{-/-}$ female.

First of all, I performed qRT-PCR to analyze gonadotropin genes *fshb* and *lhb* (Figures 2-3A and B), which are expressed in the pituitary and play roles in folliculogenesis and ovulation, respectively in teleosts [15]. Significant differences between *esr2b*$^{+/-}$ and *esr2b*$^{-/-}$ female were not observed in either *lhb* nor *fshb* expressions, suggesting that *esr2b* is not involved in the regulation of gonadotropin genes expression.

Next, I analyzed the expression of female secondary sex characteristics, which is thought to be expressed depending on the sex steroid hormones, especially estrogen (Figure 2-3C). Female medaka show some secondary sex characteristics such as triangular anal fin, non-notched dorsal fin, and thickened UGP, which is a fleshy protrusion behind the anus and is developed in an estrogen dependent manner [82-85]. I found that *esr2b*$^{-/-}$ females showed normal female secondary sex characteristics, similar to that of *esr2b*$^{+/-}$ females, which suggests that *esr2b*$^{-/-}$ female normally secreted estrogen and received it in the peripheral tissues such as UGP, via blood circulation.

In addition, there was no distinguishable differences in the external appearance of the ovaries (Figures 2-3D), and significant difference was not found in the GSI between the genotypes (Figures 2-3E). To further understanding the ovarian architecture, I performed histological examination and found that *esr2b*$^{-/-}$ ovaries had stem cells, oocyte like cells at zygotene/pachytene/diplotene, and oocytes filled with accumulated yolk were enclosed by follicular cells, namely, granulosa/theca cell. Also, the ovarian cavity was normally formed in the *esr2b*$^{-/-}$ ovaries (Figures 2-3F).

These results indicate that *esr2b* KO does not influence the expression of secondary sex characteristics and ovarian formation.

esr2b KO females did not show transition to the clasping behavior, although they were normally approached by males

Next, I analyzed the sexual behavior of *esr2b*$^{-/-}$ female. There were no significant differences in the indices of following behavior (Figures 2-4B, D, and E), suggesting that WT males can perform the following behavior toward the *esr2b*$^{-/-}$ female as frequently as toward the *esr2b*$^{+/-}$ female, and *esr2b*$^{-/-}$ females normally accepted the following behavior. On the other hand, the significant difference was detected in the latency to first clasping, the frequency of courtship, and the percentage of following with successful courtship (Figures 2-4C, F, and G), which indicate that *esr2b*$^{-/-}$ female avoided the courtship display by male and failed to be clasped by male. Taken together, these results suggest that *esr2b* KO females shows the decline of female receptivity, therefore they refuses male courtship, which results in failure in spawning.

Discussion

In the present chapter, I examined the possible involvement of estrogen and its receptor *esr2b* in the activation of female sexual behavior by pharmacological manipulation of the internal estrogen levels and analyzed the *esr2b* KO female. I showed by behavioral analysis of the female medaka treated with pharmacological inhibitor of estrogen synthesis that estrogen is essential for promoting the clasping behavior. This result is consistent with the other result that estrogen administration partially reinstated the clasping behavior of ovariectomized female. Also, I demonstrated that *esr2b* KO females did not show spawning behavior, although they were normally approached by male. It should be noted that *esr2b* KO females showed normal ovarian function and secondary sex characteristics. In the previous study, it was shown that *esr2b* is expressed in the brain [29, 30]. Taken together, it is suggested that *esr2b*-expressing neuron in the brain plays a pivotal role in the activation of female receptivity.

Female receptivity is facilitated by estrogen, probably via *esr2b*-expressing neurons in the brain

I showed by pharmacological analysis using estrogen synthesis inhibitors (Figure 2-1) and estrogen administration to ovariectomized females (Figure 2-3) that female medaka performs spawning behavior in an estrogen-dependent manner. By using a gene knocked out medaka, I also obtained evidence to suggest that one of the estrogen receptors, Esr2b play a key role in the activation of female receptivity (Figure 2-3). This is consistent with the previous studies which showed that *esr2b* is expressed in some brain nuclei that are supposed to be involved in the regulation of sexual behavior in teleosts [29, 30]. Sex steroid hormones modulate the neural architecture and neurosecretory properties in various vertebrate species [86-94], and some studies

in mice show that these modulations actually function to drive female receptivity [22, 23]. Also, it has been reported that some estrogen-receptive neurons in the female medaka brain can change their cellular size, transcriptional properties, and spontaneous firing activity in an estrogen dependent manner [95-99]. Thus, it is suggested that *esr2b*-expressing neurons in the female medaka brain contribute to the activation of female receptivity by changing the release of neurotransmitters in an estrogen-dependent manner. Further analysis in the future is expected to elucidate the contribution of the estrogen/*esr2b* signaling. It should be noted that Fad-administered female showed normal acceptance of courtship display (Figures 2-1E and F), although significant decrease was found in the acceptance of courtship display in *esr2b*$^{-/-}$ female (Figures 2-4F and G). I speculated that this discrepancy was caused by the difference in the periods of inhibition of estrogen/*esr2b* signaling. In Fad-administered females, estrogen/*esr2b* signaling was inhibited only during three-day period, whereas the estrogen/ *esr2b* signaling never worked in *esr2b*$^{-/-}$ female.

Recently, Nishiike *et al.* (2021) described the phenotype of *esr2b* KO female medaka [100], which is basically similar to that of the present study; *esr2b*-deficient female medaka showed dysfunction in the activation of female receptivity but not in the ovarian function and the sex steroid milieu.

Some unknown ovarian factors in addition to estrogen should be involved in the activation of female receptivity

As described above, estrogen/*esr2b* signaling plays a key role in the female receptivity, but it does not mean that estrogen is necessary and sufficient to accomplish the entire female sexual behavior. Sexual behavior of medaka consists of several sequentially occurring stereotypical repertoires; following, courtship, clasping, and spawning, and sometimes these are halted by

female when female is not receptive. In the present chapter, I showed that Fad-administered (estrogen-deficient) and *esr2b* KO females showed normal acceptance of the male following behavior (Figures 2-1B and D, 2-4B, D, and E), although there was some difference in the courtship acceptance between these two female groups (Figures 2-1E and F, 2-4F and G). On the other hand, OVX failed to accept not only the courtship display but also the following behavior by male (Figure 2-2), which is more severe phenotype than the Fad-administered and *esr2b* KO females. Furthermore, estrogen administration to OVX females partially reinstated clasping behavior alone (Figure 2-2C), while kept failing to accept the male following behavior (Figures 2-2D and E). These results suggest that some ovarian factor(s) other than estrogen may affect the male receptive behavior prior to the courtship behavior.

Although the nature of the ovarian substance that is involved in the acceptance of following behavior by male has yet to be determined, several studies have suggested that substances other than estrogen may also play a role in female sexual behavior. Unpublished study in our laboratory have shown that female medaka whose *gnrh*/*lhb* genes had been knocked out and have never ovulated do not show the clasping behavior in spite of normal reception of male courtship display, and administration of progesterone, which is one of the ovarian sex steroid hormones, reinstated the clasping behavior (Shimomai, unpublished). This finding may suggest that 17α,20β-dihydroxy-4-pregnen-3-one (DHP), which is considered to be equivalent to progesterone in telsosts, is also involved in some process(es) of the clasping behavior. Also, preliminary experiments in our lab showed that intracellular nuclear progesterone receptor, *pr* is expressed in some brain nuclei that are supposed to be involved in the control of sexual behavior (Shimomai and Tomihara, unpublished), and I found that some of the membrane-bound progesterone receptor subtypes, *paqr3*, *paqr6*, *paqr7b* are highly expressed in the brain (data not shown). These results suggest that ovarian progesterone, which is secreted concomitantly with the ovulation, contributes

to the facilitation of female receptivity and/or activation of the clasping behavior, perhaps via progesterone receptors that are expressed in the brain. Since it has been reported that *pr*-expressing neurons is essential for the female sexual behavior in mice [101, 102], and progesterone administration reinforces the estrogen effect on the activation of lordosis behavior in female rats [103], it is likely that both estrogen and progesterone may activate the female sexual behavior also in the teleosts.

In addition, there is some evidence that non-steroid factor is also involved in the activation of the sexual behavior in other teleost species. Prostaglandin F2α (PGF2α), a kind of physiologically active lipid, elicits female sexual behavior in goldfish, cichlid and zebrafish [43, 104-106]. However, it is revealed that another prostaglandin subtype PGE2, which is functionally equivalent to goldfish PGF2α in medaka ovulation, failed to activate female sexual behavior (Mori, unpublished). Furthermore, because prostaglandins are generally considered to function locally because of its rapid elimination (e.g. pain signals), it is presumable that PGF2α synthesized in the brain locally activate sexual behavior, even if it acts also in medaka.

Evolutionary insights into the function of estrogen and its receptor signaling

Taken together with the present results, the importance of estrogen in the activation of female sexual behavior is considered to be conserved in mammals and teleosts. Importantly, I demonstrated that estrogen/*esr2b* signaling is involved in the activation of female receptivity but does not contribute to the ovarian functions, at least in a teleost, medaka. Teleosts generally possess three Esr subtypes, *esr1*, *esr2a*, and *esr2b*, which are generated by gene duplication of ancestral Esr genes in the early gnathostome lineage (when *esr1* and *esr2* were generated), and another gene duplication of *esr2* in the third-round whole genome duplication that has occurred specifically in teleost ancestors (*esr2a* and *esr2b* were generated) [80, 107, 108]. In a recent study,

it has been reported that *esr1* is dispensable for reproductive function including the activation of sexual behavior in medaka [81], and *esr2a* is involved in the negative sex steroid feedback regulation of gonadotropin secretion in the pituitary [17]. Although there are some different phenotypes among the species, it is known that *esr2a* and *esr2b* deficiencies cause severe dysregulation of reproductive function, but *esr1*-deficiency does not induce any dysfunction that causes infertility in other teleost species [31, 109, 110]. Taken together, it is suggested that *esr2a* and/or *esr2b* are mainly involved in the female reproductive functions in teleosts, with a possible sub-functionalization between the two genes. Also, recent studies demonstrated that *esr2* but not *esr1* is responsible for the activation of sexual behavior in avian species [111]. Taken together, it is suggested that *esr2* rather than *esr1* is involved in reproductive functions in non-mammalian species.

In contrast, *esr1* plays more important roles than *esr2* in female reproductive functions in mammals. Actually, *esr1* KO mice shows severe gonadal defect and behavioral dysfunction leading to infertility [21, 112, 113], whereas *Esr2*-deficiency reduces litter sizes but does not cause complete infertility [114-116].

These findings suggest that swapping of the main functions of Esr subtypes as to the control of physiological functions and sexual behavior may have occurred in mammalian and nonmammalian species during evolution, and it may be speculated that this swapping of Esr subtypes may have been caused by difference in neural circuitries involved in reproductive regulations. Kisspeptin neural system may be the prime example of this phenomenon. In mammals, a neuropeptide kisspeptin play a pivotal role in the regulation of HPG axis by modyfing the neuronal activity of GnRH-releasing neurons. Kisspeptin neurons express *esr1*, and are supposed to be the target of well-known sex steroid feedback regulation [3-8]. However, growing body of evidence suggests that kisspeptin is not involved in the HPG axis regulation in non-

mammalian vertebrates [16, 71], although estrogen itself should have a role in the feedback regulation of GnRH neurons via non-kisspeptin neural system [117], suggesting that the site of the action of steroid feedback regulation in the hypothalamus are different between mammalian and non-mammalian species, although estrogen/Esr feedback as a phenomenone seems to be commonly exist in veretebrates. The result in this chapter demonstrated that *esr2b* but not *esr1* is involved in the control of sexual behavior in teleost medaka. It suggests that the neurons receives estrogen to avtivate sexual behavior should be different between mammals and teleost, which is in a similar situation to the in HPG axis regulation as described above. Further analysis of the estrogen/*esr2b* neuroendocrine mechanism will contribute to elucidate the evolution of estrogen-related neural mechanism activating the sexual behavior among vertebrates.

In summary, I have shown in chapter2 that estrogen/*esr2b* signaling in the brain plays a crucial role in the activation of female receptivity. This process may be considered as one of the most important mechanisms eliciting the sexual behavior in synchrony with the gonadal maturation.

Table 2-1

The list of primers used for probe preparations in chapter 2. the primers for genotyping of *esr2b* KO were gifted by Dr. Daichi Kayo (The University of Tokyo). Also, the sequences of primers for qRT-PCR were also described in Kayo *et al.*, 2019 [17].

Primer name	Purpose	Sequence
erb2 melt se	Genotyping of *esr2b* KO	5′-CTTTTGCCTGCCATGTACAGCC-3′
erb2 melt as2	Genotyping of *esr2b* KO	5′-GGACTATAGAAGGTCAACGGTCCAG-3′
erb2 Wtonly AS2	Genotyping of *esr2b* KO	5′-TAGTCATGGCTGCTGTCCGT-3′
qPCR LHb F new	qRT-PCR for *lhb* gene	5′-TGCCTTACCAAGGACCCCTTGATG-3′
qPCR LHb R new	qRT-PCR for *lhb* gene	5′-AGGGTATGTGACTGACGGATCCAC-3′
qPCR FSHb Fw new	qRT-PCR for f*shb* gene	5′-TGGAGATCTACAGGCGTCGGTAC-3′
qPCR FSHb Rv new	qRT-PCR for f*shb* gene	5′-AGCTCTCCACAGGGATGCTG-3′
RPS13-SE	qRT-PCR for *lhb* /*fshb*	5′-GTGTTCCCACTTGGCTCAAGC-3′
RPS13-AS	qRT-PCR for *lhb* /*fshb*	5′-CACCAATTTGAGAGGGAGTGAGAC-3′

Figure legends

Figure 2-1

Female receptivity is decreased in the females whose estrogen synthesis was pharmacologically inhibited. (A) Time-courses of behavioral sequences during 30-minute period observation of sexual behavior are shown as raster plots. Each trace represents data from a single pair of male and female. “Before”, “During”, and “After” indicates before Fad-administration, during Fad-administration, and after Fad-administration, respectively. Yellow, black, cyan and red bands indicates the period of following, courtship, clasping and spawning, respectively. A red triangle is placed on the right side of each red band for the sake of easier detection of the occurrence of spawning (red band, which is very short). (B, C) The latency data were further analyzed using Kaplan-Meier plots. Red, khaki, and blue curves indicates “Before”, “During”, and “After”, respectively. (B) The females during administration received the first following by males later than the females before/after administration (Latency to the first following (min.): Before; 95.33 ± 29.87, During; 49.11 ± 15.76, After; 59.56 ± 11.18, $P = 0.2626$ by Log-Rank Test, (C) Latency to the first clasping (min.): Before; 218.78 ± 67.11, During; 1485.00 ± 189.00, After; 489.67 ± 193.01, $^{**}P = 0.001422$ between Before and During, $^{***}P = 0.00018$ between During and After by Log-Rank Test). (D-G) Various parameters were measured and compared among the data for three periods. Red, khaki, and blue dots represent “Before”, “During”, and “After”, respectively. (D) There was no significant difference among the data for three periods in the percentage of time spent for following (%) (Before; 27.81 ± 4.56, During; 41.44 ± 3.55, After; 40.66 ± 6.93, $P = 0.1043$ by Kruskal-Wallis Test), (E) frequency of courtship (/min.) (Before; 0.707 ± 0.165, During; 0.715 ± 0.150, After; 1.078 ± 0.262, $P = 0.4942$ by Kruskal-Wallis Test (E)), and (F) percentage of following with successful courtship (%) (Before; 48.25 ± 5.92, During; 42.36 ± 6.05, After; 49.68 ± 7.66, $P = 0.4326$ by Kruskal-Wallis Test). (G) The percentage of spawned

female. The females during administration rarely spawned. (H) Representative photographs of ovaries. There are many oocytes with accumulated yolk (arrowheads) in the ovary of DMSO-administered females (+DMSO), although they were not observed in the ovary of Fad-administered females (+Fad). Scale bar = 200 μm.

Figure 2-2

Ovariectomized (OVX) females failed to accept (or rather appeared to actively refuse) the following by male, and estrogen administration partially reinstated the clasping behavior. (A) Time-courses of behavioral sequences during 30-minute period observation of sexual behavior are shown as raster plots. Yellow, black, cyan and red bands represent the timing and duration of following, courtship, clasping and spawning, respectively. The red triangles are the same as in Figure 2-1. (B, C) The latency data were further analyzed using Kaplan-Meier plots. Blue, Red, and khaki curves represent Sham, OVX, OVX+E, respectively. (C) OVX females never perform clasping behavior with male, although a part of OVX+E females (3/5 females) showed the clasping behavior that occurred significantly late (Latency to first following (min.): Sham; 1.69 ± 0.47, OVX; 2.22 ± 0.35, OVX+E; 1.58 ± 0.24, $P = 0.4288$, Latency to first clasping (min.): Sham; 12.48 ± 0.81, OVX; not detected, OVX+E; 26.18 ± 6.47 (n = 3), $^{**}P = 0.00552$ between Sham and OVX, $^{**}P = 0.00552$ between Sham and OVX+E, by Log-Rank Tests). (D-G) Various parameters were measured and compared among Sham, OVX, and OVX+E, which are represented as blue, red, and khaki dots, respectively. It was not found the significant difference in percentage of the time spent for following (%) (Sham; 42.77 ± 1.63, OVX; 52.14 ± 7.28, OVX+E; 51.62 ± 2.68, $P = 0.1583$ by Kruskal-Wallis Test (D)), although number of following trial was significantly higher in OVX and OVX+E compared to Sham (Sham; 43.2 ± 2.63, OVX; 87.2 ± 11.50, OVX+E; 104.0 ± 7.93, $^{**}P = 0.02449$ between Sham and OVX, $^{**}P = 0.02449$

between Sham and OVX+E by Steel-Dwass Tests (E)), and frequency of courtship (/min.) (Sham; 1.44 ± 0.088, OVX; 2.91 ± 0.383, OVX+E; 3.47 ± 0.264, $^{**}P = 0.02341$ between Sham and OVX, $P = 0.02395$ between Sham and OVX+E by Steel-Dwass Tests (F)) and percentage of following with successful courtship (%) (Sham; 82.82 ± 3.56, OVX; 31.02 ± 4.36, OVX+E; 23.90 ± 2.17, $^{**}P = 0.02449$ between Sham and OVX, $^{**}P = 0.02449$ between Sham and OVX+E by Steel-Dwass Tests (G)) were significantly lower in OVX and OVX+E compared to Sham.

Figure 2-3

Various analyses on the physiological functions of *esr2b* KO female. "+/-" and "-/-" indicate the data of $esr2b^{+/-}$ and $esr2b^{-/-}$ female, respectively. (A, B) Expression levels of *lhb* (A) and *fshb* (B) in the pituitary. Significant difference between $esr2b^{+/-}$ and $esr2b^{-/-}$ female was not detected in either *lhb* or *fshb* expression (*lhb*: +/-; 29.4 ± 4.01, -/-; 16.7 ± 3.46, $P = 0.0601$, *fshb*: +/-; 74.6 ± 8.06, -/-; 50.8 ± 10.2, $P = 0.173$, by Mann-Whitney *U* Tests), which is consistent with the previous study [17]. (C) Representative photographs of caudal part of the body of $esr2b^{+/-}$ and $esr2b^{-/-}$ female. There was no visible difference in the appearance of secondary sex characteristics: dorsal fin, anal fin, and UGP (arrowhead). Scale bar = 5 mm. (D-F) Morphological features of the ovaries. There was no discernible difference in gross morphology (D) and histological architecture (F), and GSI (%) (+/-; 6.31 ± 0.67, -/-; 6.61 ± 1.64, $P = 0.5827$ (E)).

Figure 2-4

$esr2b^{-/-}$ female shows lower receptivity. "+/-" and "-/-" indicate the data of $esr2b^{+/-}$ and $esr2b^{-/-}$ female, respectively. (A) Time-courses of behavioral sequences during 30-minute period observation of sexual behavior are shown as raster plots. Yellow, black, cyan and red bands represent the timing and duration of following, courtship, clasping and spawning, respectively.

The red triangles are the same as in Figure 2-1. (B, C) The latency data were further analyzed using Kaplan-Meier plots. Red and blue curves represent *esr2b*$^{+/-}$ and *esr2b*$^{-/-}$, respectively. (C) The latency data of first clasping indicated that *esr2b*$^{-/-}$ female rarely performed clasping behavior (Latency to first following (min.): +/-; 1.77 ± 0.80, -/-; 1.08 ± 0.41, $P = 0.4426$, Latency to first clasping (min.): +/-; 6.61 ± 2.07, -/-; 16.08 ± 7.08 (n = 2), ***$P = 0.0005$ by Log-Rank Tests). (D-G) Various parameters were measured and compared between *esr2b*$^{+/-}$ and *esr2b*$^{-/-}$ female, which were represented as red and blue dots, respectively. From the result that there was no significant difference in percentage of the time spent for following (%) (+/-; 33.1 ± 5.46, -/-; 44.3 ± 5.29, $P = 0.2298$ (D) by Mann-Whitney *U* Test) and number of following trials (+/-; 61.2 ± 7.04, -/-; 54.2 ± 6.50, $P = 0.5752$ (E) by Mann-Whitney *U* Test), *esr2b*$^{-/-}$ female suggested to be normally followed by male, although frequency of courtship (/min.) (+/-; 1.16 ± 0.12, -/-; 0.73 ± 0.16, *$P = 0.03006$ (F) by Mann-Whitney *U* Test) and percentage of following with successful courtship (%) (+/-; 58.1 ± 3.68, -/-; 38.6 ± 4.68, *$P = 0.01307$ (G) by Mann-Whitney *U* Test) was significantly lower than that of *esr2b*$^{+/-}$ female.

Figure 2-1

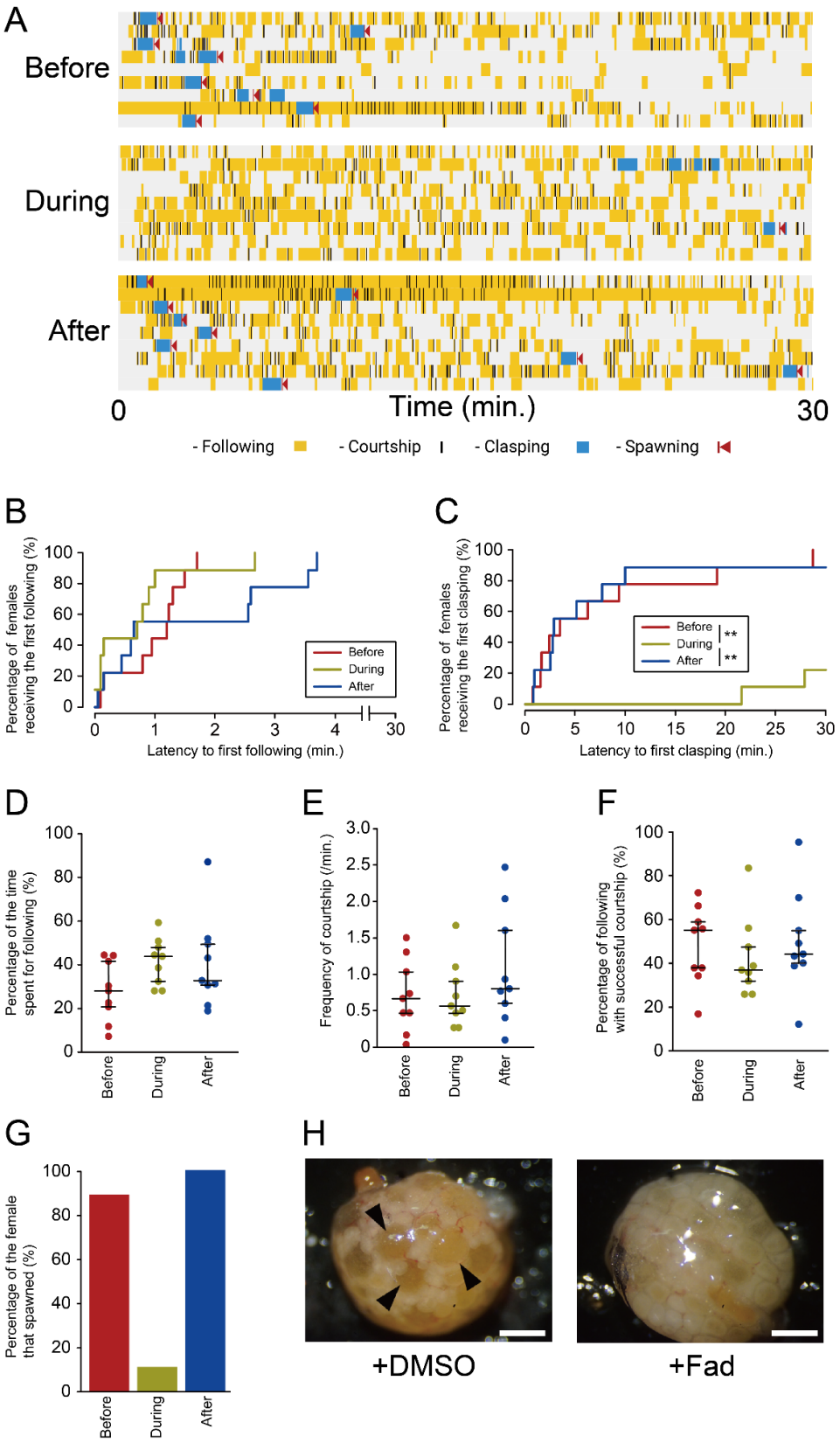
A
Before
During
After
0
Time (min.)
30
- Following
- Courtship
- Clasping
- Spawning
B
Percentage of females receiving the first following (%)
Latency to first following (min.)
Before
During
After
C
Percentage of females receiving the first clasping (%)
Latency to first clasping (min.)
Before
During
After
**
**
D
Percentage of the time spent for following (%)
Before
During
After
E
Frequency of courtship (/min.)
Before
During
After
F
Percentage of following with successful courtship (%)
Before
During
After
G
Percentage of the female that spawned (%)
Before
During
After
H
+DMSO
+Fad

Figure 2-2

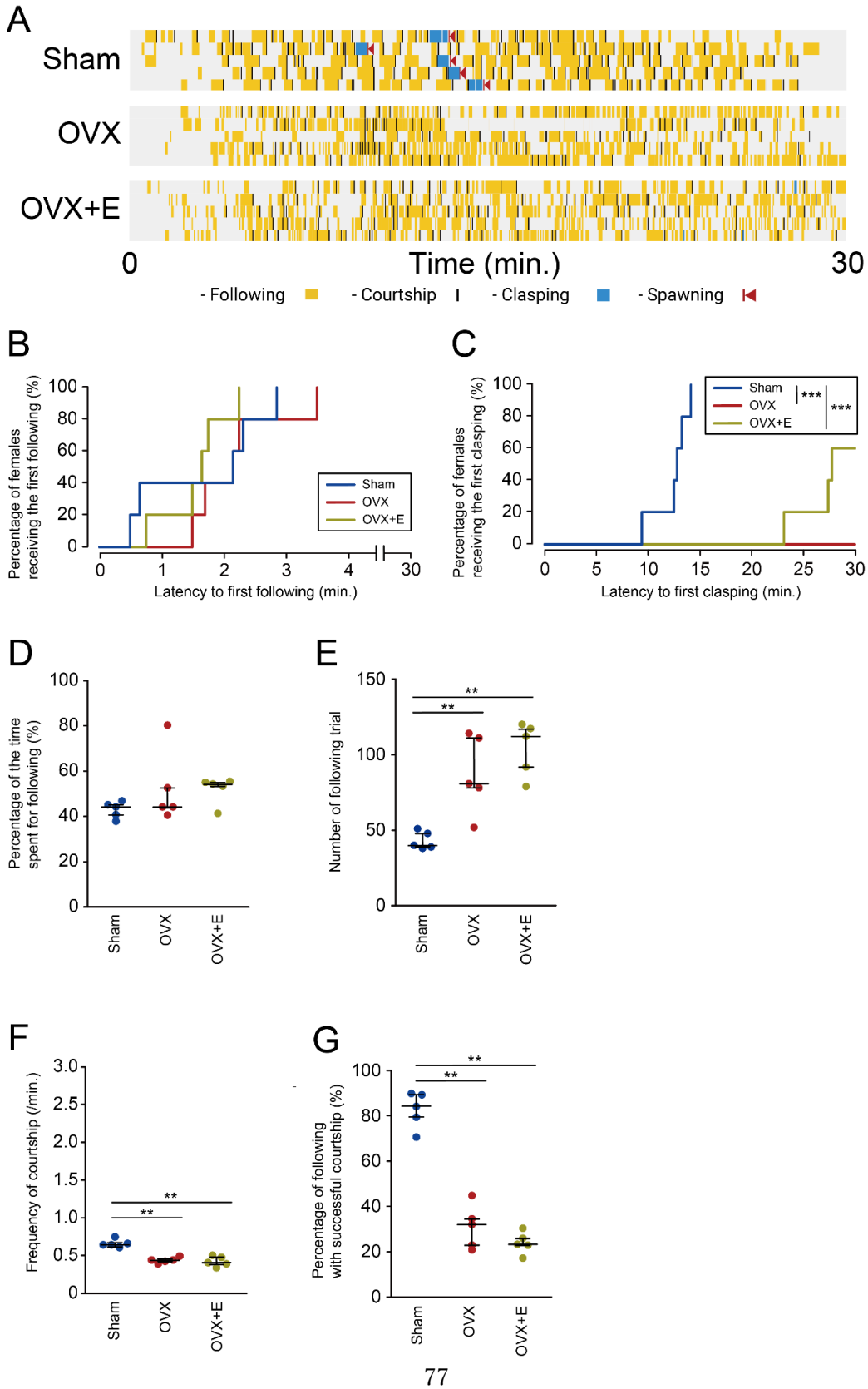
A
Sham
OVX
OVX+E
0
Time (min.)
30
- Following
- Courtship
- Clasping
- Spawning
B
Percentage of females receiving the first following (%)
Latency to first following (min.)
Sham
OVX
OVX+E
C
Percentage of females receiving the first clasping (%)
Latency to first clasping (min.)
***
***
D
Percentage of the time spent for following (%)
E
Number of following trial
**
**
F
Frequency of courtship (/min.)
G
Percentage of following with successful courtship (%)

Figure 2-3

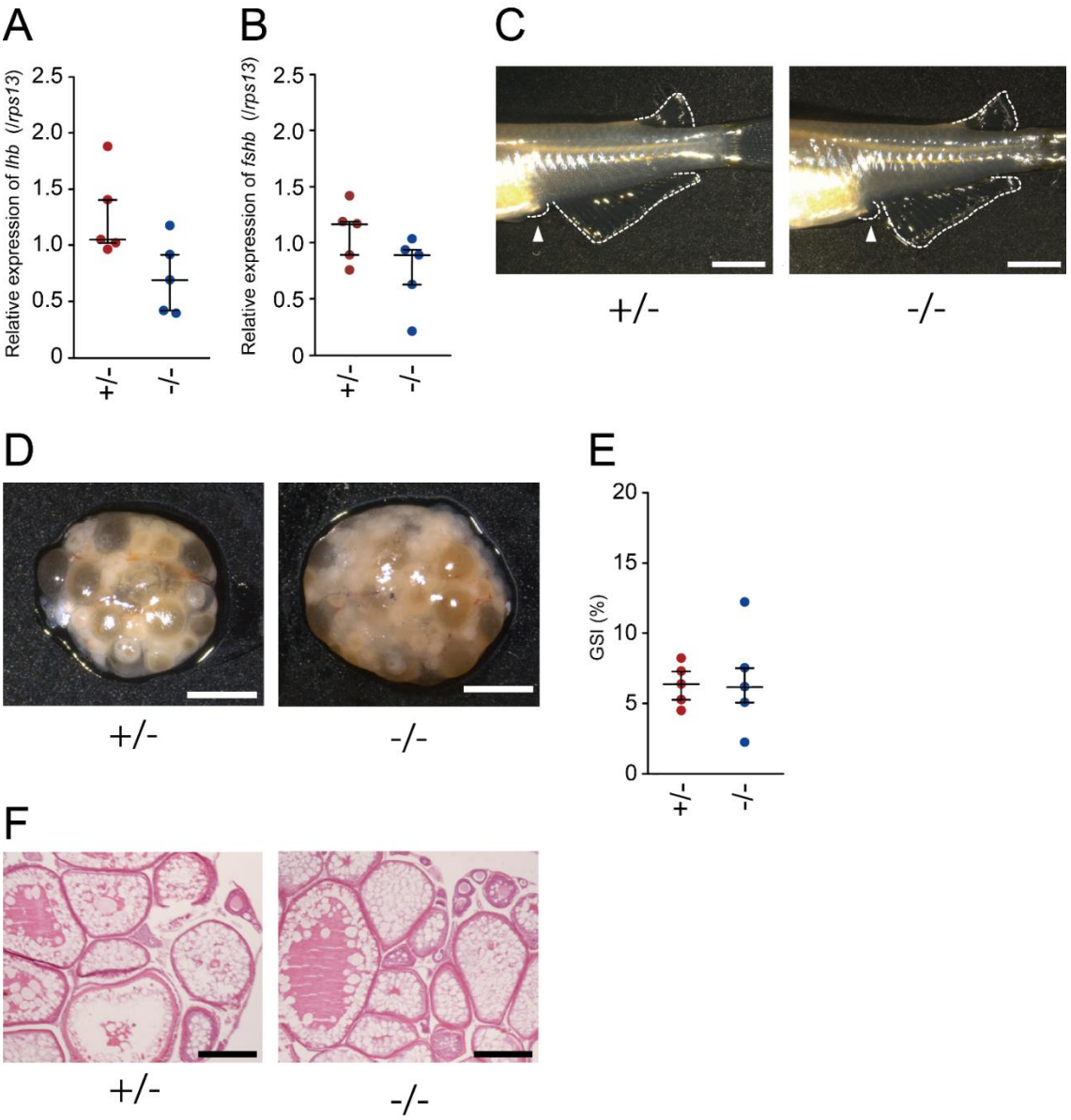
A
Relative expression of lhb (/rps13)
2.5
2.0
1.5
1.0
0.5
0
+/-
-/-
B
Relative expression of fshb (/rps13)
2.5
2.0
1.5
1.0
0.5
0
+/-
-/-
C
+/-
-/-
D
+/-
-/-
E
GSI (%)
20
15
10
5
0
+/-
-/-
F
+/-
-/-

Figure 2-4

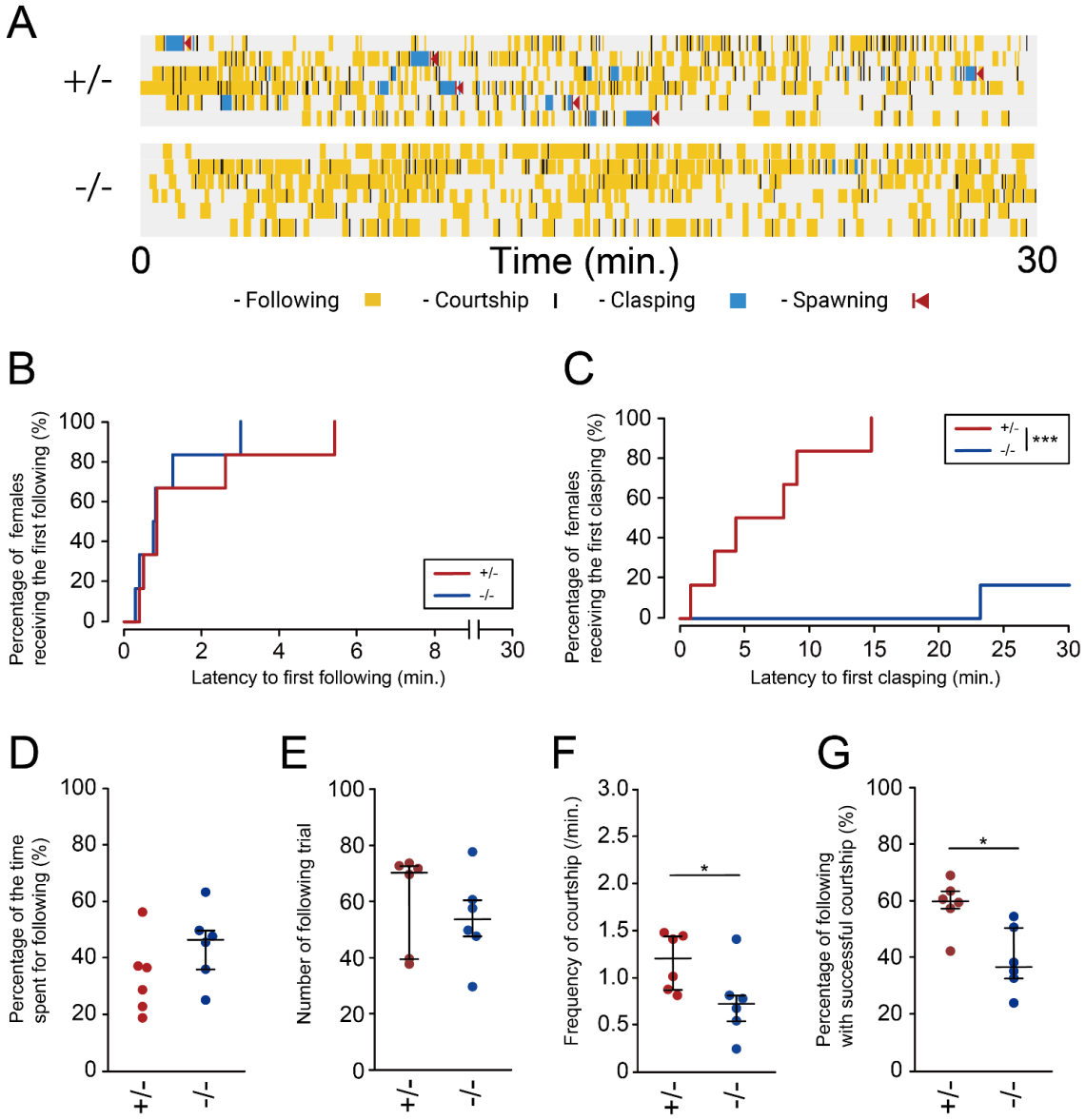
A
+/-
-/-
0
Time (min.)
30
- Following
- Courtship
- Clasping
- Spawning
B
Percentage of females receiving the first following (%)
Latency to first following (min.)
+/-
-/-
C
Percentage of females receiving the first clasping (%)
Latency to first clasping (min.)
***
D
Percentage of the time spent for following (%)
E
Number of following trial
F
Frequency of courtship (/min.)
*
G
Percentage of following with successful courtship (%)
*

Chapter 3

Neural circuit for eliciting female spawning behavior following activation of estrogenic signaling via *esr2b*-expressing neurons

Abstract

Vertebrates perform sexual behavior as an innate behavior for generating offspring, which is regulated to be activated in a flexible manner according to the internal and external environments by neuroendocrinological/neuroethological mechanisms. For such regulation, it has generally been suggested that estrogen, one of the sex steroid hormones, plays pivotal roles by controlling the neural circuit for the sexual behavior, which should involve neurons expressing estrogen receptors. Although many studies have been conducted about this circuit in mammals, there are only a few studies on the circuitry system of non-mammalian species including teleosts.

In chapter 3, I used a teleost, medaka, and explored the neural circuit that elicits the female sexual behavior following activation of estrogenic signaling by using brain activity mapping with immediate early gene (IEG) and histological techniques. I found a neural population in Vd/Vs/Vp brain region of females that shows high neural activity during spawning behavior culminating in oviposition. This population of neurons expressed a GABA marker gene, *gad1.1*, suggesting that GABAergic inhibitory neurotransmission is involved in the female sexual behavior for successful spawning. In addition, estrogen receptor 2b (*esr2b*)– expressing neurons, which are suggested to be involved in female sexual behavior, was located adjacent to the the GABAergic neurons, which were shown to be active during spawning. Furthermore, by using LMD/RNA-seq analysis followed by dual ISH analysis, I identified neuropeptide B, cholecystokinin, and C-type natriuretic peptide 1 as the candidate neuropeptides expressed by those neurons, which are most probably used as neuromodulators activating their specific receptors expressed by the target neurons. Interestingly, the genes of receptors for these peptides were expressed in the ventral telencephalic region where the above-mentioned GABAergic neurons were located. These anatomical results may suggest the existence of local peptidergic neuromodulation between these

two populations in the ventral telencephalon. Because the ventral telencephalic region described in this chapter closely corresponds to the brain regions in himé/kokanee salmon and goldfish that have been shown to trigger specific sexual behaviors in these fish when they received local electrical stimulations, the findings in chapter 3 may give us important general insights into the neural circuit for activating the sexual behavior of female teleosts in general.

Introduction

Sexual behavior is the innate behavior for reproduction in animals, which exhibits sexually dimorphic behavioral patterns. In many cases, male shows the courtship behavior, in some cases accompanied by clasping, and if female accepts the male as a mating partner, they both culminate in spawning behaviors to release sperms and eggs. These sequential behaviors are supposed to be regulated by the neural circuits that are also modulated by physiological conditions of the individual [118]. Among the modulators, gonadal sex steroids are ones of the most important factors for activating the sexual behavior [119, 120], which is also evidenced by the strong correlation between the occurrence of sexual behavior and gonadal maturation.

In females, estrogen, which is secreted from mature ovary, has been supposed to play crucial roles in this neuroendocrine signaling in many vertebrate species [120, 121]. Regarding such regulatory systems, it has been investigated in many studies using mammalian species, especially rodents. In mammalian species that show lordosis behavior, which is a female sexual behavior observed mainly in rodents, rising up their posterior pelvis for facilitating penis intromission into vagina, the lordosis behavior has been suggested to be elicited in an estrogen-dependent manner [18, 74, 76]. It has been also elucidated that estrogen is directly received by estrogen-receptive neurons in the brain, which express estrogen receptors (Esr), and these neurons are involved in the activation of lordosis. Actually, electrolytic lesion of VMH or Esr-knock out (KO) or genetic ablation of Esr1 (one of the Esr subtypes)-expressing neurons in the ventrolateral part of ventromedial hypothalamus (VMHvl) resulted in severe defects in lordosis [19, 21, 44, 101]. Moreover, it has been reported that estrogen/Esr1 signaling modifies the gene expression patterns and synaptic connection of VMHvl neurons [22, 23]. Thus, there are accumulating evidence for the neural circuits of estrogen-dependent regulation of sexual behaviors in mammals, especially

in rodents. However, in non-mammalian species, the neural mechanisms of estrogen-dependent control of sexual behaviors still remain unclear compared to these of mammals, and experimental analyses on this topic have been long awaited.

In chapter 3, I focused on a teleost medaka for the studies of the neural mechanisms activating sexual behavior, because such studies in non-mammalian vertebrates have mostly used teleosts. In the 1980s, several studies using electrolytic local brain lesions and electrical stimulation of local brain regions suggested that ventral telencephalon and preoptic area are involved in the activation of sexual behavior in several teleost species [24-26]. In more recent studies, expression of the genes of sex steroid hormone receptors have been localized to such brain regions [27-30]. These studies suggest that there is a neural circuit that receives the sex steroid signals and promotes the sexual behaviors that are functionally equivalent to those in mammals. To elucidate this neural mechanism, I used a teleost medaka in the present study. Medaka is an advantageous model for experiments in the neuroendocrinological studies. There is an accumulating information about their genome, mechanisms of neuroendocrine regulation of reproduction including the sex steroid hormones, and sophisticated experimental methods, such as molecular genetic techniques [33]. Also, medaka shows stereotypical patterns of sexual behavior, which makes it easy to quantitatively analyze the behavior (Chapter 1) [36]. Moreover, I have shown in chapter 2 that some components of female sexual behaviors are severely affected by gene KO of estrogen receptor 2b (*esr2b*), one of the estrogen receptor subtypes expressed in the brain, which suggests that *esr2b*-expressing neurons may be involved in the activation of sexual behavior (Chapter 2) [100].

In the present chapter, I first identified GABAergic neurons in the ventral telencephalon that are activated during spawning behavior leading to oviposition in female, which is supposed to be one of the major components in the neural circuit for activation of female sexual behavior. Also, my

results suggested that *esr2b*-expressing neurons closely located to these neurons use local neuromodulatory signaling to facilitate the GABAergic neurons to trigger the motor pattern generator circuitries for spawning behavior.

Materials and Methods

Animals

Female and male wild type (WT) d-rR medaka (*Oryzias latipes*) and the transgenic (Tg) lines of *esr1*:*egfp*, which were generated in Zempo *et al.*, 2018 [122] were used in this study. All fish were maintained in shoals until it was possible to distinguish their sex by their sexually dimorphic appearance. After breeding in shoals, I made the pairs (one female and one male) or the harems (two to three females and one male) in fish tank with water circulation (Labreed, IWAKI Co., Ltd., Tokyo, Japan) under 14-h light/10-h dark photoperiod (light on at 08:00 and off at 22:00) condition at a water temperature of 27 ± 2 °C. I fed live brine shrimp and/or commercial flake food (Tetra Medaka-bijin; Spectrum Brands, Yokohama, Japan) for three or four times per day. All of the fish maintenance and the experiments were conducted in accordance with the protocols approved by the Animal Care and Use Committee of the University of Tokyo (permission number 17-1).

Quantification of tail-bending behavior

To quantitatively comparing the tail-bending behavior performed during the clasping behavior culminating/not culminating in oviposition, I obtained the video-captures at the timing of clasping behavior from the video of intact female and male pairs (Figure 3-1). I traced the posture by drawing two lines from anus (This point is called “point P”) to the rostral edge (This point is called “point Q”) and the root of the tail fin (This point is called “point R”). Then I quantified the angles of ∠QPR for each capture of clasping by using ImageJ, subtracted it from 180 °, and compared this value (termed as “tail angle”) between the clasping culminating/not culminating in oviposition.

Behavioral experiment

The day before the experimental day, I prepared the several pairs of medaka describes below (Figure 3-2). I used sexually matured females that were confirmed to show the spawning for three consecutive days before preparation. I placed the pairs to the experimental tank (described in chapter 1) [36], separated individually until the analysis by putting a transparent perforated partition diagonally across the tank. The behavioral experiments were carried out the next morning. After experiment session, I anesthetized the females by immersion in 0.02 % tricaine methanesulfonate (MS-222) and perform the tissue preparation steps.

The flow of conditioning sessions is described below.

Female and male pair

I paired the female with the intact male and placed the pairs to the experimental tank with partition (Figure 3-2A). At 9:00-10:00 of the experimental day, I removed the partition to allow females and males to interact, then picked up the females 25 minutes after they showed spawning behavior. They were immediately anesthetized and performed the tissue preparation steps described below.

Female and female pair

I paired the female with the intact female and placed the pairs to the experimental tank with partition (Figure 3-2B). At 9:00-10:00 of the experimental day, I removed the partition to allow females to interact. I picked up the females 60 minutes after partition-removal, then I immediately anesthetized and performed the tissue preparation steps.

Female and fin-removed male pair

In the previous studies, males embrace females using their dorsal and anal fins when clasping; wrapping female and quivering together [34]. Actually, the pairs of which the male is removed their dorsal and anal fins impair the spawning behavior and consequently cannot obtain fertilized eggs [123]. I excised male's dorsal and anal fins using surgical razor and recovered them overnight in 0.8 % NaCl water. The day before conditioning, I paired them with intact female and placed the pairs to the experimental tank with partition (Figure 3-2C). At 9:00-10:00 of the experimental day, I removed the partition to allow females and males to interact, then picked up the females I picked up the females 60 minutes after partition-removal, then I immediately anesthetized and performed the tissue preparation steps.

Partitioned female and male

The pairs are prepared by the same method of female and male pair. Until 10:00-11:00 of the experimental day, the females and males were remained separated, then females were picked up, immediately anesthetized by immersion in 0.02 % MS-222, and carried on the tissue preparation steps (Figure 3-2D).

In situ hybridization

Immediately after anesthetizing of females, I quickly fixed them by perfusion with 4 % paraformaldehyde (Nakarai Tesque, Kyoto, Japan) in 1.0 × phosphate-buffered saline (PBS) (Takara Bio, Shiga, Japan) for 30 seconds from the bulbus arteriosus using a borosilicate glass pipette made from capillaries with 1.5-mm outer diameters (GD-1.5; Narishige, Tokyo, Japan). After perfusion, I decapitated, dissected out the whole brain, and soaked it in 4 % PFA in 1.0 × PBS for ten minutes at room temperature. And then I substituted with 30 % (w/v) sucrose

(FUJIFILM Wako Pure Chemical Corporation, Osaka, Japan) in 1.0 × PBS overnight at 4 °C. I embedded the brain with 5 % ultra-low melting agarose (Sigma-Aldrich, Darmstadt, Germany) / 20 % sucrose (w/v) in 1.0 × PBS and prepared cryosections by frontal cutting serially at 25 μm intervals by using a cryostat (CM 3050S; Leica Microsystems, Wetzlar, Germany). The sections were mounted onto CREST-coated glass slides (Matsunami, Osaka Japan).

I prepared digoxigenin (DIG)-labeled sense and anti-sense cRNA probes. Template cDNA was prepared from the female brain by reverse-transcription PCR. The primer sequences for this reaction are described in Table 3-1. PCR product was inserted in a pCR®2.1-TOPO® Vector (Invitrogen, Waltham, MA) and transcribed *in vitro* for three hours at 37 °C, using a DIG labeling kit (Roche Applied Science, Manheim, Germany). Transcription products were extracted, which were used as cRNA probes.

In situ hybridization (ISH) was performed on the brain cryosections. All the specimens were washed with 3 % Triton X-100 (FUJIFILM) in 1.0 × PBS (1.0 ×PBST), postfixed with 4 % PFA in 1.0 × PBS for ten minutes, treated with 2 mg/mL glycine in 1.0 × PBS, and incubated with 0.25 % acetic anhydride in 0.1 M triethanolamine for ten minutes. Then the specimens were incubated for 90 minutes at 58 °C with hybridization buffer containing 50 % formamide, 3.0 × saline sodium citrate (SSC), 0.12 M phosphate buffer, 1.0 × Denharldt's solution (Sigma-Aldrich), 100 μg/mL calf thymus DNA solution (Invitrogen), 10 % Dextran sulfate (Sigma-Aldrich), and 125 μg/mL tRNA solution (Roche). The specimens were incubated overnight at 58 °C with hybridization buffer containing 100 ng/mL DIG-labeled *egr1* cRNA probe. After hybridization, the specimens were twice washed with 50 % formamide in 2.0 × SSC for 15 minutes at 58 °C and incubated with 20 μg/mL RNase A for 30 minutes at 37 °C in TNE buffer (1 % 1M Tris-HCl (pH 7.5) / 10 % 5 M NaCl / 0.2 % 0.5 M EDTA (v/v)). The slides were washed for ten minutes at 37 °C once, 2.0 × SSC for 15 minutes at 58 °C twice, 0.5 × SSC for 15 minutes at 58 °C, and then

soaked in pH 7.6 Tris buffered saline with Tween 20 (TBS-T) (Sigma-Aldrich) for five minutes. Blocking treatment was performed with 1.5 % blocking reagent (Roche) in TBS-T for 30 minutes.

For the detection of *egr1* mRNA, DIG signals are fluorescently visualized. I incubated the slides with a horseradish peroxidase-conjugated anti-DIG antibody (Roche) diluted 1:500 with TBS-T for 2 hours, washed with TBS-T, then applied Tyramide Signal Amplification / Cyanine 3 (TSA/Cy3) detection kit (Perkin Elmer, Waltham, MA) for ten minutes at room temperature. After washing the slides with 1.0 × PBST, I applied 4',6-diamidino-2-phenylindole (DAPI) (Dojindo laboratories, Kumamoto, Japan) diluted 1:1,000 with 1.0 × PBS for the fluorescent visualization of nucleus localization. The slides were observed and photographed the brain nuclei, which are known to express *esr2b*; ventral telencephalon pars dorsalis/supracommissuralis/posterior (Vd/Vs/Vp), rostral part of nucleus preopticus pars parvocellularis (rPOp), nucleus preopticus pars magnocellularis (POm), nucleus posterioris peroventricularis (NPPv), nucleus ventralis tuberis (NVT) [29, 30] under a LSM-710 confocal laser-scanning microscope (Carl Zeiss, Oberkochen, Germany). The nomenclature of the medaka brain nuclei was identified following the previous study [124], while it should be noted that Vd/Vs/Vp is regarded as the ventral telencephlic region of posterior-Vd to Vp in the present study.

On the other hand, I detected the signals of other genes except for *egr1* by chemogenic detection. After blocking step, I incubated the slides with an alkaline phosphatase-conjugated anti-DIG antibody diluted 1:1000 with TBS-T (Roche) for 1 hours, washed with TBS-T, then applied NBT/BCIP as chemogenic substrates. The slides were observed and photographed the region containing Vd/Vs/Vp under a Leica DM5000 B equipped with a digital camera Leica DFC310 FX (Leica).

I counted the number of signal-positive cells and by using a plugin function "*Cell Counter*" of ImageJ (https://imagej.nih.gov/ij/). Cell counting was performed by blind test.

Dual *in situ* hybridization

To analyze the co-expression of two genes, whether I performed dual *in situ* hybridization. The brain samples were obtained from the females that were confirmed to show the spawning for three consecutive days before sampling. Also, for dual ISH for *egr1* and another gene, behavioral conditionings were performed as well as single ISH for *egr1* in the female that interact with female/male. Slide preparation and cRNA probe preparation were performed in the same methods for single ISH, while cRNA probes for another gene were labeled with fluorescein (FL), using a FL labeling kit (Roche) The primer sequences for probe preparation are described in Table 3-1. All the procedures up to the DIG signal detection step were performed as described in the previous section (*in situ* hybridization), except for the hybridization step that the sections were incubated overnight at 58 °C with hybridization buffer containing 100 ng/mL DIG-labeled cRNA probe / 200 ng/mL FL-labeled cRNA probe. After the detection of DIG signal, I incubated the slides with 3 % H_2O_2 in 1.0 × PBS for 60 minutes in order to quenching the peroxidase activity for the detection of DIG signal. Blocking treatment was performed with 1.5 % blocking reagent in TBS-T for 30 minutes, and I incubated the slides with a horseradish peroxidase-conjugated anti-FL antibody (Roche) diluted 1:500 with TBS-T for two hours, then applied Tyramide Signal Amplification / Plus Biotin (TSA/biotin) detection kit (Akoya Biosciences, Marlborough, MA) for ten minutes at room temperature. I applied VECTASTAIN ABC Elite kit for signal-amplification (Vector laboratories, Burlingame, CA) before visualization with Alexa Fluor 488-conjugated streptavidin (Invitrogen).

The slides were observed and photographed the region containing Vd/Vs/Vp under a LSM-710 confocal laser-scanning microscope, with visualization DIG/FL signals to magenta/green, respectively. Cell counting was performed by the same method described in the session "*in situ* hybridization".

Laser microdissection microscopy

At 10:00-11:00, I deeply anesthetized *esr1*:*egfp* Tg female medaka with 0.02 % MS-222, decapitated and dissected out the whole brain. Then I quickly rinsed the brain with 1.0 × PBS, embedded in 5 % ultra-low melting agarose / 20 % sucrose (w/v) in 1.0 × PBS, and prepared cryosections by frontal cutting serially at 8 μm intervals by using a cryostat (CM 3050S). The sections were mounted onto polyethylene naphthalate film-coated glass slides (Leica) and stored at –80 °C until laser-microdissection (LMD).

Before LMD, the slides were immediately air dried using a blower. The regions express *egr1* or *esr2b* in Vd/Vs/Vp were laser-microdissected using the LMD7000 (Leica) with observing GFP fluorescence expressed in *esr2b*-expressing neuron as a landmark, and collected into the cap of a 0.2 mL microtube (Ina-Optika, Osaka, Japan). Six serial sections were collected from each female, and I prepared three tubes that were pooled samples for two individuals. The tissue samples were spun down to the bottom of microtubes by centrifugation at 15,000 × g for one minute.

RNA-sequencing and data analysis

I applied NEBNext Single Cell/Low Input RNA Library Prep Kit for Illumina (New England Biolabs, Ipswich, MA) for the preparation of the sequencing libraries. The laser-microdissected tissue samples were dissolved in lysis buffer and then used as template for reverse-transcription. Sequencing libraries were prepared according to the manufacture's protocols. Barcode-sequence ligation was conducted with using NEBNext Multiplex Oligos for Illumina (New England Biolabs). The concentration and length of sequencing libraries were measured using Qubit Fluorometer (Thermo Fisher Scientific, Waltham, MA) and Tapestation (Agilent Technologies, Santa Clara, CA), respectively. Sequencing was performed using the illumina NovaSeq 6000 (2 × 150) at Nippon Genetics (Tokyo, Japan).

The obtained reads were trimmed using PRINSEQ++ v0.20.4 [125] and mapped on the *O. latipes* reference assembly using STAR v2.7.9a [126] with default parameters. The mapped read numbers and TPM (transcripts per kilobase million) value of each gene were counted using RSEM v1.3.3 [127]. I selected the candidate genes judging from TPM values in the obtained data.

Quantification of tail-bending behavior

To quantitatively comparing the tail-bending behavior performed during the clasping that showed/did not oviposition, I obtained the video-capture at the timing of clasping behavior from the video of intact female and male pairs (Figure 3-2). I traced the posture by drawing two lines from anus (This point is called “point P”) to the rostral edge (This point is called “point Q”) and the root of the tail fin (This point is called “point R”). Then I quantified the angles of ∠QPR are quantified for each capture of clasping by using ImageJ, subtracted it from 180 °, and compared this value (termed as “tail angle”) between the clasping that showed/did not show oviposition.

GFP immunohistochemistry

I deeply anesthetized *esr1*:*egfp* Tg female medaka with 0.02 % MS-222, quickly fixed them by perfusion with 4 % PFA in 1.0 × PBS, decapitated, and dissected out their whole brain. Cryosections were obtained by the same methods for ISH, washed by 1.0 × PBST, and incubated with anti-GFP rabbit IgG diluted 1:2000 with 5 % normal goat serum in 1.0 × PBST overnight. The sections were washed with 1.0 × PBST, and applied biotinylated anti-rabbit IgG goat IgG diluted 1:200 with 1.0 × PBST at room temperature for two hours. Then I washed the specimens, applied VECTASTAIN ABC Elite kit for signal-amplification, and visualized signals with Alexa Fluor 488-conjugated streptavidin (Invitrogen). The slides were observed and photographed the region containing Vd/Vs/Vp under a LSM-710 confocal laser-scanning microscope.

Dual labeling of *esr2b in situ* hybridization and GFP immunohistochemistry

All the procedures up to the application of biotinylated anti-rabbit IgG antibody were performed as described in the previous section (GFP immunohistochemistry), then I perform the ISH steps from washing the specimen with 1.0 ×PBST, to fluorescent visualization of *esr2b* mRNA signals by using *esr2b*-specific DIG-labeled cRNA probe and TSA/Cy3. After washing specimen, applied VECTASTAIN ABC Elite kit for signal-amplification, and visualized GFP-immunoreactive (ir) signals with Alexa Fluor 488-conjugated streptavidin (Invitrogen). The slides were observed and photographed the region containing Vd/Vs/Vp under a LSM-710 confocal laser-scanning microscope with visualization *esr2b* mRNA/GFP-ir signals to magenta/green, respectively.

Statistical analysis

All the values are presented as mean ± standard error of the mean (SEM). Statistical analyses and graph drawing were performed by using R (R Core Team 2020). For comparing between two groups, Mann–Whitney *U* test was employed, except for the analysis of tail-bending behavior, which was analyzed by Welch's *t* test. On the other hand, data were analyzed by the non-parametric Kruskal-Wallis test followed by Dunn-Bonferroni test using the *Dunn.test* package (https://cran.r-project.org/web/packages/dunn.test/index.html) for more than two groups. All parameters are shown by the whisker and scatter plot. We used the *beeswarm* package to perform the scatter plot. A *P*-value less than 0.05 was considered statistically significant.

Results

Female medaka bend their body during the spawning behavior culminating in oviposition

First of all, for better understanding of the phases of female sexual behaviors, I observed the postures of female during the clasping behavior (Figure 3-1). I quantified the maximum angle of the female tail-bending while it is clasped by a male. Here I found a clear difference in this maximum angle between the clasping culminating in spawning (termed as "Culminating (in spawning)") and clapsing that failed to spawn (termed as "Not culminating (in spawning)") (Figures 3-1A and B). This result suggests that females bend and thrust their body to the male (termed as "tail-bending") only during the successful spawning behavior leading to oviposition. Thus, the tail-bending can be regarded as a fixed action pattern of spawning behavior for oviposition (egg release).

Neurons in the ventral telencephalon showed higher expression of *egr1* in the female that performed tail-bending behavior

To identify neural populations that are involved in female clasping behavior, I performed *in situ* hybridization (ISH) for an immediate early gene (IEG), *egr1*, with special reference to the brain nuclei, ventral telencephalon, preoptic area, and hypothalamic region, where *esr2b*, an estrogen receptor subtype involved in sexual behavior is expressed (Figure 3-3). Here, I found that significantly more *egr1*-expressing cells were found in Vd/Vs/Vp of females paired with males (that had physical contacts and received various sensory stimuli from males, and performed sexual behaviors) compared to those of females paired with females (that did not perform sexual behaviors), suggesting that this *egr1* expression may be associated with the sexual behavior (Figures 3-3A and B).

For detecting more precise timing of *egr1* induction in Vd/Vs/Vp during sexual behavior in female, I further performed *egr1* ISH in the control females who were partitioned with an intact male, those who interacted with a dorsal and anal fin-removed male, and those who interacted with an intact male (Figures 3-3C and D). Female separated from male was not able to physically interact with the male, so they were only courted by the male from the opposite side of the partition. On the other hand, since the fin-removed males could not clasp the female for successful spawning, the females were clasped by fin-removed male for a much shorter time. Therefore, the females rarely showed tail-bending and subsequent spawning leading to oviposition. Actually, in the present experiment, four out of six females did not show tail-bending behavior accompanied by oviposition. The number of *egr1*-expressing cells were significantly higher in the females who interacted with the intact male (group A in Figure 3-2) than in the females separated from the male (group D in Figure 3-2) and that in females with fin-removed male (group C in Figure 3-2) (Figures 3-3C and D). It should be noted that more *egr1*-expressing cells were found in females that clasped and spawned with fin-removed male than that in females did not spawned with fin-removed male, which appeared to resemble those expression in females interacted with intact male. These findings indicate that Vd/Vs/Vp neurons show high neural activity with *egr1* expression in females that performed persistent clasping leading to oviposition, which was manifested by tail-bending behavior. Hereafter, these neurons are termed as *egr1*$^{Vd/Vs/Vp}$ neurons.

egr1$^{Vd/Vs/Vp}$ neurons did not express *esr2b*

From the expression pattern of *egr1*, it is suggested that the neural population involved in the female spawning behavior is located in Vd/Vs/Vp, which was shown to express *esr2b* [29, 30]. Considering this fact, I next performed dual ISH for *egr1* and *esr2b* to investigate whether *egr1*$^{Vd/Vs/Vp}$ neurons also express *esr2b* (Figure 3-4). I found that the *egr1*-positive signals were

located in dorsolateral subpopulation of Vd/Vs/Vp, wheareas *esr2b* signals were located in the ventromedial subpopulation of Vd/Vs/Vp. The cells that showed both *egr1* and *esr2b* signals were barely found. It suggests that the *egr1*$^{Vd/Vs/Vp}$ neurons are distinct from the *esr2b*-expressing neurons in Vd/Vs/Vp (hereafter called the *esr2b*$^{Vd/Vs/Vp}$ neurons).

RNA-seq analysis identified the candidate neurotransmitter/neuromodulators of *egr1*$^{Vd/Vs/Vp}$ and *esr2b*$^{Vd/Vs/Vp}$ neurons

For characterization of *egr1*$^{Vd/Vs/Vp}$ and *esr2b*$^{Vd/Vs/Vp}$ neurons, I performed gene-expression RNA-sequencing (RNA-seq) analysis of the micro-dissected brain area including *egr1*$^{Vd/Vs/Vp}$ or *esr2b*$^{Vd/Vs/Vp}$ neurons by using laser-microdissection microscopy (LMD). Results of the RNA-seq of the brain area including *egr1*$^{Vd/Vs/Vp}$ neurons (Total reads: 20737172.67 ± 223235.75, aligned base rate (%): 42.85 ± 0.92) showed approximately 130 genes that have high TPM values (> 1000) regarded as the candidate gene for their neurotransmitters/neuromodulators or markers. Among these genes, I found that *gad1.1*, which is a gene coding an enzyme for γ-aminobutanoic acid (GABA) synthesis (ENSORLG ID: ENSORLG00000009208) was highly expressed in this region (TPM value; 1017 ± 116.67). Subsequent analysis of the co-expression of *gad1.1* and *egr1* by dual ISH in the female that clasped with male indicated that almost 80 % of *egr1*-positive cells co-express *gad1.1* (Figures 3-5A-C), which suggests that most of *egr1*$^{Vd/Vs/Vp}$ neurons are GABAergic (*gad1.1*/*egr1*$^{Vd/Vs/Vp}$ neurons).

Also, I analyzed the RNA-seq results of the area including *esr2b*$^{Vd/Vs/Vp}$ neurons (Total reads: 22377249.33 ± 3243901.34, aligned base rate (%): 41.34 ± 3.77) aiming at identifying the neurotransmitters/neuromodulators or markers of these neurons. I found that several genes coding for neuropeptides, such as neuropeptide B (*npb*, ENSORLG ID: ENSORLG00000025130), cholecystokinin (*cck*, ENSORLG ID: ENSORLG00000005949), and C-type natriuretic peptide-

1 (*cnp1*, ENSORLG ID: ENSORLG00000012204) showed high TPM values (TPM value: *npb*; 34209.65 ± 7019.55, *cck*; 1475.63 ± 293.61, *cnp1*; 2003.01 ± 317.08). To confirm the co-expression of these candidate genes and *esr2b* in Vd/Vs/Vp, I conducted dual ISH for *npb* / *cck* / *cnp1* and *esr2b* and found that mRNA signals of all these three genes were clearly co-localized with *esr2b* mRNA signal (Figure 3-5D). From these results, NPB / CCK / CNP1 were identified as neuromodulators that are released from *esr2b*$^{Vd/Vs/Vp}$ neurons; I here prefer neuromodulator to neurotransmitter, since these are considered to be neuropeptides whose receptors are GPCR or guanylyl cyclase. Among them, *npb* has been also reported to show female-biased expression in *esr2b* expressing neurons [100, 128], which is consistent with my dual ISH results here.

Some of the *esr2b*$^{Vd/Vs/Vp}$ neurons appear to project to the lateral region of Vd/Vs/Vp in which *gad1.1*/*egr1*$^{Vd/Vs/Vp}$ neurons are located

Next, I performed EGFP immunohistochemistry (IHC) in the brain of *esr1*:*egfp* transgenic (Tg) female medaka in which most of the EGFP-ir neurons express *esr2b*, and the IHC signals in the neurites may be regarded as the neurites of *esr2b*$^{Vd/Vs/Vp}$ neurons (Figure 3-6A). It sould be noted that some neurons in Vd/Vs/Vp co-express several subtypes of Esr [122], which is consistent with the results here that EGFP-ir neurons in Vd/Vs/Vp co-express *esr2b*. I observed axonal projections of EGFP-positive neurons in Vd/Vs/Vp and found that a part of EGFP-positive fibers was detected in ventral part from Vd/Vs/Vp. However, EGFP-positive fibers were also detected in lateral part of Vd/Vs/Vp, which is a region that *gad1.1*/*egr1*$^{Vd/Vs/Vp}$ neurons are located (Figure 3-6B). In addition, I observed several varicosities along the neurites arising from the cell bodies (Figure 3-6C, arrowheads), which have been considered to represent structures for the accumulation and release of neuromodulators. Taken together, it may be suggested that at least some of the *esr2b*$^{Vd/Vs/Vp}$ neurons may release the above-mentioned neuropeptides to act as

neuromodulators affecting neurons including the *gad1.1*/*egr1*$^{Vd/Vs/Vp}$ neurons.

GABAergic neurons in Vd/Vs/Vp appear to express *cckbr* and *olgc7*, receptor genes for CCK and CNP1

I analyzed the data for RNA-seq of *egr1*$^{Vd/Vs/Vp}$ again and searched for the receptor genes for the neuropeptides, NPB / CCK / CNP1, assuming a possible existence of peptidergic neuromodulatory signaling from *esr2b*$^{Vd/Vs/Vp}$ neurons to the *gad1.1*/*egr1*$^{Vd/Vs/Vp}$ neurons. I found that *cckbr* (ENSORLG ID: ENSORLG00000024681) and *olgc7* (ENSORLG ID: ENSORLG00000001459), which are receptor gene for CCK, and CNP1, respectively, were possibly expressed in *egr1*$^{Vd/Vs/Vp}$ neurons, whereas NPB receptor *npbwr2* (ENSORLG ID: ENSORLG00000016815) did not appear to be expressed considering the TPM values (*npbwr2*; 4.44 ± 2.51, *cckbr*; 95.43 ± 9.86, *olgc7*; 33.70 ± 10.56). Although it is preliminary, single ISH results showed that mRNA signals of *cckbr*/*olgc7* were located in the ventrolateral part of Vd/Vs/Vp in which *gad1.1*-expressing neurons are located (Figure 3-7). Taken together with this result and the properties of *gad1.1*/*egr1*$^{Vd/Vs/Vp}$ neuron, it is conceivable to be exist the neuromodulatory signaling from the *esr2b*$^{Vd/Vs/Vp}$ neurons to the *gad1.1*/*egr1*$^{Vd/Vs/Vp}$ neurons via neuropeptides such as CCK, and/or CNP1.

Discussion

In this chapter, I quantitatively analyzed the female sexual behavior “tail-bending”, which is actively performed by female medaka during the successful spawning behavior leading to oviposition. I also performed histological analysis and found that a neural population in Vd/Vs/Vp is activated during the spawning behavior. Interestingly, these neurons were distinct from *esr2b*-expressing neurons that has been suggested to play a role in female specific sexual behavior. LMD/RNA-seq analysis followed by dual ISH analysis identified GABA and NPB/CCK/CNP1 as neurotransmitter/neuromodulators used by the *egr1* and *esr2b* -expressing neurons in Vd/Vs/Vp, respectively. Further analysis suggested the existence of peptidergic neuromodulatory signaling using CCK and/or CNP1 from *esr2b*-expressing neurons to the *egr1*-expressing neurons in Vd/Vs/Vp.

Quantitative description of the active repertoires of sexual behavior in female medaka

Sexual behavior of medaka can be largely divided into four behavioral repertoires: following, courtship, clasping, and spawning (each repertoire was referred to as approaching to courting orientation, head-up I to courting round dance, head up II to copulation, and spawning, respectively in the previous literature [34]). Following and courtship is initiated by a male, and a female perceives these behaviors and appear to “make decision” as to accept or refuse the male. Including these two behavioral repertoires, males appear to start the clasping behavior by wrapping the female with their dorsal and anal fins. After this wrapping by a male, the female and male quiver their bodies and start spawning, and I follow this nomenclature in the present thesis. Although these sequential behaviors mainly lead by males have been well investigated previously, there are a few reports that mentioned an active behavior by female as short descriptions and did

not quantitatively analyze them [129]. In the present study, I identified and quantitatively analyzed a behavioral repertoire actively performed by female, and termed it as “tail bending”, bending their caudal body during clasping behavior leading to spawning, simultaneously with the male (Figure 3-2). Tail-bending is considered to be equivalent to the repertoire termed “quivering” in the previous studies [34], judging from the order of the behavioral repertoires. However, quivering behavior and its importance in the behavioral context have never been analyzed in detail because of its difficulty in quantification. The present study enabled quantifying quivering behavior by measuring tail angles. It is suggested that the tail-bending behavior is prerequisite for spawning leading to oviposition, which also agrees well with the previous study [129]. Taken together, it is natural that not only male but also female actively perform the sexual behavior for successful reproduction also in medaka.

GABAergic neurons in ventral telencephalon appear to elicit the tail-bending and/or oviposition in female

Ventral telencephalon has been suggested to play a pivotal role in the activation of sexual behavior in some teleosts. Local electrolytic lesion of this region disrupted the male sexual behavior in goldfish (*Carassius auratus*) [24]. Also, local electrical stimulation of Vd/Vs/Vp of himé/kokanee salmon (*Oncorhynchus nerka*) and goldfish elicits the sexual behavior in both female and male [25, 26]. It should be noted that himé/kokanee salmon female performed “spawning act” immediately after stimulation, which suggests that the neurons in the ventral telencephalon directly activates spawning behavior by rapid neural transmission. In the present study, I used one of the IEGs, *egr1* expression for labeling the neurons that are activated during the sexual behavior. Although IEGs generally have low time resolution (minutes to tens of minutes), I succeeded in labeling specific neural population that is responsible for a specific

behavior by using the experimental protocol used in the present thesis. *egr1* was increased specifically in some neurons in Vd/Vs/Vp of female medaka that performed tail-bending and subsequent spawning/oviposition (Figure 3-3). Interestingly, such *egr1* induction was not observed in the females that were separated from male or in the females who interacted with fin-removed males (Figure 3-3C and D), suggesting that *egr1* expression in Vd/Vs/Vp is enhanced in females that perform spawning behavior, not in the females that approached by male and considered to have increased their sexual motivation. Considering results of the previous studies in the other species of teleosts described above, my present results suggests that the *egr1* neurons in Vd/Vs/Vp may be responsible for tail-bending/spawning in female medaka.

The results of RNA-seq and dual ISH for *egr1* and *gad1.1* indicated that *egr1*$^{Vd/Vs/Vp}$ neurons are GABAergic (Figures 3-5A-C). GABA is a major neurotransmitter for fast inhibitory transmission in the central nervous system. It is consistent with the present hypothesis that the neurons in Vd/Vs/Vp can evoke instantaneous and acute activation of the sexual behavior, although the neural target to be inhibited is yet to be identified.

To my knowledge, the identified neurons in the present study were the first reported GABAergic neurons involved in the sexual behavior in teleost. Taken together with the previous studies in other teleost species reporting the importance of Vd/Vs/Vp in sexual behavior, it is conceivable that GABAergic neurons in medaka Vd/Vs/Vp are one of the major components of the neural circuit for promoting female spawning behavior, which may be conserved in teleost species.

Vd/Vs/Vp GABAergic neural subpopulation possibly receive the peptidergic signaling from the adjacent estrogen-receptive neurons

In the present study, I showed that GABAergic neurons in Vd/Vs/Vp showed high neural activity labeling with *egr1* during female tail-bending / spawning behavior (*gad1.1*/*egr1*$^{Vd/Vs/Vp}$

neurons). However, this subpopulation did not express *esr2b*, and *esr2b*-expressing neural subpopulation (*esr2b*$^{Vd/Vs/Vp}$ neurons) are located adjacent to *gad1.1*/*egr1*$^{Vd/Vs/Vp}$ neurons (Figure 3-4). *esr2b*-expressing neurons is considered to be important for female receptivity, because KO female medaka avoid the courtship display by male and do not show clasping behavior despite their normal gonadal maturation (Chapter 2) [100]. Thus, it is suggested that *esr2b*-expressing neurons and *gad1.1*/*egr1*$^{Vd/Vs/Vp}$ neurons are involved in different phase of the female sexual behavior, female receptivity and spawning behavior leading to oviposition, respectively, which is consistent with the present results that *gad1.1*/*egr1*$^{Vd/Vs/Vp}$ neurons are anatomically distinct from *esr2b*-expressing neurons. Although *esr2b*-expressing neurons were not labeled by *egr1* ISH, it does not mean they are not activated, because immediate early genes including *egr1* are considered to label not all, but only a small portion of, the activated neurons. Because *esr2b* plays an important role in the female receptivity, they should rather be considered to be activated at some phase of sexual behavior. Recently, it was shown that the gene for NPB, *npb* is expressed in *esr2b*-expressing neurons in Vd/Vs/Vp and POm in mature female medaka [97, 100, 128], which is consistent with my present result of RNA-seq and dual ISH analysis that showed co-expression of *esr2b* and *npb* (Figure 3-5D). Also, regarding *npb* and *npbwr2*, which is a NPB receptor gene, KO females of either of these genes showed the delay in the first clasping and spawning, which indicates that estrogen/*esr2b*-regulated NPB/NPBWR2 signaling partially contributes to the female receptivity in medaka [128], while the neural circuit involved in NPB/NPBWR2 signaling remains unclear.

On the other hand, histological analysis indicated that some of *esr2b*$^{Vd/Vs/Vp}$ neurons appeared to extend neurites with varicosity-like structures to the region where *gad1.1*/*egr1*$^{Vd/Vs/Vp}$ neurons are localized (Figure 3-6). I further identified candidates of ligand-receptor combinations for this peptidergic signaling, *cck*/*cckbr* and *cnp1*/*olgc7* by RNA-seq from laser-microdissected tissues.

Subsequent analysis by *in situ* hybridization indicated that *cck* and *cnp1* are expressed in *esr2b*$^{Vd/Vs/Vp}$ neurons (Figure 3-5D). In addition to this, my preliminary experiments showed that *cckbr*/*olgc7* were expressed in the dorsolateral part of Vd/Vs/Vp in which *gad1.1*/*egr1*$^{Vd/Vs/Vp}$ neurons are localized (Figure 3-7). From these findings, I hypothesized that *gad1.1*/*egr1*$^{Vd/Vs/Vp}$ neurons may receive peptidergic signaling from *esr2b*$^{Vd/Vs/Vp}$ neurons via CCK and/or CNP1. This peptidergic signaling probably results in some kinds of neuromodulatory effects on the activation of tail-bending/spawning behavior. Contrary to CCK and CNP1, NPB are not considered to contribute to the neural pathway from *esr2b*$^{Vd/Vs/Vp}$ neuron to *gad1.1*/*egr1*$^{Vd/Vs/Vp}$ neuron, because gene-expression level of *npbwr2* was very low in the laser-microdissected tissue including *gad1.1*/*egr1*$^{Vd/Vs/Vp}$ neuron (TPM value was shown in the Results section). Although the previous study demonstrated that *npbwr2* is expressed in Vs/Vp [128], my RNA-seq analysis of either dorsal or ventral part of Vd/Vs/Vp in the present study showed a low level of *npbwr2* transcripts. This discrepancy may be explained by a possibility that the area examined are different between these two studies along the rostro-caudal axis.

While CCK was first identified as one of the gastrointestinal hormones [130], another CCK subtype consisting of 8 amino acids is expressed in the brain and supposed to serve as a neurotransmitter that is associated with anxiety and social behavior [131-134]. Furthermore, it has been reported that the gene expression of CCK and their receptor is regulated by estrogen and is supposed to be involved also in female sexual behavior in rodent species [23, 135]. In the present study, I have shown that *esr2b*$^{Vd/Vs/Vp}$ neurons appear to release CCK as a neuromodulator. Thus, CCK may contribute to female sexual behavior in an estrogen-dependent manner also in medaka, and this mechanism may be conserved among vertebrates. Further analyses of CCK and CCK-releasing neurons may prove this possible functions of this neural system in medaka.

In addition to CCK, I identified CNP1 as another candidate neuromodulator for the neural

circuit consisting of *esr2b*$^{Vd/Vs/Vp}$ neuron and *gad1.1*/*egr1*$^{Vd/Vs/Vp}$ neuron. CNP is a neuropeptide that belongs to the same family as atrial natriuretic peptide (ANP) and B-type natriuretic peptide (BNP), which regulates circulatory and fluid homeostasis in vertebrates [136]. In medaka, CNP1 is specifically expressed in the central nervous system [137], although its function is yet to be determined. Preliminary analysis indicated that OlGC7, which is one of the CNP receptor subtypes, is expressed in the Vd/Vs/Vp of female medaka (Figure 3-7). OlGC7 is a membrane-bound guanylate cyclase, which eventually modifies the properties of ion channels the second messenger, cyclic GMP (cGMP) [137-139]. Considering these results, it is suggested that *esr2b*$^{Vd/Vs/Vp}$ neurons may modulate firing activity or excitability of *gad1.1*/*egr1*$^{Vd/Vs/Vp}$ neurons.

For the elucidation of the existence of such neuromodulatory effect, further multidisciplinary analyses are required; for example, IHC using anti-CCK/CNP1 antibody, electrophysiological examination of the effects of these peptides on the *gad1.1*/*egr1*$^{Vd/Vs/Vp}$ neurons. By performing these lines of multidisciplinary analyses, it is hoped that the functional characteristics of the estrogenic neuromodulation on the neural circuit for activation of tail-bending/spawning behavior will be unraveled in the near future.

In summary, I identified GABAergic neurons in the ventral telencephalon Vd/Vs/Vp that show high level of neural activity labeling with *egr1* during female spawning behavior (*gad1.1*/*egr1*$^{Vd/Vs/Vp}$ neuron), which are probably involved in the activation of tail-bending/spawning behavior in female. These neurons are distinct from the *esr2b*-expressing neurons, which are also distributed in Vd/Vs/Vp (*esr2b*$^{Vd/Vs/Vp}$ neuron), which is located close to the *gad1.1*/*egr1*$^{Vd/Vs/Vp}$ neurons. In addition, histological analyses suggested that there may be a local neural circuit consist of *esr2b*$^{Vd/Vs/Vp}$ and *gad1.1*/*egr1*$^{Vd/Vs/Vp}$ neurons using neuropeptide, CCK and/or CNP1 for neuromodulation, which may contribute to the sensing and signaling of

the gonadal status. Further analysis of this neural circuitry will reveal the neural mechanisms by which the female sexual behavior is activated in synchrony with gonadal maturation in teleosts.

Table 3-1

The list of primers used for probe preparations in Chapter 3. *esr2b* probes and the constructs for *npb* probe preparation were gifted by Drs. Daichi Kayo and Kataaki Okubo (The University of Tokyo), respectively. Also, primer sequences of *cck* probes are described in Nakajo *et al.*, 2018 [71].

Primer name	Purpose	Sequence
egr1 cds-F70	Preparation of *egr1* probes for ISH	5'-GAAGGTGCAGGCTTTGGCTC-3'
egr1 cds-R1293	Preparation of *egr1* probes for ISH	5'-GATGGTGGATGCAACCGAGG-3'
esr2b-F	Preparation of *esr2b* probes for ISH	5′-AAGAGGTAGATGCCAGCAAAGC-3′
esr2b-R	Preparation of *esr2b* probes for ISH	5'-GGATCTTCTTGGCCCAGCTGA-3'
MfGAD1-1 SE	Preparation of *gad1.1* probes for ISH	5'-GAGGCTGTGACTCATGGGTG-3'
MfGAD1-1 AS	Preparation of *gad1.1* probes for ISH	5'-TGGTCGGACAGCTCCAGGTTG-3'
npb-F1	Preparation of *npb* probes for ISH	5'-AGCACACAGCCGTTTCCACTGAG-3'
npb-R1	Preparation of *npb* probes for ISH	5'-GAAATTACAGCTCACATATGTACATTCATC-3'
mf_SP6-CCK_Fw	Preparation of *cck* probes for ISH	5′-TTATTTAGGTGACACTATAGATCACACGCTCAACTTCTCTCC-3′
mf_SP6-CCK_Rev	Preparation of *cck* probes for ISH	5′-AATTCTAATACGACTCACTATAGGGAACCTTCTCCATCCCAAATGATTAAG-3′
*cnp1*_probe_Fwd1	Preparation of *cnp1* probes for ISH	5'-ATGCTGTGTCCTGTGCTGC-3'
*cnp1*_probe_Rev1	Preparation of *cnp1* probes for ISH	5'-CTAACAGCCCAGTCCACTCATTG-3'

Figure legends

Figure 3-1

Tail-bending behavior analysis. (A) Snapshots of tail-bending behavior leading to oviposition (successful spawning) and unsuccessful spawning that failed to lead to oviposition. Tail angle was defined as the acute angle made by the bent body lines. (B) Tail angle shown during clasping leading to oviposition (Culminating (in spawning)) showed significantly larger than that which failed to show spawning (Not Culminating (in spawning)) (Culminating; 54.41 ± 3.98 °, Not culminating; 12.80 ± 2.56 °, ***P = 0.00000144).

Figure 3-2

Schematic diagram of the behavioral experiment. Four experimental groups were prepared as described below. (A) A female was allowed to interact with intact male. Twenty-five minutes after they showed spawning leading to oviposition, the female was removed. (B) A female who interacted with a female. In this condition, both of the two females never exhibited any sexual behavior. Sixty minutes after partition-removal, the females were removed and was subjected to histological analysis. (C) The pair of a male whose dorsal and anal fins were removed frequently failed to show spawning. Four out of six pairs did not spawn in the present study. The female was removed 60 minutes after removal of the partition, regardless of the occurrence of spawning. (D) A female was partitioned from an intact male with transparent perforated partition; the female can ‘see’ the male’s courtship display (or perhaps can also receive the male’s pheromonal signal) but cannot interact physically. The female was removed and was subjected to histological analysis at the same time when (B, C) females were removed.

Figure 3-3

In situ hybridization (ISH) for *egr1* in the brain areas that have been reported to express *esr2b*. (A) Representative ISH images for *egr1* (red channel) after behavioral experiment counterstained with DAPI (blue channel) (scale bar: 20 μm). Behavioral experiment was conducted by allowing females to interact with male or female. (B) Number of *egr1*-expressing cells in the brain nuclei of interest (aligned from left to right, rostral to caudal) in the females that were allowed to interact with male (navy dots) and those with female (khaki dots) (n = 5, each group). Significantly more *egr1*-expressing cells were detected only in Vd/Vs/Vp (Vd/Vs/Vp: with male; 108.6 ± 12.64, with female; 57.6 ± 6.40, $P = 0.01219$, rPOp: with male; 27.8 ± 13.45, with female; 18.2 ± 4.27, $P = 0.6714$, POm: with male; 12.4 ± 2.84, with female; 5.6 ± 1.69, $P = 0.07491$, NPPv: with male; 16.4 ± 7.00, with female; 18.8 ± 4.60, $P = 0.6004$, NVT: with male; 17.2 ± 6.51, with female; 14.4 ± 4.45, $P = 0.6752$). (C) Representative ISH images for *egr1* in Vd/Vs/Vp of the females that had been differentially conditioned behavior. The behavioral experiment was conducted by allowing females to interact with intact male (Figure 3-2A), fin-removed male (Figure 3-2C), and partitioned with intact male (Figure 3-2D). (D) Number of *egr1*-expressing cells in Vd/Vs/Vp of the females who interacted with intact male (navy dots, n = 4), females who interacted with fin-removed male (spawned: blue dots, n = 2; not spawned: sky blue dots, n = 4), and females partitioned from female (green dots, n = 4). Number of *egr1*-expressing cells is significantly higher in the female who interacted with intact male than the female partitioned from female, and who interacted with fin-removed male (separated with male; 64.5 ± 4.52, with fin-removed male; 68.5 ± 15.21, with intact male; 155.0 ± 11.58, $*P = 0.0337$ between separated with male and with intact male, $*P = 0.0222$ between with fin-removed male and with intact male by Dunn-Bonferroni test). Note that females that spawned together with fin-removed male showed the number of *egr1*-expressing cells same as the female that interacted with intact male.

Figure 3-4

Representative dual *in situ* hybridization photographs showing the localization of *egr1* (magenta) and *esr2b* (green) expression in the females who interacted with intact male and female (scale bar: 20 μm). Although *egr1*-expressing cells appears to be increased in the females who interacted with female, the cells that express both *egr1* and *esr2b* signals were barely found, suggesting that *egr1*-expressing cells can be distinguished from the *esr2b*-expressing neuron in Vd/Vs/Vp.

Figure 3-5

Dual *in situ* hybridization (ISH) for the two genes. (A) Representative dual ISH images showing colocalization of *egr1* (magenta) and *gad1.1* (green) counterstained with DAPI (blue) in Vd/Vs/Vp of the female who interacted with intact male (scale bar: 20 μm). The inset in the overlay image shows an enlarged image of the region in square with 10 μm sides. (B) Number of *egr1*-expressing cells (magenta), number of *egr1*/*gad1.1*-co-expressing cells (green) after interaction with intact male (n = 3). Magenta and green bar represents the average number respectively. Circle, triangles, and squares correspond to each individuals. (C) The percentage of *egr1*-expressing cells colocalized with *gad1.1*. Approximately 75 % of *egr1*-expressing cells co-expressed *gad1.1* (103.67 ± 10.92 / 130 ± 11.53), which suggests that most of highly activated neurons with *egr1* activity labeling were GABAergic. (D) Representative dual ISH photographs showing colocalization of candidate genes for neurotransmitters of *esr2b*$^{Vd/Vs/Vp}$ neuron (magenta) and *esr2b* (green) (scale bar: 20 μm). The insets in the overlay photograph show enlarged images of the region in squares with 20 μm sides. mRNA signals of *npb*, *cck*, and *cnp1* as candidate genes were clearly colocalized with *esr2b* mRNA signal.

Figure 3-6

EGFP immunohistochemistry (IHC) in *esr1*:*egfp* Tg female medaka (scale bar: 20 μm). (A) Representative photograph of dual labeling by *esr2b* ISH and EGFP IHC. Most of the EGFP-ir cells express *esr2b* (arrows). (B) Representative image of EGFP IHC of left side of Vd/Vs/Vp of *esr1*:*egfp* Tg female. The area on the lower left/upper right across the dotted line are regarded as ventromedial/lateral part of Vd/Vs/Vp, respectively. EGFP-immunoreactive (ir) signals shows that neurons located in ventromedial part of Vd/Vs/Vp send neurites to the lateral part of Vd/Vs/Vp where the *gad1.1*/*egr1*$^{Vd/Vs/Vp}$ neurons are located. (C) Enlarged microphotograph of the square in (B). The existance of several varicose structures (arrowheads) on the neurites arising from the EGFP-ir neurons indicate that these neurons have varicosities on their neurites.

Figure 3-7

Representative photographs of ISH for *cckbr* and *olgc7* in Vd/Vs/Vp of females. Both *cckbr* and *olgc7* signals were detected in Vd/Vs/Vp. The region was identified, judging from the anatomical relationship with the anterior commissure, which was located below the photographed areas.

Figure 3-1

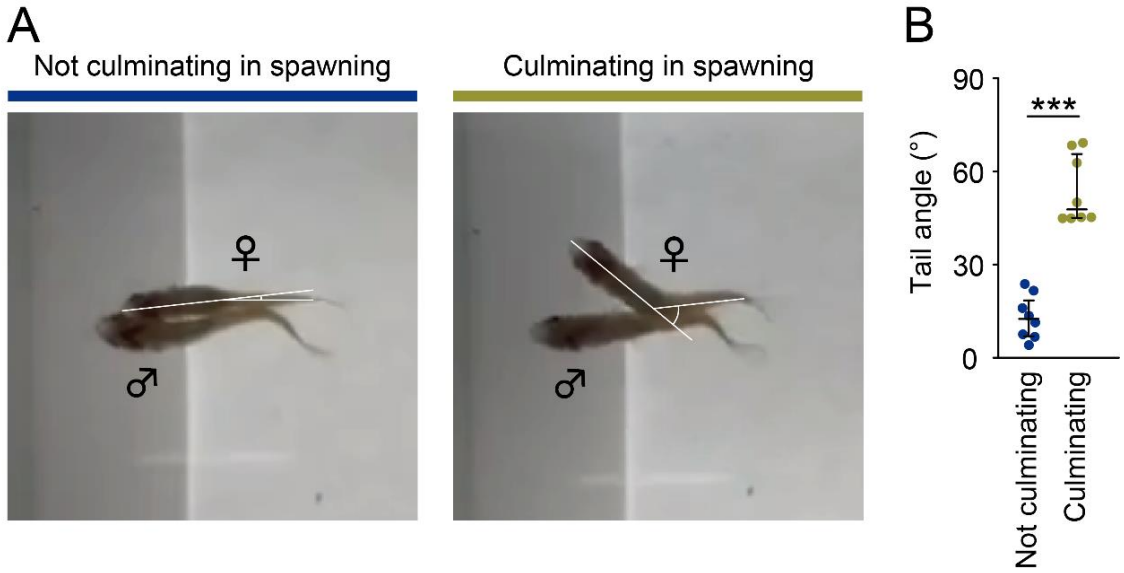
A
Not culminating in spawning
Culminating in spawning
♀
♂
♀
♂
B
Tail angle (°)
90
60
30
0
***
Not culminating
Culminating

Figure 3-2

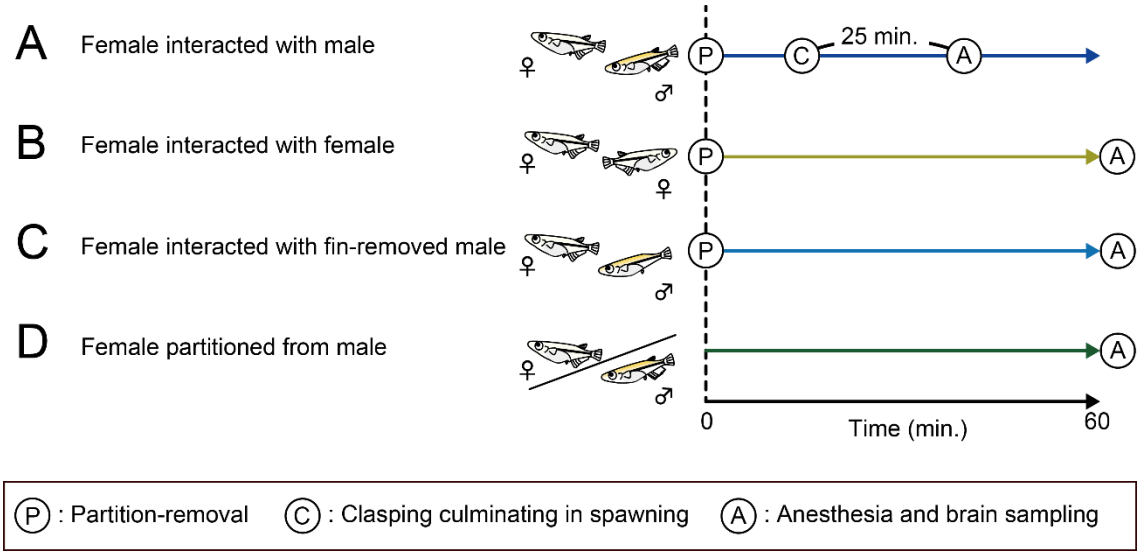
A
Female interacted with male
B
Female interacted with female
C
Female interacted with fin-removed male
D
Female partitioned from male
♀
♂
P
C
25 min.
A
0
Time (min.)
60
P : Partition-removal
C : Clasping culminating in spawning
A : Anesthesia and brain sampling

Figure 3-3

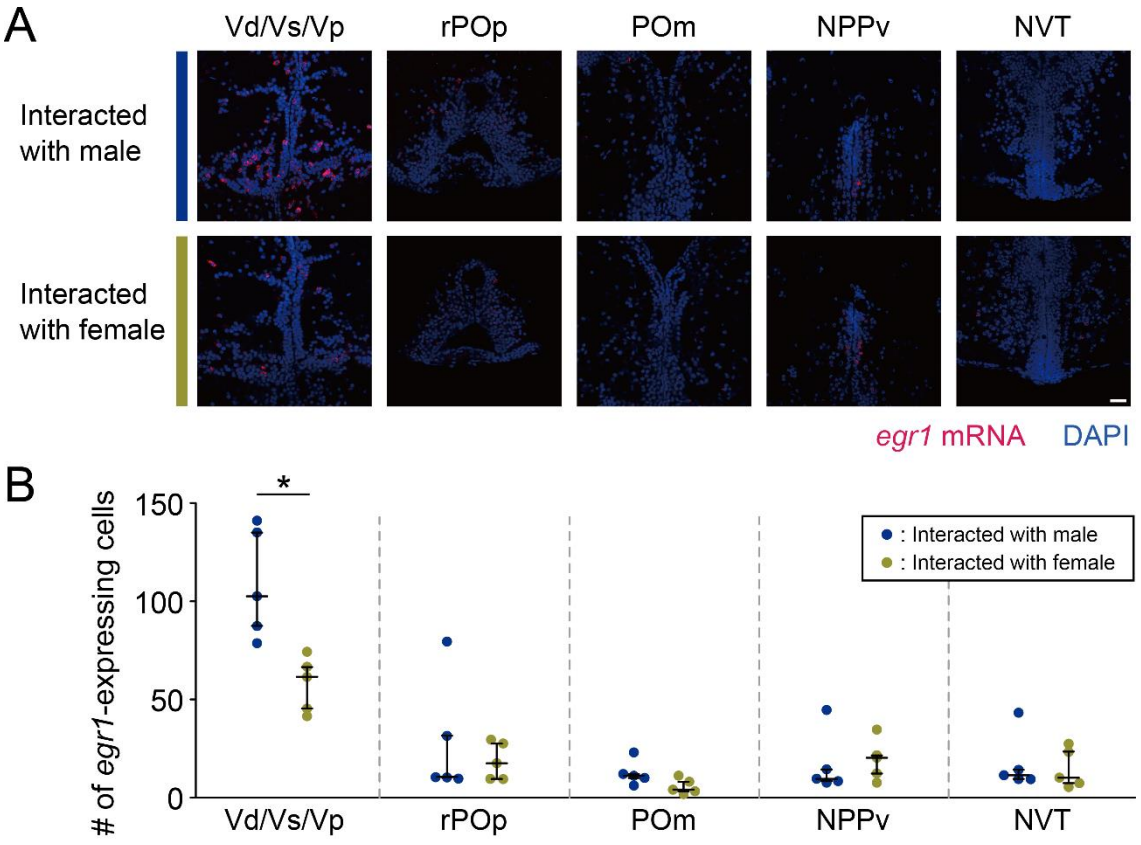
A
Vd/Vs/Vp
rPOp
POm
NPPv
NVT
Interacted with male
Interacted with female
egr1 mRNA
DAPI
B
*
# of egr1-expressing cells
150
100
50
0
: Interacted with male
: Interacted with female
Vd/Vs/Vp
rPOp
POm
NPPv
NVT

Figure 3-3

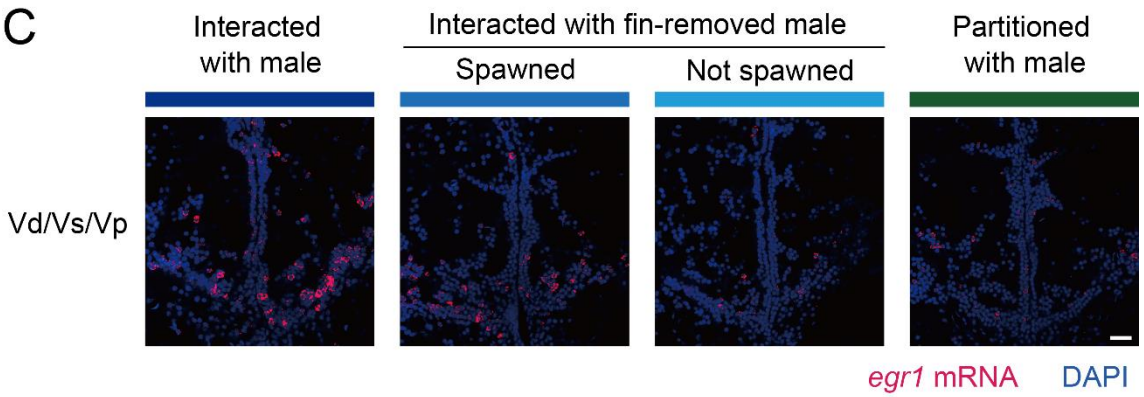
C
Interacted with male
Interacted with fin-removed male
Spawned
Not spawned
Partitioned with male
Vd/Vs/Vp
egr1 mRNA
DAPI

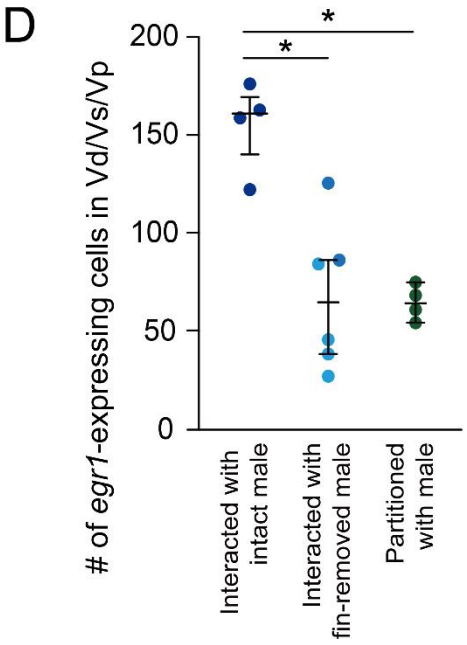
D
# of egr1-expressing cells in Vd/Vs/Vp
200
150
100
50
0
*
*
Interacted with intact male
Interacted with fin-removed male
Partitioned with male

Figure 3-4

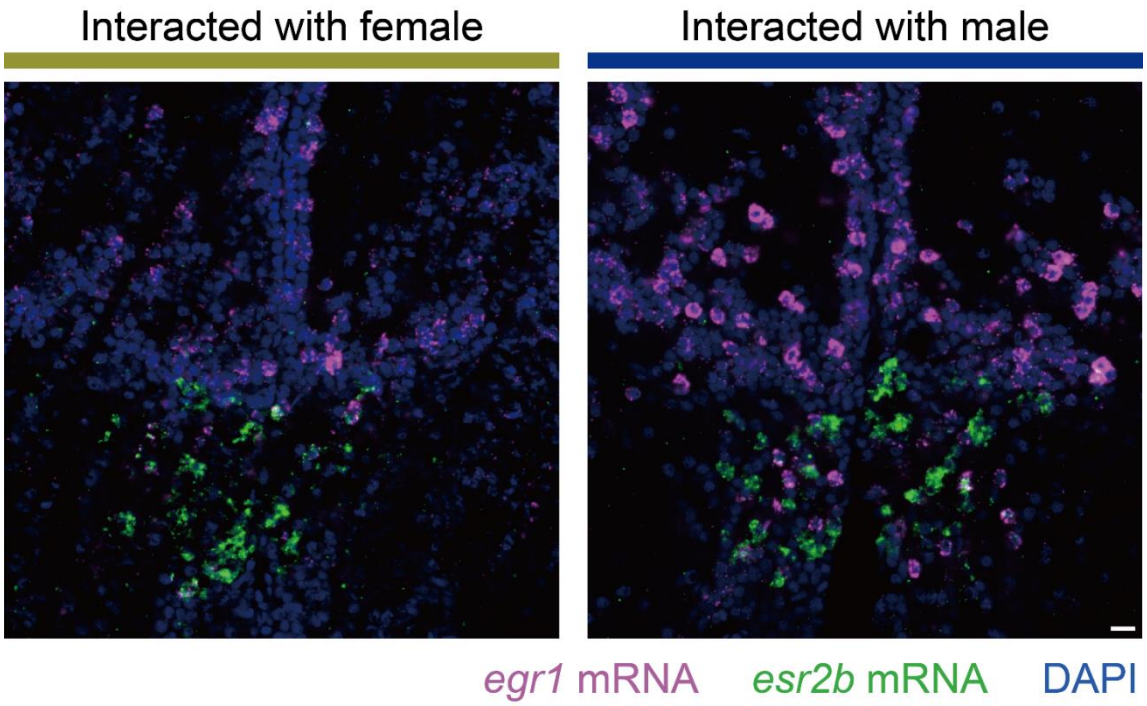
Interacted with female
Interacted with male
egr1 mRNA
esr2b mRNA
DAPI

Figure 3-5

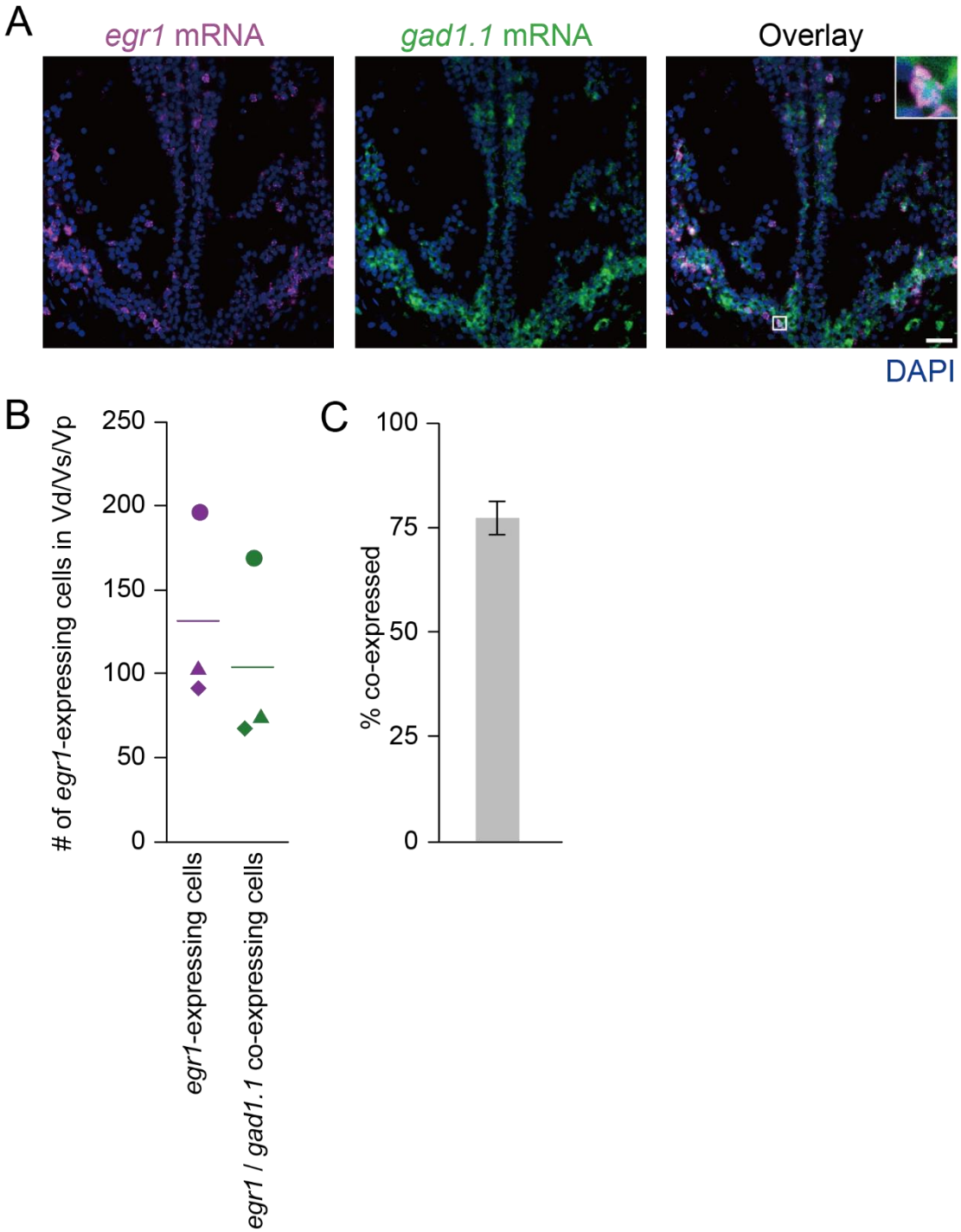
A
egr1 mRNA
gad1.1 mRNA
Overlay
DAPI
B
# of egr1-expressing cells in Vd/Vs/Vp
250
200
150
100
50
0
egr1-expressing cells
egr1 / gad1.1 co-expressing cells
C
% co-expressed
100
75
50
25
0

Figure 3-5

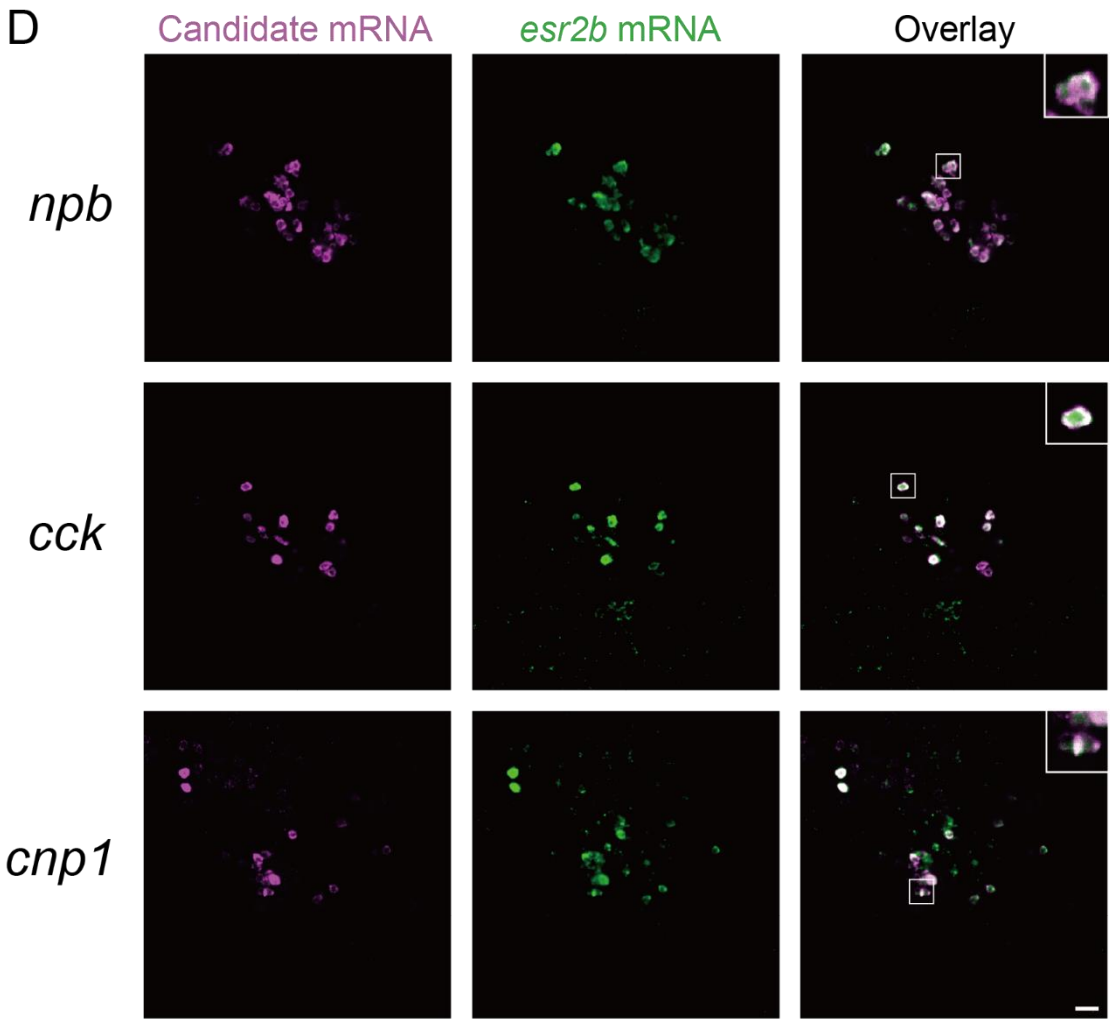

Figure 3-6

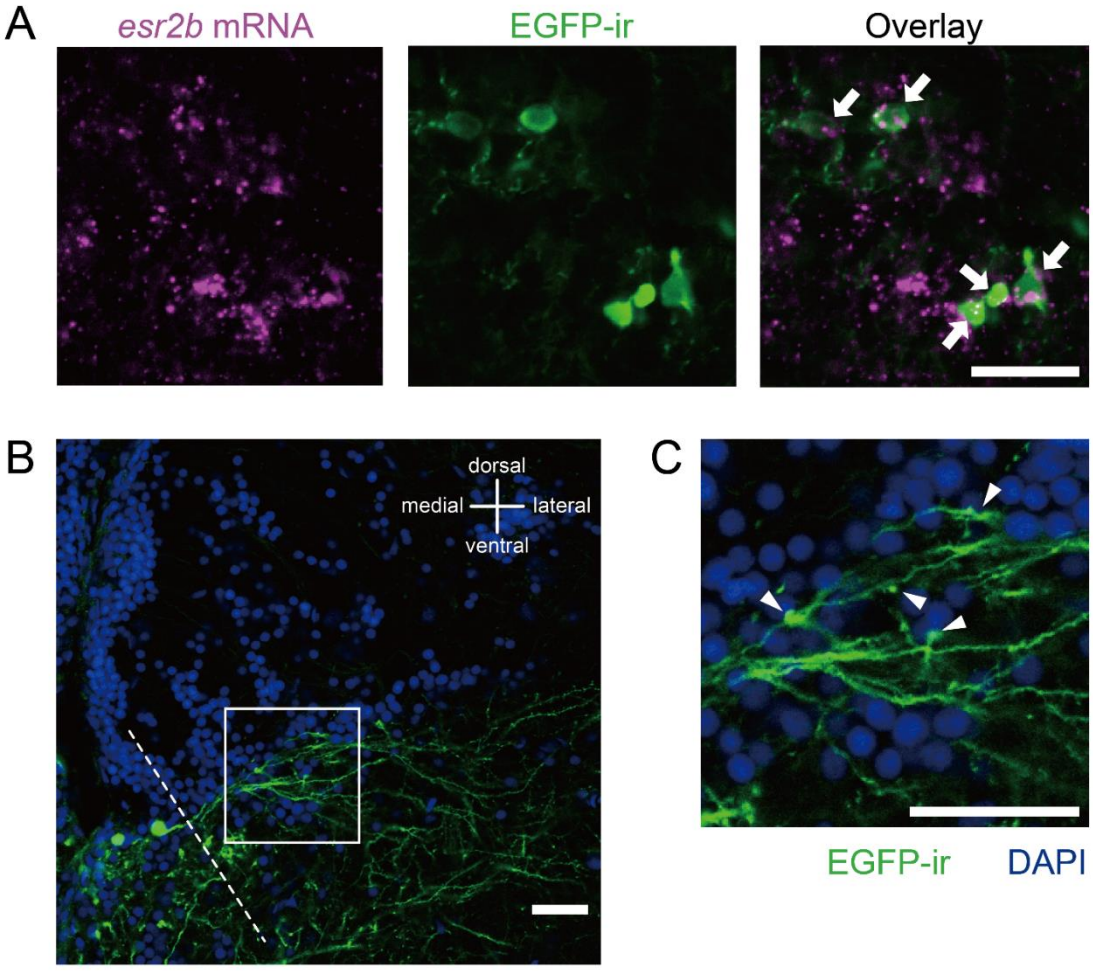
A
esr2b mRNA
EGFP-ir
Overlay
B
dorsal
medial
lateral
ventral
C
EGFP-ir
DAPI

Figure 3-7

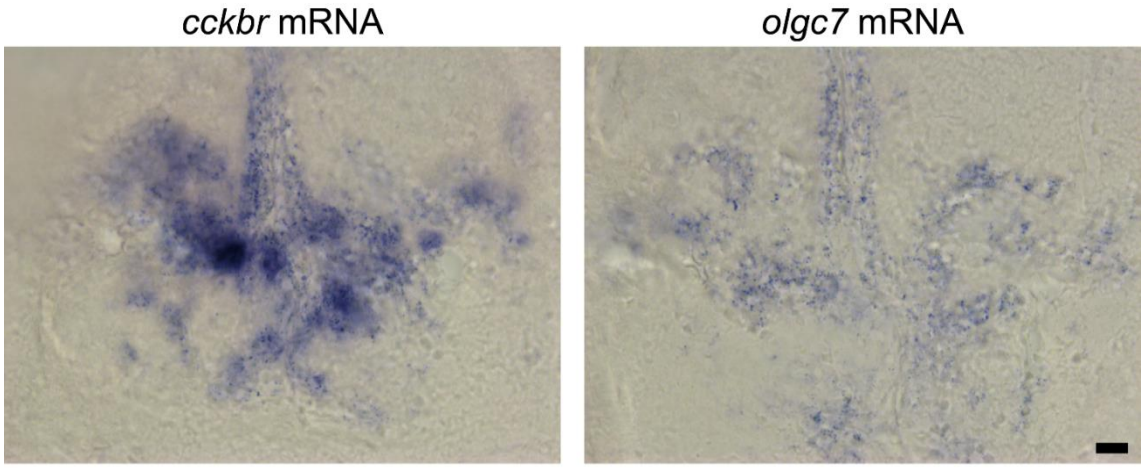

General Discussion

The present thesis aimed to elucidate the neuroendocrine mechanisms that elicit the female sexual behavior in teleosts, using medaka as a teleost model, which have many experimental advantages for the analysis. In chapter 1, I established an open-source analysis suite for behavioral recording/annotation by using a single-board computer Raspberry Pi and Microsoft Excel Macro, which allows us to perform efficient and sophisticated analyses of animal behaviors, including sexual behavior of medaka. In chapter 2, I focused on one of the sex steroid hormones, estrogen, and examined its possible involvement in the activation of female sexual behavior in medaka. Behavioral analysis revealed that Esr2b, one of the estrogen receptor subtypes is necessary for the activation of female receptivity. In chapter 3, I explored the neural circuitry for activating female sexual behavior by IEG activity mapping and found evidence to suggest that neurons in the ventral telencephalon may play important roles in triggering the spawning behavior leading to the oviposition. Furthermore, I obtained histological results to suggest that *esr2b*-expressing neural population may activate these neurons (probably by neuromodulatory actions) via peptidergic signaling. These results suggest the existence of local neural circuitry for the estrogen-dependent neuromodulatory activation of the motor pattern generators leading to oviposition.

Behavioral analysis system that can be widely applied to the analyses of various animal behaviors

Since animals flexibly change their behaviors in response to various signals from the external environment, it is important for behavioral analyses to minimize the unintentional disturbances of their behavior by the observers. To overcome such problems, I established an open-source automated behavioral recording system using the Raspberry Pi, which can also be applied to the automation of simple experimental operations such as feeding and electrical stimulation by manipulating appropriate external devices via GPIO interface (Figures 1-1, 2, and 7). Since we

can remotely operate this system, the time required for the observation near the behaving animals could be minimized, which resulted in the reduction of human errors. In addition, the system automates not only recording but also the subsequent file-sorting and encoding, which are laborious and usually take much time. Thus, the behavioral analyses can be carried out more efficiently and systematically. Actually, the time spent for video-recording and file-sorting of 16 pairs of medaka was drastically shortened compared to the conventional method (Figure 1-5).

Difficulty of behavioral analysis tends to increase as the behavioral annotation becomes laborious. Although there are several automated behavioral annotation systems, most of them are specialized for specific behaviors of certain animals such as rodents [48-52] and fruit flies [53-57], which are less flexible for application to various animal behaviors. Therefore, for the analyses of unique behaviors of various animal species including non-model animals, we are forced to perform painstaking behavioral annotation that requires, e.g., video-recoding of behavioral sequences and pausing the video and note-taking the timing and duration manually, each time the behavior occurs. The Microsoft Excel macro "*Ethogramer*", which I developed in the present study, may be one of the possible solutions for such problem (Figure 1-3). *Ethogramer* enables us to perform behavioral annotation by only pressing the PC keys, while watching the videos of animal behavior, then frees us from laborious annotation procedure as described above. Furthermore, since *Ethogramer* has the function for generating raster plots showing the behavioral time course, we can also visually understand the temporal transition of the behavior. Recetly, automated behavioral annotation systems have been established by using machine learning method [58, 59], which may become frequently used in the future. However, since current studies that cannot apply these methods require manual analyses, the present study helps researchers to perform these manual analyses.

By using the analysis suite, I succeeded in efficiently and quantitatively analyzing the sexual

behavior in medaka and found a difference in sexual motivation between laboratory and wild strain, presumably resulting from domestication (Figure 1-6). I applied this suite for the behavioral analyses in chapters 2 and 3 (Chapter. 1).

Neuroendocrine mechanisms that elicit the female sexual behavior in teleosts

Available evidence concerning the mechanisms of coordinated occurrence of gonadal maturation and activation of sexual behavior seem to suggest that the substance(s) released from mature gonads, mainly sex steroid hormones, may play an important role in signaling the gonadal status to the brain. However, the neuroendocrine mechanism for coordinated regulation for activation of sexual behavior and gonadal maturation is poorly understood. In chapter 2, I examined the contribution of estrogen, one of the sex steroid hormones secreted from mature ovary, to the activation of female sexual behavior by using ovariectomy and estrogen-receptor gene knockout models. In addition, in chapter 3, I explored neurons that are activated during female sexual behavior.

Estrogen/*esr2b* signaling is essential for the activation of female sexual behavior, presumably by driving female receptivity

In chapter 2, I demonstrated that the activation of female sexual behavior is regulated in an estrogen-dependent manner, in which estrogen receptor 2b (*esr2b*) plays a role. Administration of fadrozole hydrochloride, an inhibitor of estrogen synthesis, disrupted the clasping behavior despite normal acceptance of courtship display by male (Figure 2-1). However, it should be noted that this result may also arise from secondary effects of unexpected changes in the other ovarian sex steroids (Figure 2-1H). On the other hand, removal of the entire gonad by ovariectomy (OVX) elicited avoidance behavior of females from males (Figures 2-2D-G), and estrogen administration

to OVX (OVX+E) females reinstated the clasping behavior (Figures 2-2C), although the subsequent process of the sexual behavior (e.g. oviposition) was eliminated by OVX. These results suggest that estrogen may play a role in the female's acceptance of male. This suggestion is consistent with the observation that *esr2b*$^{-/-}$ female refused courtship behavior by male and failed to perform clasping behavior with male, although they did not escape from following behavior by male (Figure 2-4). Therefore, it is suggested that estrogen/*esr2b* signaling contributes to the regulation of the female receptivity.

On the other hand, OVX females were not receptive and apparently avoided the male following and courtship, which is more severe phenotype of avoidance behavior compared with that of *esr2b*$^{-/-}$ female. Also, estrogen administration did not alleviate this avoiding behavior, which suggests that some ovarian substance(s) other than estrogen may be involved in the regulation of the acceptance behavior of male courtship. Although the identity of the substance remains unclear so far, it is interesting to note that *fshb* KO females, which are supposed to be unable to secrete the sex steroid hormones from their immature ovary, do not show such severe avoidance behavior (Shimomai, unpublished), suggesting that the substance may be something other than the steroid hormones.

The difference between mammals and teleosts in the contribution of estrogen receptors for the reproductive functions

Analysis of *esr2b* KO female revealed that *esr2b*-expressing neurons in the brain are essential for the activation of female sexual behavior. *esr2a* and *esr2b* are the duplicates of the ancestral *esr2* generated during the third-round whole genome duplication, which are considered to have occurred in the common ancestor of teleosts [80, 107, 108]. However, mammalian *Esr2*, the ortholog of teleost *esr2a* and *esr2b*, has been shown to lack critical functions in the female sexual

behaviors in mammals [116]. Instead, *esr1* has been shown to be mainly involved in the female sexual behavior in mammals [21, 112, 113]. Thus, replacement of the main functional subtype of Esr for sexual behavior may have occurred during evolution. The replacement of the main functional Esr may have also occurred in the HPG axis regulation for gonadal functions. *esr1* and *esr2a* are mainly involved in the estrogen feedback regulation of HPG axis in mammals [3-8] and teleost [12-17], respectively. While the importance of estrogen has been conserved during evolution of vertebrates, it is interesting to note that the main functional Esr subtypes appear to have been exchanged between *esr1* and *esr2*, which may be due to the difference in the neural circuitry that is involved in reproductive functions (Chapter. 2).

Elucidation of the neural circuitry for the activation of female spawning behavior

A working hypothesis of the neural circuitry for the activation of female spawning behavior is shown in Figure 4-1. In chapter 3, I identified *gad1.1*/*egr1*$^{Vd/Vs/Vp}$ neurons as the neurons eliciting the female spawning behavior, the final trigger for the oviposition. Here, RNA-seq followed by histological analysis suggested that the neurons in the ventral telencephalon are GABAergic (Figures 3-5A-C). The tail-bending behavior of female medaka observed in chapter 3 is a fixed action pattern leading to oviposition and is equivalent to the spawning behavior, which has been described in the other teleost species, such as the dwarf gourami and himé/kokanee salmon [25, 42]. It is intriguing to note that in himé/kokanee salmon, electrical stimulation of the ventral telencephalon rapidly elicits the spawning act leading to oviposition, suggesting that the neurons in the ventral telencephalon may play a role in the immediate triggering of the spawning behavior [25]. Taken together, it is speculated that GABAergic *gad1.1*/*egr1*$^{Vd/Vs/Vp}$ neurons in medaka may be involved in the simultaneous triggering of the motor pattern generator (MPG) circuitries that elicit the stereotypical pattern of spawning behavior including tail-bending and egg release. Since

the GABAergic neurotransmission is usually inhibitory, it may be postulated that these key neurons in medaka (Figures 3-5A-C) have a disinhibitory action on the MPG circuitries for the female spawning behavior (Figure 4-1).

I also found in chapter 3 that *esr2b*-expressing neurons are closely located in *gad1.1*/*egr1*$^{Vd/Vs/Vp}$ neurons (*esr2b*$^{Vd/Vs/Vp}$ neurons) (Figure 3-4), which appeared to send axonal projections to the lateral part of Vd/Vs/Vp, in which *gad1.1*/*egr1*$^{Vd/Vs/Vp}$ neurons are localized (Figures 3-6B and C). Furthermore, my preliminary RNA-seq followed by histological analysis also suggested the existence of peptidergic neuromodulation, by using CCK and/or CNP1, from *esr2b*$^{Vd/Vs/Vp}$ neurons to *gad1.1*/*egr1*$^{Vd/Vs/Vp}$ neurons (Figures 3-5D and 7). This peptidergic neuromodulation may be involved in sensing and relaying the information on the presence of ovulated eggs in the mature ovary via estrogen/*esr2b* signaling (green arrows in Figure 4-1) and lowering threshold for triggering sexual behaviors in females in response to the key stimuli, the nature of which remains to be determined. This process may be equivalent to the neurophysiological notion of "facilitation".

Independent mechanisms controlling reception of male and facilitation of spawning behavior

As described in chapter 2, estrogen/*esr2b* signaling contributes to the regulation of the receptivity in which the female accepts male courtship/clasping, which is displayed prior to oviposition, and it is conceivable that the proceptive behavior reflects the sexual motivation/receptivity of females. On the other hand, in chapter 3, I suggested that *gad1.1*/*egr1*$^{Vd/Vs/Vp}$ neurons elicits spawning behavior, and this action was suggested to be modulated by *esr2b*$^{Vd/Vs/Vp}$ neurons. These findings suggest a possibility that *esr2b*-expressing neurons in Vd/Vs/Vp are involved in both facilitation of spawning behavior (see the preceding

paragraph) and receptivity of males. It may also be possible that different populations of *esr2b*-expressing neurons play a role in facilitation of spawning behavior of female medaka (Vd/Vs/Vp neurons) and regulation of receptivity (neurons in the other regions), respectively. This is because *esr2b* is also expressed in the brain nuclei other than Vd/Vs/Vp [29, 30], and *esr2b*$^{Vd/Vs/Vp}$ neurons also project to the regions other than the lateral part of Vd/Vs/Vp where *gad1.1*/*egr1*$^{Vd/Vs/Vp}$ neurons are located (data not shown). Several studies in female rodents suggested that closely located different subpopulations are involved in proceptive/solicitatory behavior and lordosis behavior, respectively [72, 73], which may be a similar situation with *gad1.1*/*egr1*$^{Vd/Vs/Vp}$ neurons and *esr2b*$^{Vd/Vs/Vp}$ neurons suggested here in medaka (Chapter. 3).

In conclusion, from the results of chapters 1, 2, and 3, I propose a working hypothesis of the neural circuitries for activation of female sexual behavior in medaka in response to ovarian maturation. Previous behavioral studies using brain stimulation and lesioning in teleosts, such as himé/kokanee salmon and goldfish [24-26], have identified the brain nuclei for activating sexual behavior. However, the cellular and molecular mechanisms of the neural circuitry involved in the control of sexual behavior have not previously been elucidated. In the present thesis, I identified neurons that are considered to elicit spawning behavior leading to oviposition (*gad1.1*/*egr1*$^{Vd/Vs/Vp}$ neurons) by using the IEG brain activity mapping. I also found estrogen-receptive neurons (*esr2b*$^{Vd/Vs/Vp}$ neurons) that are considered to play a role in sensing and relaying the information on the presence of ovulated eggs in the mature ovary via estrogen/*esr2b* signaling. Furthermore, I found possible local neural circuitry from *esr2b*$^{Vd/Vs/Vp}$ neurons to *gad1.1*/*egr1*$^{Vd/Vs/Vp}$ neurons that are considered to modulate the excitability of the latter via peptides such as CCK and CNP1. Since the ventral telencephalon is suggested to be involved in the immediate activation of sexual behavior in some teleost species , the neural circuit described above may facilitate the key

stimulus input from male to trigger MPG circuitries for the spawning behavior of female medaka. Furthermore, I propose that estrogen/*esr2b* signaling of the same or the other populations of neurons may be involved in the receptivity of males by females (see Figure 4-1). Considering the involvement of neurons in the ventral telencephalon in the control of sexual behaviors in goldfish, himé/kokanee salmon, and medaka, such neural circuitry may be common to many species of teleost as well.

I wish that the present thesis paves the way towards understanding the neuroethological/neuro-endocrinological mechanisms for the regulation of female sexual behavior generally in teleost that have enormous diversity.

Figure 4-1

Working hypothesis of the neuroendocrinological/neuroethological mechanism that regulate the female sexual behavior in medaka in response to ovarian maturation. Speculated parts are illustrated by gray and dotted lines. *gad1.1*/*egr1*$^{Vd/Vs/Vp}$ neurons in medaka may be involved in triggering the motor pattern generator (MPG) circuitries via GABAergic signaling, which has disinhibitory action on the MPG circuitries for the female spawning behavior. In addition, it is suggested that there is a peptidergic neuromodulation using CCK and/or CNP1, from *esr2b*$^{Vd/Vs/Vp}$ neurons to *gad1.1*/*egr1*$^{Vd/Vs/Vp}$ neurons for facilitation, lowering threshold for triggering spawning behavior on the presence of ovulated eggs in the mature ovary via estrogen/*esr2b* signaling (green arrows). On the other hand, *esr2b*-expressing neurons also contribute to the regulation of female receptivity in which NPB is supposed to play a role. Also, there may be other ovarian substance(s) that is involved in the regulation of receptivity (deep-pink arrow).

Figure 4-1

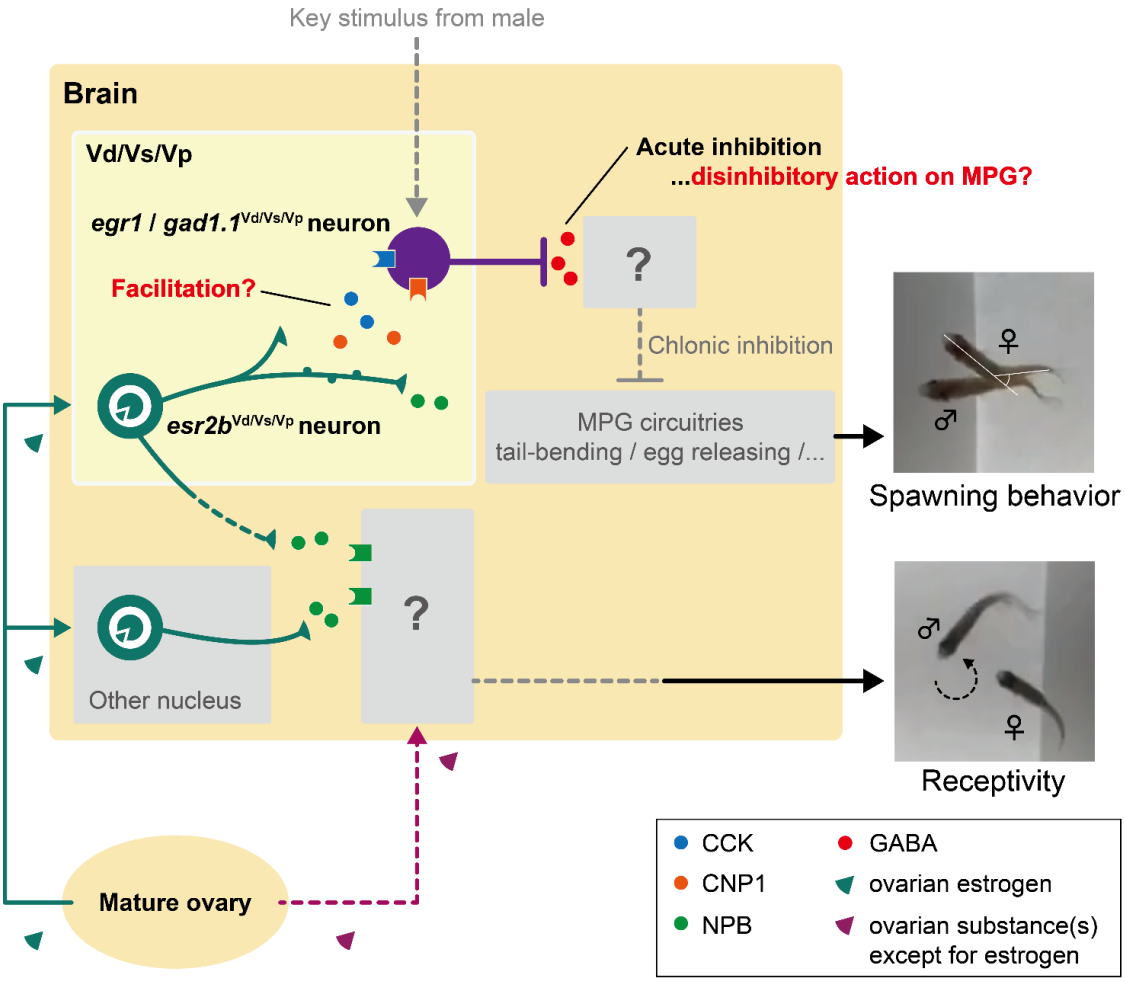
Key stimulus from male
Brain
Vd/Vs/Vp
egr1 / gad1.1Vd/Vs/Vp neuron
Facilitation?
esr2bVd/Vs/Vp neuron
Acute inhibition
...disinhibitory action on MPG?
?
Chlonic inhibition
MPG circuitries
tail-bending / egg releasing /...
Spawning behavior
Other nucleus
?
Receptivity
Mature ovary
CCK
CNP1
NPB
GABA
ovarian estrogen
ovarian substance(s) except for estrogen

Acknowledgements

I heartily express my great gratitude to Associate professor Shinji Kanda, Laboratory of Physiology, Department of Marine Bioscience, Division of Marine Life Science, Atomosphere and Ocean Research Institute (AORI), The University of Tokyo, and emeritus professor Yoshitaka Oka, Laboratory of Biological Signaling, Department of Biological Sciences, Graduate School of Science, The University of Tokyo, for their constant guidance, encouragement, and valuable discussion during the entire course of my study. I am also indebted to Drs. Chie Umatani (Graduate School of Science), Mikoto Nakajo (Osaka Medical and Pharmaceutical University), Kana Ikegami (Graduate School of Science), Chika Fujimori (AORI), Daichi Kayo (Graduate School of Agricultural and Life Sciences, The University of Tokyo), Genki Yamagishi (Tokyo University of Science), and Min Kyun Park (Graduate School of Science) for their helpful advice, instruction, discussion, and encouragement.

I sincerely wish to thank to Drs. Kiyoshi Naruse (National Institute for Basic Biology) and Daichi Kayo for a generous gift of wild individuals of Kiyosu strain and cRNA probes, respectively, Dr. Satoshi Ansai (Tohoku University) for generation and providing the genome-edited medaka strain (not shown in the present thesis), Ms. Fumika Muguruma, Hiroko Tsukamoto, Hisako Kohno, Miho Kyokuwa, Natsuko Itoh, and Fujiko Masui (The University of Tokyo) for their excellent care of the fish used in the present study. Thanks are also due to Hiroki Tomida (Graduate School of Science) for helping construct the equipment for the analysis of sexual behavior described in chapter 1, and Rinko Shimomai (Graduate School of Science) for allowing to mention her unpublished data. I also greatly thank all the members of Laboratory of Physiology and Laboratory of Biological Signaling for their helphul support.

I am sincerely grateful to Professor Susumu Hyodo, Professor Takeo Kubo (Graduate School of Science), Professor Yuichi Iino (Graduate School of Science), Associate professor Kataaki Okubo, and Associate professor Shinji Kanda for critical reading of the present thesis and valuable discussion.

This work was supported by Grants-in-Aid from Japan Society for the Promotion of Science Grants (Grant Number: 19J21828) and World-leading INnovative Graduate Study Program for Life Science and Technology (WINGS-LST), the University of Tokyo WISE Program (Doctoral Program for World-leading Innovative & Smart Education), MEXT, Japan.

Finally, I would like to express my deep gratitude to my parents, Kiyomasa and Yoshiko Tomihara and my brother, Takuma Tomihara, for their constant support and heartfelt encouragement.

References

1. Legan, S.J., and Winans, S.S. (1981). The photoneuroendocrine control of seasonal breeding in the ewe. General and comparative endocrinology *45*, 317-328.
2. Ikegami, K., and Yoshimura, T. (2016). Comparative analysis reveals the underlying mechanism of vertebrate seasonal reproduction. General and comparative endocrinology *227*, 64-68.
3. Adachi, S., Yamada, S., Takatsu, Y., Matsui, H., Kinoshita, M., Takase, K., Sugiura, H., Ohtaki, T., Matsumoto, H., Uenoyama, Y., Tsukamura, H., Inoue, K., and Maeda, K. (2007). Involvement of anteroventral periventricular metastin/kisspeptin neurons in estrogen positive feedback action on luteinizing hormone release in female rats. The Journal of reproduction and development *53*, 367-378.
4. Clarkson, J., d'Anglemont de Tassigny, X., Moreno, A.S., Colledge, W.H., and Herbison, A.E. (2008). Kisspeptin-GPR54 signaling is essential for preovulatory gonadotropin-releasing hormone neuron activation and the luteinizing hormone surge. The Journal of neuroscience : the official journal of the Society for Neuroscience *28*, 8691-8697.
5. Clarkson, J., and Herbison, A.E. (2009). Oestrogen, kisspeptin, GPR54 and the pre-ovulatory luteinising hormone surge. J Neuroendocrinol *21*, 305-311.
6. Clarkson, J., Han, S.K., Liu, X., Lee, K., and Herbison, A.E. (2010). Neurobiological mechanisms underlying kisspeptin activation of gonadotropin-releasing hormone (GnRH) neurons at puberty. Molecular and cellular endocrinology *324*, 45-50.
7. Dubois, S.L., Acosta-Martinez, M., DeJoseph, M.R., Wolfe, A., Radovick, S., Boehm, U., Urban, J.H., and Levine, J.E. (2015). Positive, but not negative feedback actions of estradiol in adult female mice require estrogen receptor alpha in kisspeptin neurons. Endocrinology *156*, 1111-1120.
8. Herbison, A.E. (2016). Control of puberty onset and fertility by gonadotropin-releasing hormone neurons. Nature reviews. Endocrinology *12*, 452-466.
9. Schally, A.V., Arimura, A., Kastin, A.J., Matsuo, H., Baba, Y., Redding, T.W., Nair, R.M., Debeljuk, L., and White, W.F. (1971). Gonadotropin-releasing hormone: one polypeptide regulates secretion of luteinizing and follicle-stimulating hormones. Science (New York, N.Y.) *173*, 1036-1038.
10. Cattanach, B.M., Iddon, C.A., Charlton, H.M., Chiappa, S.A., and Fink, G. (1977). Gonadotrophin-releasing hormone deficiency in a mutant mouse with hypogonadism. Nature *269*, 338-340.

11. Kumar, T.R., Wang, Y., Lu, N., and Matzuk, M.M. (1997). Follicle stimulating hormone is required for ovarian follicle maturation but not male fertility. Nature genetics *15*, 201-204.
12. Kanda, S., Okubo, K., and Oka, Y. (2011). Differential regulation of the luteinizing hormone genes in teleosts and tetrapods due to their distinct genomic environments--insights into gonadotropin beta subunit evolution. General and comparative endocrinology *173*, 253-258.
13. Karigo, T., Kanda, S., Takahashi, A., Abe, H., Okubo, K., and Oka, Y. (2012). Time-of-day-dependent changes in GnRH1 neuronal activities and gonadotropin mRNA expression in a daily spawning fish, medaka. Endocrinology *153*, 3394-3404.
14. Karigo, T., Aikawa, M., Kondo, C., Abe, H., Kanda, S., and Oka, Y. (2014). Whole brain-pituitary in vitro preparation of the transgenic medaka (Oryzias latipes) as a tool for analyzing the differential regulatory mechanisms of LH and FSH release. Endocrinology *155*, 536-547.
15. Takahashi, A., Kanda, S., Abe, T., and Oka, Y. (2016). Evolution of the Hypothalamic-Pituitary-Gonadal Axis Regulation in Vertebrates Revealed by Knockout Medaka. Endocrinology *157*, 3994-4002.
16. Kanda, S. (2018). Evolution of the regulatory mechanisms for the hypothalamic-pituitary-gonadal axis in vertebrates-hypothesis from a comparative view. General and comparative endocrinology.
17. Kayo, D., Zempo, B., Tomihara, S., Oka, Y., and Kanda, S. (2019). Gene knockout analysis reveals essentiality of estrogen receptor β1 (Esr2a) for female reproduction in medaka. Scientific reports *9*, 8868.
18. Davidson, J.M., Rodgers, C.H., Smith, E.R., and Bloch, G.J. (1968). Stimulation of female sex behavior in adrenalectomized rats with estrogen alone. Endocrinology *82*, 193-195.
19. Pfaff, D.W., and Sakuma, Y. (1979). Deficit in the lordosis reflex of female rats caused by lesions in the ventromedial nucleus of the hypothalamus. J Physiol *288*, 203-210.
20. Pfaff, D.W. (1980). Estrogens and brain function. RU Authors *149*.
21. Rissman, E.F., Early, A.H., Taylor, J.A., Korach, K.S., and Lubahn, D.B. (1997). Estrogen receptors are essential for female sexual receptivity. Endocrinology *138*, 507-510.
22. Inoue, S., Yang, R., Tantry, A., Davis, C.-h., Yang, T., Knoedler, J.R., Wei, Y., Adams, E.L., Thombare, S., Golf, S.R., Neve, R.L., Tessier-Lavigne, M., Ding, J.B., and Shah, N.M. (2019). Periodic Remodeling in a Neural Circuit Governs Timing of Female Sexual Behavior. Cell *179*, 1393-1408.e1316.
23. Xu, X., Coats, Jennifer K., Yang, Cindy F., Wang, A., Ahmed, Osama M., Alvarado, M.,

Izumi, T., and Shah, Nirao M. (2012). Modular Genetic Control of Sexually Dimorphic Behaviors. Cell *148*, 596-607.

24. Koyama, Y., Satou, M., Oka, Y., and Ueda, K. (1984). Involvement of the telencephalic hemispheres and the preoptic area in sexual behavior of the male goldfish, Carassius auratus: a brain-lesion study. Behavioral and neural biology *40*, 70-86.
25. Satou, M., Oka, Y., Kusunoki, M., Matsushima, T., Kato, M., Fujita, I., and Ueda, K. (1984). Telencephalic and preoptic areas integrate sexual behavior in hime salmon (landlocked red salmon, Oncorhynchus nerka): results of electrical brain stimulation experiments. Physiology & behavior *33*, 441-447.
26. Koyama, Y., Satou, M., and Ueda, K. (1985). Sexual Behavior Elicited by Electrical Stimulation of the Telencephalic and Preoptic Areas in the Goldfish, Carassius auratus. Zoological science *2*, 565-570.
27. Menuet, A., Pellegrini, E., Anglade, I., Blaise, O., Laudet, V., Kah, O., and Pakdel, F. (2002). Molecular characterization of three estrogen receptor forms in zebrafish: binding characteristics, transactivation properties, and tissue distributions. Biology of reproduction *66*, 1881-1892.
28. Munchrath, L.A., and Hofmann, H.A. (2010). Distribution of sex steroid hormone receptors in the brain of an African cichlid fish, Astatotilapia burtoni. J Comp Neurol *518*, 3302-3326.
29. Hiraki, T., Takeuchi, A., Tsumaki, T., Zempo, B., Kanda, S., Oka, Y., Nagahama, Y., and Okubo, K. (2012). Female-specific target sites for both oestrogen and androgen in the teleost brain. Proc Biol Sci *279*, 5014-5023.
30. Zempo, B., Kanda, S., Okubo, K., Akazome, Y., and Oka, Y. (2013). Anatomical distribution of sex steroid hormone receptors in the brain of female medaka. J Comp Neurol *521*, 1760-1780.
31. Lu, H., Cui, Y., Jiang, L., and Ge, W. (2017). Functional Analysis of Nuclear Estrogen Receptors in Zebrafish Reproduction by Genome Editing Approach. Endocrinology *158*, 2292-2308.
32. Ishikawa, T., Murakami, Y., Fujimori, C., Kinoshita, M., Naruse, K., and Kanda, S. (2022). Chapter 9 - Medaka as a model teleost: characteristics and approaches of genetic modification. In Laboratory Fish in Biomedical Research, L. D'Angelo and P. de Girolamo, eds. (Academic Press), pp. 185-213.
33. Umatani, C., Nakajo, M., Kayo, D., Oka, Y., and Kanda, S. (2022). Chapter 10 - Integrated analyses using medaka as a powerful model animal toward understanding various aspects of reproductive regulation. In Laboratory Fish in Biomedical Research, L. D'Angelo and P. de Girolamo, eds. (Academic Press), pp. 215-243.

34. Ono, Y., and Uematsu, T. (1957). Mating ethogram in *Oryzias latipes*. Hokkaido University Collection of Scholarly and Academic Papers *13*, 197-202.
35. Walter, R.O., and Hamilton, J.B. (1970). Head-up movements as an indicator of sexual unreceptivity in female medaka, Oryzias latipes. Animal Behaviour *18*, 125-127.
36. Tomihara, S., Oka, Y., and Kanda, S. (2021). Establishment of open-source semi-automated behavioral analysis system and quantification of the difference of sexual motivation between laboratory and wild strains. Scientific reports *11*, 10894.
37. Bogdanove, A.J., and Voytas, D.F. (2011). TAL Effectors: Customizable Proteins for DNA Targeting. Science (New York, N.Y.) *333*, 1843-1846.
38. Jinek, M., Chylinski, K., Fonfara, I., Hauer, M., Doudna, J.A., and Charpentier, E. (2012). A Programmable Dual-RNA–Guided DNA Endonuclease in Adaptive Bacterial Immunity. Science (New York, N.Y.) *337*, 816-821.
39. Joung, J.K., and Sander, J.D. (2013). TALENs: a widely applicable technology for targeted genome editing. Nature Reviews Molecular Cell Biology *14*, 49-55.
40. Wang, H., Hu, Y.-C., Markoulaki, S., Welstead, G.G., Cheng, A.W., Shivalila, C.S., Pyntikova, T., Dadon, D.B., Voytas, D.F., Bogdanove, A.J., Page, D.C., and Jaenisch, R. (2013). TALEN-mediated editing of the mouse Y chromosome. Nature Biotechnology *31*, 530-532.
41. Satou, M., Oka, Y., Kusunoki, M., Matsushima, T., Kato, M., Fujita, I., and Ueda, K. (1984). Telencephalic and preoptic areas integrate sexual behavior in hime salmon (landlocked red salmon, Oncorhynchus nerka): Results of electrical brain stimulation experiments. Physiology & behavior *33*, 441-447.
42. Yamamoto, N., Oka, Y., and Kawashima, S. (1997). Lesions of Gonadotropin-Releasing Hormone-lmmunoreactive Terminal Nerve Cells: Effects on the Reproductive Behavior of Male Dwarf Gouramis. Neuroendocrinology *65*, 403-412.
43. Yabuki, Y., Koide, T., Miyasaka, N., Wakisaka, N., Masuda, M., Ohkura, M., Nakai, J., Tsuge, K., Tsuchiya, S., Sugimoto, Y., and Yoshihara, Y. (2016). Olfactory receptor for prostaglandin F2alpha mediates male fish courtship behavior. Nature neuroscience *19*, 897-904.
44. Ishii, K.K., Osakada, T., Mori, H., Miyasaka, N., Yoshihara, Y., Miyamichi, K., and Touhara, K. (2017). A Labeled-Line Neural Circuit for Pheromone-Mediated Sexual Behaviors in Mice. Neuron *95*, 123-137.e128.
45. Seeholzer, L.F., Seppo, M., Stern, D.L., and Ruta, V. (2018). Evolution of a central neural circuit underlies Drosophila mate preferences. Nature *559*, 564-569.
46. Simon, V., Hyacinthe, C., and Rétaux, S. (2019). Breeding behavior in the blind Mexican cavefish and its river-dwelling conspecific. PLOS ONE *14*, e0212591.

47. Yamashita, J., Takeuchi, A., Hosono, K., Fleming, T., Nagahama, Y., and Okubo, K. (2020). Male-predominant galanin mediates androgen-dependent aggressive chases in medaka. eLife *9*, e59470.
48. Patel, T.P., Gullotti, D.M., Hernandez, P., O'Brien, W.T., Capehart, B.P., Morrison, B., 3rd, Bass, C., Eberwine, J.E., Abel, T., and Meaney, D.F. (2014). An open-source toolbox for automated phenotyping of mice in behavioral tasks. Front Behav Neurosci *8*, 349.
49. Samson, A.L., Ju, L., Ah Kim, H., Zhang, S.R., Lee, J.A., Sturgeon, S.A., Sobey, C.G., Jackson, S.P., and Schoenwaelder, S.M. (2015). MouseMove: an open source program for semi-automated analysis of movement and cognitive testing in rodents. Scientific reports *5*, 16171.
50. Hong, W., Kennedy, A., Burgos-Artizzu, X.P., Zelikowsky, M., Navonne, S.G., Perona, P., and Anderson, D.J. (2015). Automated measurement of mouse social behaviors using depth sensing, video tracking, and machine learning. Proceedings of the National Academy of Sciences *112*, E5351-E5360.
51. Reeves, S.L., Fleming, K.E., Zhang, L., and Scimemi, A. (2016). M-Track: A New Software for Automated Detection of Grooming Trajectories in Mice. PLoS Comput Biol *12*, e1005115.
52. Ben-Shaul, Y. (2017). OptiMouse: a comprehensive open source program for reliable detection and analysis of mouse body and nose positions. BMC Biology *15*, 41.
53. Fontaine, E.I., Zabala, F., Dickinson, M.H., and Burdick, J.W. (2009). Wing and body motion during flight initiation in Drosophila revealed by automated visual tracking. Journal of Experimental Biology *212*, 1307-1323.
54. Dankert, H., Wang, L., Hoopfer, E.D., Anderson, D.J., and Perona, P. (2009). Automated monitoring and analysis of social behavior in Drosophila. Nature Methods *6*, 297-303.
55. Kain, J., Stokes, C., Gaudry, Q., Song, X., Foley, J., Wilson, R., and de Bivort, B. (2013). Leg-tracking and automated behavioural classification in Drosophila. Nature Communications *4*, 1910.
56. Scaplen, K.M., Mei, N.J., Bounds, H.A., Song, S.L., Azanchi, R., and Kaun, K.R. (2019). Automated real-time quantification of group locomotor activity in Drosophila melanogaster. Scientific reports *9*, 4427.
57. Günel, S., Rhodin, H., Morales, D., Campagnolo, J., Ramdya, P., and Fua, P. (2019). DeepFly3D, a deep learning-based approach for 3D limb and appendage tracking in tethered, adult Drosophila. eLife *8*, e48571.
58. Kabra, M., Robie, A.A., Rivera-Alba, M., Branson, S., and Branson, K. (2013). JAABA: interactive machine learning for automatic annotation of animal behavior. Nature Methods *10*, 64-67.

59. Mathis, A., Mamidanna, P., Cury, K.M., Abe, T., Murthy, V.N., Mathis, M.W., and Bethge, M. (2018). DeepLabCut: markerless pose estimation of user-defined body parts with deep learning. Nature neuroscience *21*, 1281-1289.
60. Freedman, A.H., and Wayne, R.K. (2017). Deciphering the Origin of Dogs: From Fossils to Genomes. Annual Review of Animal Biosciences *5*, 281-307.
61. Trut, L., Oskina, I., and Kharlamova, A. (2009). Animal evolution during domestication: the domesticated fox as a model. Bioessays *31*, 349-360.
62. Matsumoto, Y., Goto, T., Nishino, J., Nakaoka, H., Tanave, A., Takano-Shimizu, T., Mott, R.F., and Koide, T. (2017). Selective breeding and selection mapping using a novel wild-derived heterogeneous stock of mice revealed two closely-linked loci for tameness. Scientific reports *7*, 4607-4607.
63. Weber, K.P., De, S., Kozarewa, I., Turner, D.J., Babu, M.M., and de Bono, M. (2010). Whole genome sequencing highlights genetic changes associated with laboratory domestication of C. elegans. PLoS One *5*, e13922.
64. Stanley, C.E., and Kulathinal, R.J. (2016). Genomic signatures of domestication on neurogenetic genes in Drosophila melanogaster. BMC Evolutionary Biology *16*, 6.
65. Ruzzante, D.E. (1994). Domestication effects on aggressive and schooling behavior in fish. Aquaculture *120*, 1-24.
66. Wright, D., Nakamichi, R., Krause, J., and Butlin, R.K. (2006). QTL Analysis of Behavioral and Morphological Differentiation Between Wild and Laboratory Zebrafish (Danio rerio). Behavior Genetics *36*, 271.
67. Romeo, R.D., Richardson, H.N., and Sisk, C.L. (2002). Puberty and the maturation of the male brain and sexual behavior: recasting a behavioral potential. Neurosci Biobehav Rev *26*, 381-391.
68. Devidze, N., Lee, A.W., Zhou, J., and Pfaff, D.W. (2006). CNS arousal mechanisms bearing on sex and other biologically regulated behaviors. Physiology & behavior *88*, 283-293.
69. Juntti, S.A., and Fernald, R.D. (2016). Timing reproduction in teleost fish: cues and mechanisms. Current opinion in neurobiology *38*, 57-62.
70. Ma, X., Dong, Y., Matzuk, M.M., and Kumar, T.R. (2004). Targeted disruption of luteinizing hormone beta-subunit leads to hypogonadism, defects in gonadal steroidogenesis, and infertility. Proceedings of the National Academy of Sciences of the United States of America *101*, 17294-17299.
71. Nakajo, M., Kanda, S., Karigo, T., Takahashi, A., Akazome, Y., Uenoyama, Y., Kobayashi, M., and Oka, Y. (2018). Evolutionally Conserved Function of Kisspeptin Neuronal System Is Nonreproductive Regulation as Revealed by Nonmammalian Study.

Endocrinology *159*, 163-183.

72. Sakuma, Y. (1995). Differential control of proceptive and receptive components of female rat sexual behavior by the preoptic area. Jpn J Physiol *45*, 211-228.
73. Kato, A., and Sakuma, Y. (2000). Neuronal activity in female rat preoptic area associated with sexually motivated behavior. Brain Research *862*, 90-102.
74. Yamanouchi, K., and Arai, Y. (1976). Heterotypical sexual behavior in male rats: individual difference in lordosis response. *23*, 179-182.
75. Parsons, B., McGinnis, M.Y., and McEwen, B.S. (1981). Sequential inhibition of progesterone: effects on sexual receptivity and associated changes in brain cytosol progestin binding in the female rat. Brain Res *221*, 149-160.
76. Olster, D.H., and Blaustein, J.D. (1989). Development of steroid-induced lordosis in female guinea pigs: effects of different estradiol and progesterone treatments, clonidine, and early weaning. Hormones and behavior *23*, 118-129.
77. Kayo, D., Oka, Y., and Kanda, S. (2019). Examination of methods for manipulating serum 17beta-Estradiol (E2) levels by analysis of blood E2 concentration in medaka (Oryzias latipes). General and comparative endocrinology, 113272.
78. Royan, M.R., Kanda, S., Kayo, D., Song, W., Ge, W., Weltzien, F.A., and Fontaine, R. (2020). Gonadectomy and Blood Sampling Procedures in the Small Size Teleost Model Japanese Medaka (Oryzias latipes). J Vis Exp.
79. Sumpter, J.P., and Jobling, S. (1995). Vitellogenesis as a biomarker for estrogenic contamination of the aquatic environment. Environmental health perspectives *103 Suppl 7*, 173-178.
80. Hawkins, M.B., Thornton, J.W., Crews, D., Skipper, J.K., Dotte, A., and Thomas, P. (2000). Identification of a third distinct estrogen receptor and reclassification of estrogen receptors in teleosts. Proceedings of the National Academy of Sciences of the United States of America *97*, 10751-10756.
81. Tohyama, S., Ogino, Y., Lange, A., Myosho, T., Kobayashi, T., Hirano, Y., Yamada, G., Sato, T., Tatarazako, N., Tyler, C.R., Iguchi, T., and Miyagawa, S. (2017). Establishment of estrogen receptor 1 (ESR1)-knockout medaka: ESR1 is dispensable for sexual development and reproduction in medaka, Oryzias latipes. Development, growth & differentiation *59*, 552-561.
82. Suzuki, A., Tanaka, M., Shibata, N., and Nagahama, Y. (2004). Expression of aromatase mRNA and effects of aromatase inhibitor during ovarian development in the medaka, Oryzias latipes. Journal of experimental zoology. Part A, Comparative experimental biology *301*, 266-273.
83. Sato, T., Suzuki, A., Shibata, N., Sakaizumi, M., and Hamaguchi, S. (2008). The novel

mutant scl of the medaka fish, Oryzias latipes, shows no secondary sex characters. Zoological science *25*, 299-306.

84. Paul-Prasanth, B., Bhandari, R.K., Kobayashi, T., Horiguchi, R., Kobayashi, Y., Nakamoto, M., Shibata, Y., Sakai, F., Nakamura, M., and Nagahama, Y. (2013). Estrogen oversees the maintenance of the female genetic program in terminally differentiated gonochorists. Scientific reports *3*, 2862.
85. Ogino, Y., Hirakawa, I., Inohaya, K., Sumiya, E., Miyagawa, S., Denslow, N., Yamada, G., Tatarazako, N., and Iguchi, T. (2014). Bmp7 and Lef1 are the downstream effectors of androgen signaling in androgen-induced sex characteristics development in medaka. Endocrinology *155*, 449-462.
86. Toran-Allerand, C.D. (1976). Sex steroids and the development of the newborn mouse hypothalamus and preoptic area in vitro : Implications for sexual differentiation. Brain Research *106*, 407-412.
87. Konishi, M., and Akutagawa, E. (1985). Neuronal growth, atrophy and death in a sexually dimorphic song nucleus in the zebra finch brain. Nature *315*, 145-147.
88. Reisert, I., Han, V., Lieth, E., Toran-Allerand, D., Pilgrim, C., and Lauder, J. (1987). Sex steroids promote neurite growth in mesencephalic tyrosine hydroxylase immunoreactive neurons in vitro. International Journal of Developmental Neuroscience *5*, 91-98.
89. Frankfurt, M., Gould, E., Woolley, C.S., and McEwen, B.S. (1990). Gonadal Steroids Modify Dendritic Spine Density in Ventromedial Hypothalamic Neurons: A Golgi Study in the Adult Rat. Neuroendocrinology *51*, 530-535.
90. Montagnese, C., Poulain, D.A., and Theodosis, D.T. (1990). Influence of Ovarian Steroids on the Ultrastructural Plasticity of the Adult Rat Supraoptic Nucleus Induced by Central Administration of Oxytocin. Journal of Neuroendocrinology *2*, 225-231.
91. Fernald, R.D. (1995). Chapter 14 Social control of cell size: males and females are different. In Progress in Brain Research, Volume 105, A.C.H. Yu, L.F. Eng, U.J. McMahan, H. Schulman, E.M. Shooter and A. Stadlin, eds. (Elsevier), pp. 171-177.
92. Cooke, B.M., and Woolley, C.S. (2005). Gonadal hormone modulation of dendrites in the mammalian CNS. Journal of Neurobiology *64*, 34-46.
93. Chan, H., Prescott, M., Ong, Z., Herde, M.K., Herbison, A.E., and Campbell, R.E. (2011). Dendritic Spine Plasticity in Gonadatropin-Releasing Hormone (GnRH) Neurons Activated at the Time of the Preovulatory Surge. Endocrinology *152*, 4906-4914.
94. Balthazart, J., and Ball, G.F. (2016). Endocrine and social regulation of adult neurogenesis in songbirds. Frontiers in Neuroendocrinology *41*, 3-22.
95. Mitani, Y., Kanda, S., Akazome, Y., Zempo, B., and Oka, Y. (2010). Hypothalamic Kiss1 but Not Kiss2 Neurons Are Involved in Estrogen Feedback in Medaka (Oryzias latipes).

Endocrinology *151*, 1751-1759.

96. Maehiro, S., Takeuchi, A., Yamashita, J., Hiraki, T., Kawabata, Y., Nakasone, K., Hosono, K., Usami, T., Paul-Prasanth, B., Nagahama, Y., Oka, Y., and Okubo, K. (2014). Sexually dimorphic expression of the sex chromosome-linked genes cntfa and pdlim3a in the medaka brain. Biochemical and Biophysical Research Communications *445*, 113-119.

97. Hiraki, T., Nakasone, K., Hosono, K., Kawabata, Y., Nagahama, Y., and Okubo, K. (2014). Neuropeptide B is female-specifically expressed in the telencephalic and preoptic nuclei of the medaka brain. Endocrinology *155*, 1021-1032.

98. Hasebe, M., Kanda, S., Shimada, H., Akazome, Y., Abe, H., and Oka, Y. (2014). Kiss1 neurons drastically change their firing activity in accordance with the reproductive state: insights from a seasonal breeder. Endocrinology *155*, 4868-4880.

99. Kikuchi, Y., Hiraki-Kajiyama, T., Nakajo, M., Umatani, C., Kanda, S., Oka, Y., Matsumoto, K., Ozawa, H., and Okubo, K. (2019). Sexually Dimorphic Neuropeptide B Neurons in Medaka Exhibit Activated Cellular Phenotypes Dependent on Estrogen. Endocrinology *160*, 827-839.

100. Nishiike, Y., Miyazoe, D., Togawa, R., Yokoyama, K., Nakasone, K., Miyata, M., Kikuchi, Y., Kamei, Y., Todo, T., Ishikawa-Fujiwara, T., Ohno, K., Usami, T., Nagahama, Y., and Okubo, K. (2021). Estrogen receptor 2b is the major determinant of sex-typical mating behavior and sexual preference in medaka. Current Biology *31*, 1699-1710.e1696.

101. Yang, C.F., Chiang, M.C., Gray, D.C., Prabhakaran, M., Alvarado, M., Juntti, S.A., Unger, E.K., Wells, J.A., and Shah, N.M. (2013). Sexually Dimorphic Neurons in the Ventromedial Hypothalamus Govern Mating in Both Sexes and Aggression in Males. Cell *153*, 896-909.

102. Yang, Cindy F., and Shah, Nirao M. (2014). Representing Sex in the Brain, One Module at a Time. Neuron *82*, 261-278.

103. Satou, M., and Yamanouchi, K. (1996). Inhibitory effect of progesterone on sexual receptivity in female rats: a temporal relationship to estrogen administration. Zoological science *13*, 609-613.

104. Kobayashi, M., and Stacey, N. (1993). Prostaglandin-Induced Female Spawning Behavior in Goldfish (Carassius auratus) Appears Independent of Ovarian Influence. Hormones and behavior *27*, 38-55.

105. Kidd, M.R., Dijkstra, P.D., Alcott, C., Lavee, D., Ma, J., O'Connell, L.A., and Hofmann, H.A. (2013). Prostaglandin F2α facilitates female mating behavior based on male performance. Behavioral Ecology and Sociobiology *67*, 1307-1315.

106. Juntti, Scott A., Hilliard, Austin T., Kent, Kai R., Kumar, A., Nguyen, A., Jimenez, Mariana A., Loveland, Jasmine L., Mourrain, P., and Fernald, Russell D. (2016). A

Neural Basis for Control of Cichlid Female Reproductive Behavior by Prostaglandin F2α. Current Biology *26*, 943-949.

107. Nagler, J.J., Cavileer, T., Sullivan, J., Cyr, D.G., and Rexroad, C., 3rd (2007). The complete nuclear estrogen receptor family in the rainbow trout: discovery of the novel ERalpha2 and both ERbeta isoforms. Gene *392*, 164-173.
108. Katsu, Y., Lange, A., Miyagawa, S., Urushitani, H., Tatarazako, N., Kawashima, Y., Tyler, C.R., and Iguchi, T. (2013). Cloning, expression and functional characterization of carp, Cyprinus carpio, estrogen receptors and their differential activations by estrogens. Journal of applied toxicology : JAT *33*, 41-49.
109. Chen, Y., Tang, H., Wang, L., He, J., Guo, Y., Liu, Y., Liu, X., and Lin, H. (2018). Fertility Enhancement but Premature Ovarian Failure in esr1-Deficient Female Zebrafish. Frontiers in Endocrinology *9*.
110. Yan, L., Feng, H., Wang, F., Lu, B., Liu, X., Sun, L., and Wang, D. (2019). Establishment of three estrogen receptors (esr1, esr2a, esr2b) knockout lines for functional study in Nile tilapia. The Journal of steroid biochemistry and molecular biology *191*, 105379.
111. Court, L., Vandries, L., Balthazart, J., and Cornil, C.A. (2020). Key role of estrogen receptor β in the organization of brain and behavior of the Japanese quail. Hormones and behavior *125*, 104827.
112. Lubahn, D.B., Moyer, J.S., Golding, T.S., Couse, J.F., Korach, K.S., and Smithies, O. (1993). Alteration of reproductive function but not prenatal sexual development after insertional disruption of the mouse estrogen receptor gene. Proceedings of the National Academy of Sciences *90*, 11162-11166.
113. COUSE, J.F., and KORACH, K.S. (2001). Contrasting Phenotypes in Reproductive Tissues of Female Estrogen Receptor Null Mice. Annals of the New York Academy of Sciences *948*, 1-8.
114. Krege, J.H., Hodgin, J.B., Couse, J.F., Enmark, E., Warner, M., Mahler, J.F., Sar, M., Korach, K.S., Gustafsson, J.A., and Smithies, O. (1998). Generation and reproductive phenotypes of mice lacking estrogen receptor beta. Proceedings of the National Academy of Sciences of the United States of America *95*, 15677-15682.
115. Couse, J.F., Yates, M.M., Deroo, B.J., and Korach, K.S. (2005). Estrogen receptor-beta is critical to granulosa cell differentiation and the ovulatory response to gonadotropins. Endocrinology *146*, 3247-3262.
116. Antal, M.C., Petit-Demouliere, B., Meziane, H., Chambon, P., and Krust, A. (2012). Estrogen dependent activation function of ERbeta is essential for the sexual behavior of mouse females. Proceedings of the National Academy of Sciences of the United States of America *109*, 19822-19827.

117. Ikegami, K., Kajihara, S., Umatani, C., Nakajo, M., Kanda, S., and Oka, Y. Estrogen upregulates the firing activity of hypothalamic gonadotropin-releasing hormone (GnRH1) neurons in the evening in female medaka. Journal of Neuroendocrinology *n/a*, e13101.
118. Chen, P., and Hong, W. (2018). Neural Circuit Mechanisms of Social Behavior. Neuron *98*, 16-30.
119. McCarthy, M.M., and Arnold, A.P. (2011). Reframing sexual differentiation of the brain. Nature neuroscience *14*, 677-683.
120. Okubo, K., Miyazoe, D., and Nishiike, Y. (2019). A conceptual framework for understanding sexual differentiation of the teleost brain. General and comparative endocrinology *284*, 113129.
121. Ogawa, S., Tsukahara, S., Choleris, E., and Vasudevan, N. (2020). Estrogenic regulation of social behavior and sexually dimorphic brain formation. Neuroscience & Biobehavioral Reviews *110*, 46-59.
122. Zempo, B., Karigo, T., Kanda, S., Akazome, Y., and Oka, Y. (2018). Morphological Analysis of the Axonal Projections of EGFP-Labeled Esr1-Expressing Neurons in Transgenic Female Medaka. Endocrinology *159*, 1228-1241.
123. Egami, N. (1961). Factors initiating mating behavior and oviposition in the fish, Oryzias latipes. In Journal of the Faculty Science, University of Tokyo. Sect. Iv, Volume 9. p. 263.
124. Ishikawa, Y., Yoshimoto, M., and Ito, H. (1999). A brain atlas of a wild-type inbred strain of the medaka, Oryzias latipes(<Special Issue>A Brain Atlas of Medaka). The Fish Biology Journal Medaka, 1-26.
125. Cantu, V.A., Sadural, J., and Edwards, R. (2019). PRINSEQ++, a multi-threaded tool for fast and efficient quality control and preprocessing of sequencing datasets. (PeerJ Preprints).
126. Dobin, A., Davis, C.A., Schlesinger, F., Drenkow, J., Zaleski, C., Jha, S., Batut, P., Chaisson, M., and Gingeras, T.R. (2012). STAR: ultrafast universal RNA-seq aligner. Bioinformatics *29*, 15-21.
127. Li, B., and Dewey, C.N. (2011). RSEM: accurate transcript quantification from RNA-Seq data with or without a reference genome. BMC Bioinformatics *12*, 323.
128. Hiraki-Kajiyama, T., Yamashita, J., Yokoyama, K., Kikuchi, Y., Nakajo, M., Miyazoe, D., Nishiike, Y., Ishikawa, K., Hosono, K., Kawabata-Sakata, Y., Ansai, S., Kinoshita, M., Nagahama, Y., and Okubo, K. (2019). Neuropeptide B mediates female sexual receptivity in medaka fish, acting in a female-specific but reversible manner. Elife *8*.
129. Egami, N. (1959). Preliminary Note on the Induction of the Spawning Reflex and Oviposition in Oryzias latipes by the Administration of Neurohypophyseal Substances.

日本動物学彙報 *32*, 13-17.

130. Mutt, V., and Jorpes, J.E. (1968). Structure of porcine cholecystokinin-pancreozymin. 1. Cleavage with thrombin and with trypsin. Eur J Biochem *6*, 156-162.
131. Dockray, G.J. (1976). Immunochemical evidence of cholecystokinin-like peptides in brain. Nature *264*, 568-570.
132. Rehfeld, J.F. (1978). Immunochemical studies on cholecystokinin. II. Distribution and molecular heterogeneity in the central nervous system and small intestine of man and hog. J Biol Chem *253*, 4022-4030.
133. Bradwejn, J., and Koszycki, D. (2001). Cholecystokinin and panic disorder: past and future clinical research strategies. Scand J Clin Lab Invest Suppl *234*, 19-27.
134. Harro, J., Kiivet, R.A., Lang, A., and Vasar, E. (1990). Rats with anxious or non-anxious type of exploratory behaviour differ in their brain CCK-8 and benzodiazepine receptor characteristics. Behavioural brain research *39*, 63-71.
135. Hilke, S., Hökfelt, T., Darwish, M., and Theodorsson, E. (2007). Cholecystokinin levels in the rat brain during the estrous cycle. Brain Research *1144*, 70-73.
136. Takei, Y. (2000). Structural and functional evolution of the natriuretic peptide system in vertebrates. Int Rev Cytol *194*, 1-66.
137. Inoue, K., Naruse, K., Yamagami, S., Mitani, H., Suzuki, N., and Takei, Y. (2003). Four functionally distinct C-type natriuretic peptides found in fish reveal evolutionary history of the natriuretic peptide system. Proceedings of the National Academy of Sciences *100*, 10079-10084.
138. Yamagami, S., Suzuki, K., and Suzuki, N. (2001). Expression and Exon/Intron Organization of Two Medaka Fish Homologs of the Mammalian Guanylyl Cyclase A1. The Journal of Biochemistry *130*, 39-50.
139. Eguchi, K., Nakanishi, S., Takagi, H., Taoufiq, Z., and Takahashi, T. (2012). Maturation of a PKG-dependent retrograde mechanism for exoendocytic coupling of synaptic vesicles. Neuron *74*, 517-529.